Numerical Simulation of Transition-Edge Sensors

Master-Arbeit

zur Erlangung des Grades

Master of Science (M.Sc.)

im Studiengang Mathematik

am Department Mathematik der
Friedrich-Alexander-Universität Erlangen-Nürnberg

vorgelegt am 15.09.2017

von **Maximilian Lorenz**

Betreuer: Prof. Dr. Jörn Wilms

FRIEDRICH-ALEXANDER
UNIVERSITÄT
ERLANGEN-NÜRNBERG
NATURWISSENSCHAFTLICHE
FAKULTÄT

ecap
ERLANGEN CENTRE
FOR ASTROPARTICLE
PHYSICS

Department
MATHEMATIK

Abstract

This thesis is concerned with the numerical simulation of transition-edge sensors, a novel type of cryogenic energy sensor that will be installed on board the future X-ray observatory Athena.

Stochastic differential equations are used to accurately model the noise in these detectors. A stochastic Runge-Kutta integrator is implemented in the simulation software of the observatory. The computer simulations of the observatory will provide valuable feedback to science studies and the detector design during the development of Athena.

The simulation results of this thesis resemble previous simulations of the sensors. However, these new results are now based on a sound mathematical foundation instead of the heuristic noise simulation that was implemented in the simulation software before.

Contents

Chapter 1

Introduction

Most physical and engineering systems are too complex to provide analytical solutions. In order to study their behavior, numerical simulations are required. Numerical simulations are calculations performed by a computer program that implements a mathematical model for the physical system.

In this thesis I perform numerical simulations of transition-edge sensors, a novel type of cryogenic energy sensor. Such transition-edge sensors will be installed on board the Advanced Telescope for High ENergy Astrophysics (Athena). Athena is a future X-ray observatory of the European Space Agency that is currently under development with a launch foreseen in 2028 (Barcons et al., 2017). The performance of Athena will greatly exceed that offered by current X-ray observatories like *Chandra* and *XMM-Newton*. Athena will make an important contribution to answering some of the most pressing questions of todays astrophysics. Because X-ray radiation is absorbed by the Earth's atmosphere, the Athena observatory must be launched into space. Form there Athena will scan the universe for X-ray emission from supermassive black holes and other celestial objects.

On board Athena will be two detecting instruments. One of them, the *X-ray Integral Field Unit*, is made up of a large array of about 4000 transition-edge sensor (TES) based microcalorimeters. In order to study the performance of Athena in various science cases and to provide feedback to the detector development, simulations of this highly complex observatory are run with the *Simulation of X-ray TElescopes* (SIXTE) software package (Wilms et al., 2014). The software tool that performs detailed simulations of the TES based microcalorimeters within the SIXTE framework is named `tessim`. Since the performance of real detectors is greatly affected by various noise processes, `tessim` also simulates this detector noise. However, the method currently implemented to simulate the noise is merely heuristic and mathematically not rigorous.

The accurate description of noise in physical systems can be taken into account by *stochastic differential equations*. The main objective of this thesis is to model the noise in transition-edge sensor based microcalorimeters in the framework of stochastic differential equations and to implement a stochastic integrator into the `tessim` software tool that can solve such differential equations numerically.

In the following two chapters I present the Athena mission and the SIXTE software in more detail. Then I explain the working principle of transition-edge sensor based microcalorimeters in Chapter 4. Chapter 5 provides a detailed introduction to the

theory of stochastic differential equations. Starting with some basic definitions and concepts of stochastic calculus I gradually introduce the construction of stochastic integrals and stochastic differential equations. Next, I show methods to solve such stochastic differential equations numerically in Chapter 6 and present the algorithm that I implemented in the `tessim` software tool. In Chapter 7 I show the results of my simulations and investigate to what extent my new results differ from the simulations done before with `tessim`.

Chapter 2

The Athena X-Ray Observatory

The Advanced Telescope for High-Energy Astrophysics (Athena) is a future X-ray observatory to be launched in 2028. It is the second large class mission within the European Space Agency Cosmic Vision 2015–2035 programme and will address the *Hot and Energetic Universe* science theme (Barcons et al., 2017). A conceptual design of the Athena observatory is shown in Fig. 2.1.

Thanks to its novel optics technology and state-of-the-art detecting instruments, Athena will allow unprecedented studies of a wide range of astronomical phenomena. There are two major questions that will be studied within the Athena science theme (Barcons et al., 2015). First, how and why does ordinary matter assemble into the large-scale structures like galaxies and galaxy clusters that we see today in the Universe? Second, how do black holes grow and influence their surroundings?

In order to answer the first question Athena will map hot gas structures in the Universe and determine their physical properties. It is assumed that most of the ordinary matter, called *baryons*, in todays Universe is locked up in hot gas clouds at temperatures of more than a million Kelvin. Observations of this hot gas requires
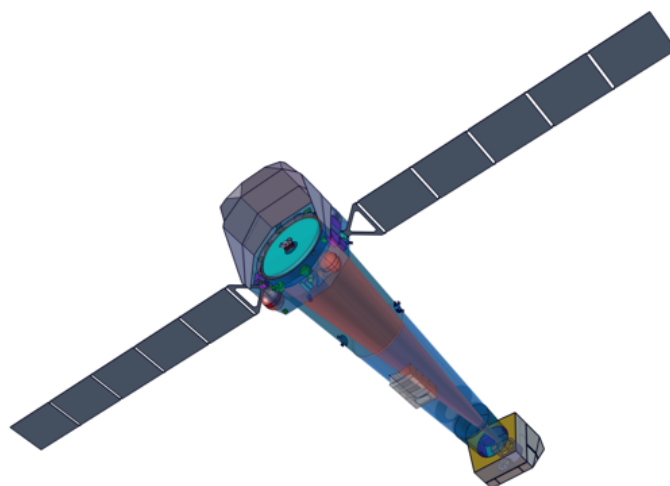

Fig. 2.1: Conceptional design of the Athena X-ray observatory. Taken from www.the-athena-x-ray-observatory.eu/mission.
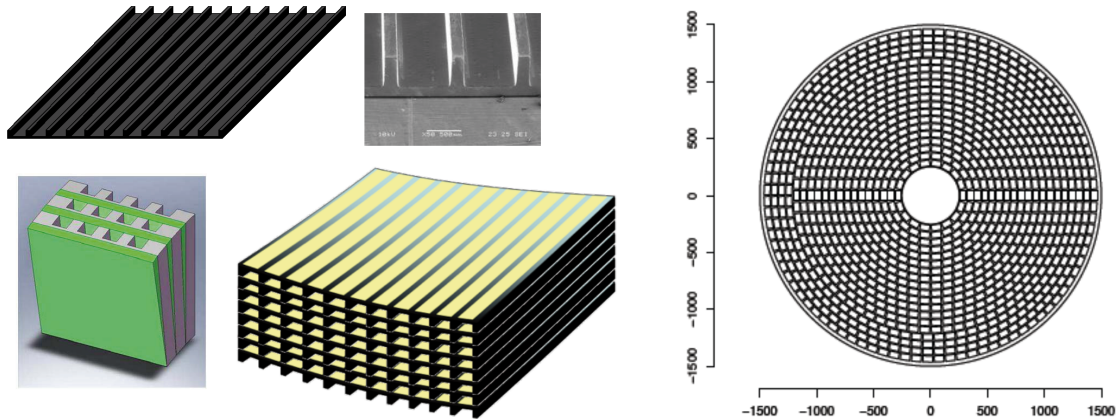
Fig. 2.2: *Left:* The manufacturing process of an SPO mirror module. The starting point is an Si plate with a width of about 60 mm. Parallel grooves with a rectangular profile are cut into the plate. Multiple plates are then stacked to create an SPO module. This way, hundreds of pores are created where each individual pore acts as a small sector of a Wolter I telescope. *Right:* The individual SPO modules are arranged in 19 rings to create the complete mirror. Figures taken from Willingale et al. (2013).

sensitive X-ray satellites. Theory and cosmological simulations predict that most of the baryons reside in filamentary structures that trace dark matter, called the *warm-hot intergalactic medium* (WHIM) (Kaastra et al., 2013). However, observational evidence of the WHIM is still lacking. One aim of the Athena mission is to reveal the WHIM and to relate its evolution and physical properties to the cosmological large-scale structure formation. Understanding of this connection is essential in order to have a complete picture of the Universe.

In order to answer the second question Athena will search for supermassive black holes. Most, if not all, galaxies harbor a black hole at their center which plays a fundamental role in their formation and evolution. Understanding the influence of black holes on the large-scale structure formation is another major goal of the Athena mission. To address this goal, Athena will find the most distant and therefore earliest supermassive black holes and trace their growth.

Besides these two major science goals, the Athena mission is expected to offer vital information on a wide range of other astrophysical research objects such as stellar winds, young stellar objects (Sciortino et al., 2013) and supernova remnants (Decourchelle et al., 2013). To meet the above science goals, Athena needs to provide a large field of view and high spectral resolution.

The Athena observatory will utilize an X-ray telescope about 3 m in diameter with a focal length of 12 m that is based on the novel *silicon pore optics* (SPO) technology (Collon et al., 2015). Simply put, the mirror is made up of multiple *SPO modules*. Each SPO module consists of a set of Si plates which are stacked together through small ribs. The individual SPO modules are then arranged in multiple rings to create the mirror. The manufacturing process of an SPO module is illustrated in Fig. 2.2. The silicon pore optics will provide a large collection area and good angular resolution while still being very lightweight.

In its focal plane Athena will carry two interchangeable detecting instruments: The Wide Field Imager (WFI) and the X-ray Integral Field Unit (X-IFU). The WFI is
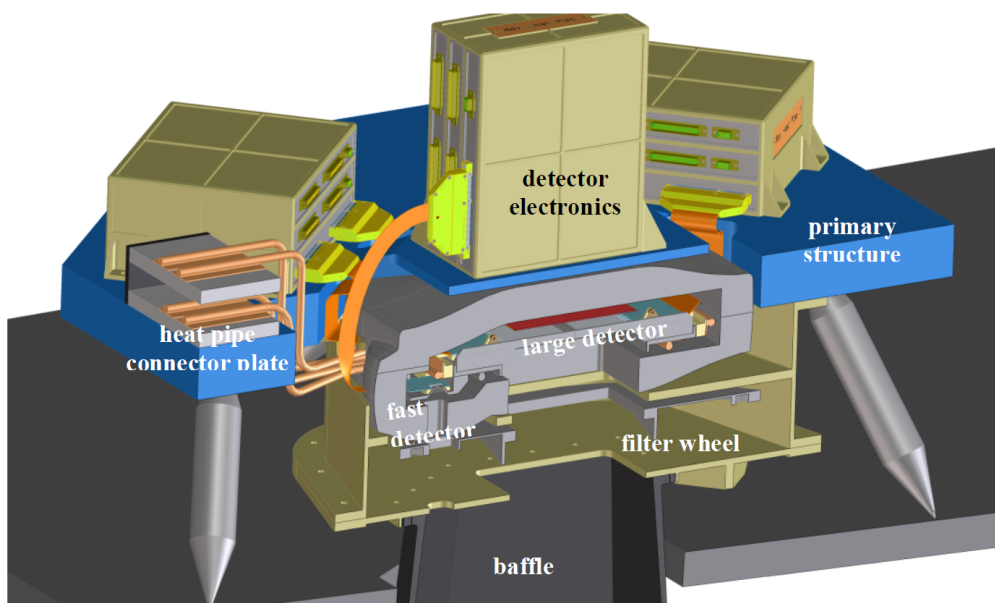
Fig. 2.3: Concept drawing of the WFI. The two detectors are installed in the center on the camera head. In front of the camera head lies the filter wheel which controls the arriving photon flux from the Athena mirror. The signal from the detector is transferred to the detector electronics which is mounted on top of the camera head. Excess heat from the detectors is removed through heat pipes. A baffle in front of the filter wheel reduces unwanted stray light. Taken from Meidinger et al. (2017).

a silicon based detector that uses DEPFET Active Pixel Sensor technology and will provide good spectral resolution over a broad energy band from 0.2 to 15 keV and a large field of view (Meidinger et al., 2017). A separate chip will allow faster readout that is appropriate for very bright sources.

The X-IFU is a cryogenic X-ray spectrometer that is made up of a large array of microcalorimeters based on superconducting transition-edge sensors (TES) operated at temperatures below 100 mK (Barret et al., 2016). Microcalorimeters are thermal detectors that measure the small temperature rise induced by the energy deposition of incident X-ray photons in the detector. By measuring this temperature rise, the photon energies can be reconstructed. The X-IFU will provide spatially resolved high-resolution X-ray spectroscopy over a small field of view with an energy resolution of 2.5 eV below 7 keV. Concept drawings of the two detectors are shown in Fig. 2.3 and Fig. 2.4.

An important part of the development of Athena will be computer simulations of the observatory (Wilms et al., 2016). By running detailed simulations of the full observatory one can estimate the performance of the detectors and make sure that the target science goals can be reached before building the hardware.

In the next chapter I present the *Simulation of X-ray Telescopes* software package. This software is used for the simulations of the Athena observatory.

50 mK Nb magnetic shield

2 K mu-metal (Cryoperm) magnetic shield

2 K structure / housing

Sensor array

300 mK support frame

Flexible sensor-to-LC interconnect

50 mK sensor readout assembly (LC filter array
+ front-end SQUID amplifiers)

Kevlar suspension unit

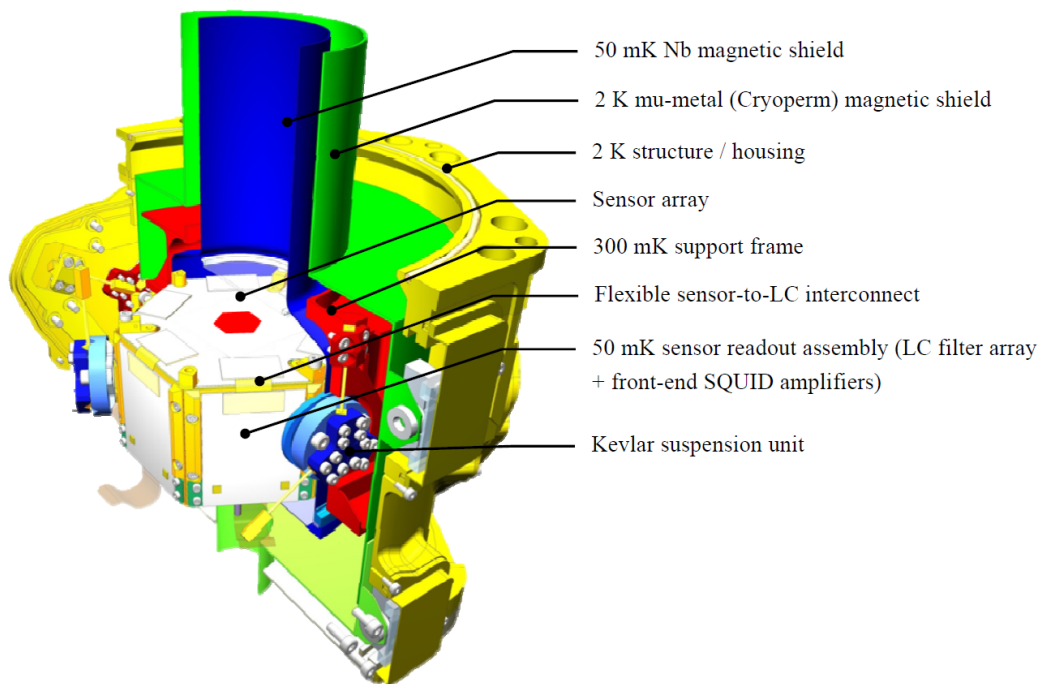**Fig. 2.4:** Design concept of the X-IFU focal plane assembly (FPA). At the core of the FPA lies the TES microcalorimeter array, consisting of 3840 pixels. Frequency domain multiplexing based on superconducting quantum interference devices (SQUIDs) is used for the readout of the TES (see Barret et al., 2016, for details). The FPA includes magnetic and stray light shielding. Taken from Jackson et al. (2016).

Chapter 3

Simulation of X-Ray Telescopes

Initially developed by Schmid (2012), the SImulation of X-ray TElescopes (SIXTE) is a software package for the simulation of observations with X-ray telescopes based on Monte Carlo methods. Since then, the software is under continuous development, with contributions from many different people and institutes. In this chapter I will briefly summarize the working principle of the simulator. A full description of the simulator is given by Schmid (2012). All software developed for the simulator is available for download at the simulator homepage[1]. Detailed instructions on its usage are given in the simulator manual[2].

The simulator performs *end-to-end* simulations, i.e., simulations of the full detection chain of an X-ray observatory. The aim of the simulator is to resemble the real observatory as closely as possible at comparably fast computation times. Starting with a description of the astrophysical source as the input, SIXTE generates a list of photons which are then propagated through the imaging and detection process. The output of a SIXTE simulation is an event list that closely resembles the output data from real telescopes. Figure 3.1 illustrates the data flow in a typical SIXTE simulation.

The simulation of future X-ray missions is a crucial step in their development process. By running simulations of the proposed observatory one can gauge its performance and make sure that the target science goals can be met before entering the construction phase. The simulations also provide important feedback to the instrument design. For example, it would be very costly and time consuming to build and test different detector designs experimentally. By running simulations of the proposed detectors one can easily change and test different pixel designs, array configurations, and other parameters in order to optimize the detector performance. For this reasons, the SIXTE software is currently used to study the performance of the instruments on board Athena (Wilms et al., 2014).

The SIXTE software is written in the C programming language and data are stored in Flexible Image Transport System (FITS) files. Most simulators for X-ray telescopes are mission specific. A big advantage of the SIXTE simulator is its flexible and modular setup. Each step of the simulation is processed by an individual simulation tool. Different telescope and instrument configurations can be implemented easily by exchanging the corresponding modules.

---

[1]http://www.sternwarte.uni-erlangen.de/research/sixte/
[2]http://www.sternwarte.uni-erlangen.de/research/sixte/data/simulator_manual.pdf
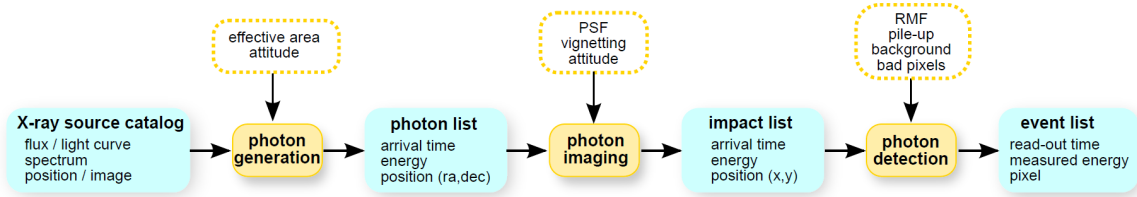
Fig. 3.1: This flow diagram shows the three major steps performed by SIXTE during the simulation process. The input of SIXTE is a description of the X-ray source to be simulated. Using this source description a list of photons is created which are then propagated through the optics. The output of the imaging process is an impact list which contains the arrival times, energies and impact positions of the photons on the detector. The last step models the detection process where the incident photons are converted into detector signals. The output of a SIXTE simulation is an event list that contains information about all detected photons in a similar way to data from real telescopes. Graphic taken from Wilms et al. (2014).

The work of my thesis contributes to the simulation of the Athena X-IFU detector. There are currently two simulation tools implemented in the SIXTE software for the X-IFU detector. One is the `xifupipeline` that is based on a simple detector model and enables fast simulations by using response matrices. A simulation of an observation by using the `xifupipeline` is shown in Fig. 3.2.

The other tool is `tessim` (Wilms et al., 2016) which is based on a much more detailed detector model and accurately simulates the physics of the transition-edge sensor based microcalorimeters that the X-IFU is made up of. This approach takes more computation time than the `xifupipeline`, but provides more realistic results and is thus much better suited for engineering studies.

The `tessim` tool is part of the third step in the SIXTE simulation chain and gets a photon impact list as its input. Put simply, `tessim` then computes a numerical solution of the differential equations that describe the response of a TES based microcalorimeter to the absorption of an X-ray photon. The output of `tessim` is a FITS file that contains the signal of the detector at each read out time. A full description of the tool is given by Wilms et al. (2016).

In order to provide realistic simulations of the detector, `tessim` also includes noise from the electronics and internal thermal fluctuations in its detector model. Currently, `tessim` uses a standard fourth order Runge-Kutta integrator to solve the system of differential equations numerically. The noise in the detector is simulated by adding appropriately scaled random numbers to the differential equations before each integration step.

This heuristic approach yields very reasonable simulation results, but is mathematically not rigorous. The correct mathematical framework to treat such differential equations affected by noise are *stochastic differential equations* (SDE). The numerical analysis of stochastic differential equations differs significantly from that of ordinary differential equations. The goal of my thesis is to model the detector noise in the framework of SDEs and implement an appropriate stochastic integrator into the `tessim` software to solve the resulting system of SDEs numerically.

Since the simulation results will provide feedback to the instrument design and science studies, it is an important task to make sure this part of the simulation is done
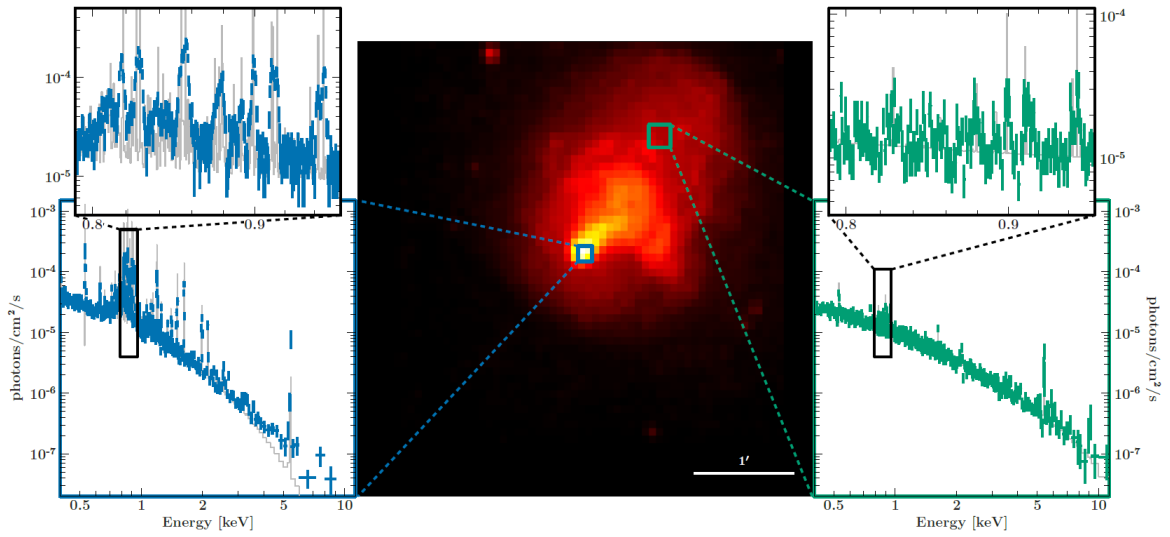
Fig. 3.2: Simulation of a 100 ks X-IFU observation of the galaxy cluster Abell 2146 by using the `xifupipeline`. The simulation result was processed with tools available in SIXTE. Spectra extracted from the two indicated regions are shown beside the image and illustrate the high resolution of the detector. Graphic taken from the SIXTE simulator manual (http://www.sternwarte.uni-erlangen.de/research/sixte/data/simulator_manual.pdf).

correctly. The `tessim` tool has already been used to study the detector performance in the past. So another question I want to answer with my thesis is if this new approach would make much of a difference to the previous simulation results. Perhaps the results of the two methods are indeed similar which would be the desired outcome.

Before proceeding to stochastic calculus and numerical methods for SDEs I will first describe the working principal of a TES based microcalorimeter in the next chapter and derive the system of differential equations that describe the detector response without noise.

Chapter 4

Transition-Edge Sensors

This chapter provides an introduction to the working principle of transition-edge sensor (TES) based microcalorimeters. The following information is obtained from Irwin & Hilton (2005) and McCammon (2005) unless otherwise stated.

Microcalorimeters are thermal detectors that can be used to measure the energy of photons. When a photon hits the detector its energy is converted into heat. By measuring the resulting temperature rise the energy of the photon can be determined.

Transition-edge sensors are superconducting thin films that can be used as very sensitive thermometers in microcalorimeters when kept within the superconducting to normal transition. Such TES based microcalorimeters can be adjusted to measure photon energies from the near infrared through gamma rays.

In the following sections I will explain the physics of a simple microcalorimeter and the transition edge-sensor and derive the system of differential equations that describe the response of the detector to the absorption of a photon. Finally, I present the fundamental noise processes that exist in such devices.

4.1 Basic Microcalorimeter Theory

A schematic view of a microcalorimeter is shown in Fig. 4.1. A simple microcalorimeter consists of an absorber with heat capacity C, a thermometer coupled to the absorber and a weak thermal link with thermal conductance G_{bath} to a cold bath at temperature T_{b}.

When a photon with an energy E_{ph} hits the absorber, its energy is converted into heat which raises the temperature of the absorber. Ideally, the energy is deposited instantaneously and the temperature of the absorber rises by $\Delta T = E_{\text{ph}}/C$. By measuring this temperature increase with the thermometer the energy of the incident photon can be determined as long as the capacity C of the absorber is known. The device then cools back to the steady state temperature through the weak thermal link. Figure 4.2 illustrates the thermal response of the device to the absorption of a photon.

The behavior of this system can be described by the power balance equation (Dreyer, 2012)

$$C\frac{dT(t)}{dt} = P_{\text{in}} - P_{\text{b}}(T, T_{\text{b}}), \quad T(0) = T_0, \tag{4.1}$$

where T is the temperature of the absorber at time t, T_0 is the initial temperature of
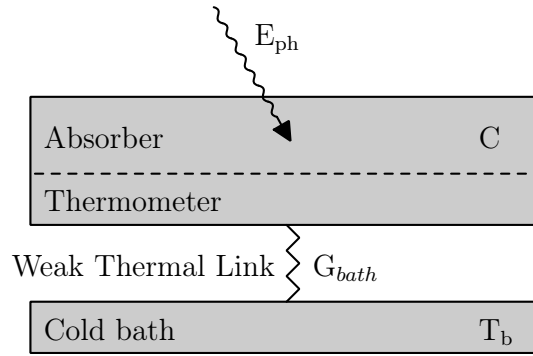
Fig. 4.1: Schematic illustration of a simple microcalorimeter (after Dreyer, 2012). A simple microcalorimeter consists of an absorber, a thermometer and a weak thermal link to a cold bath. When a photon hits the absorber its energy is thermalized. By measuring the temperature increase with a thermometer the energy of the photon can be determined. The excess heat from the absorption event is then removed through the weak thermal link to the cold bath.

the device, P_{in} is the signal power and $P_{\text{b}}(T, T_{\text{b}})$ is the heat flow from the absorber to the cold bath.

4.2   TES Based Microcalorimeters

In a TES based microcalorimeter a superconducting thin film connected to the absorber is used as the thermometer. Superconductors are materials that have zero resistance when cooled below a characteristic transition temperature T_{c} and normal resistance $R_{\text{N}} > 0$ for temperatures above T_{c}. An illustration of the resistance versus temperature curve for a TES is shown in Fig. 4.2. The critical temperature of a TES is typically of the order 0.1 K.

The superconducting film is voltage biased so that the resultant Joule heating raises the temperature of the TES to a temperature in the phase transition between the superconducting and normal state. Fig. 4.3 shows the circuit used to bias a TES and the Thevenin-equivalent circuit we will use for our analysis.

The increase of the detector temperature caused by the absorption of a photon leads to an increase of the TES resistance. This in turn leads to a reduction of the bias current. This change in current is measured using a superconducting quantum interference device (SQUID) that is inductively coupled to an input coil in series with the TES.

The electrical equation describing the system follows from Kirchhoff's voltage law, i.e., the sum of all voltages in a closed circuit is zero (Horowitz & Hill, 2015), and is given by (Irwin & Hilton, 2005)

$$L\frac{dI(t)}{dt} = V - IR_{\text{L}} - IR_{\text{TES}}(T, I), \quad I(0) = I_0, \tag{4.2}$$

where I is the electrical current through the TES, L is the inductance, V is the Thevenin-equivalent bias voltage and $R(T, I)$ is the electrical resistance of the TES, which is normally a function of the temperature and current.
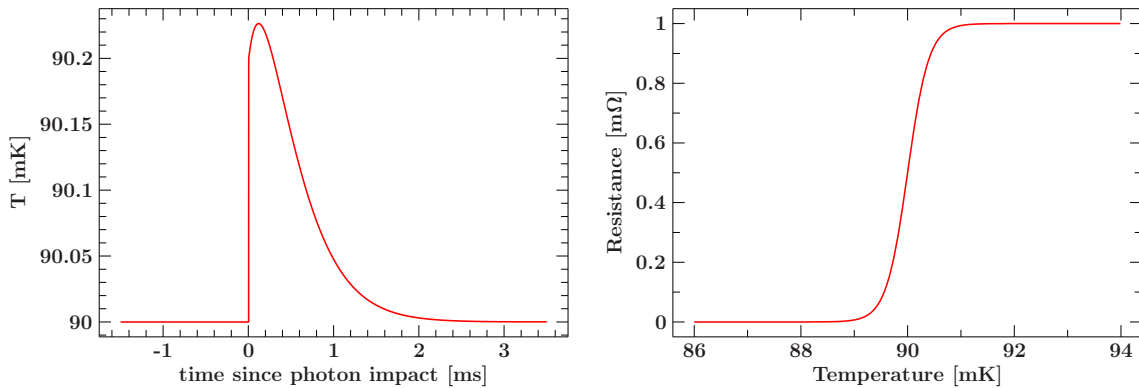
Fig. 4.2: *Left:* The time evolution of the temperature of the absorber measured with the thermometer. Initially, the microcalorimeter is at thermal equilibrium. When a photon with energy E_{ph} is absorbed, the temperature of the absorber increases by $\Delta T = E_{ph}/C$ and then cools back to the steady state temperature. *Right:* Illustration of the resistance versus temperature curve for a TES. When the TES is operated within the superconducting to normal transition, a small change in temperature leads to a large change in resistance. Within this range of temperatures the TES can be used as a very sensitive thermometer.

In the small signal limit the resistance of the TES can be expanded to first order as

$$R_{\text{TES}}(T, I) \approx R_0 + \left.\frac{\partial R}{\partial T}\right|_{(T_0, I_0)} (T - T_0) + \left.\frac{\partial R}{\partial I}\right|_{(T_0, I_0)} (I - I_0), \tag{4.3}$$

where R_0 is the steady-state resistance. We can replace the partial derivatives by defining two dimensionless parameters that describe the steepness of the superconducting transition. These parameters are the temperature sensitivity

$$\alpha \equiv \frac{T_0}{R_0} \left.\frac{\partial R}{\partial T}\right|_{(T_0, I_0)} \tag{4.4}$$

and the current sensitivity

$$\beta \equiv \frac{I_0}{R_0} \left.\frac{\partial R}{\partial I}\right|_{(T_0, I_0)}. \tag{4.5}$$
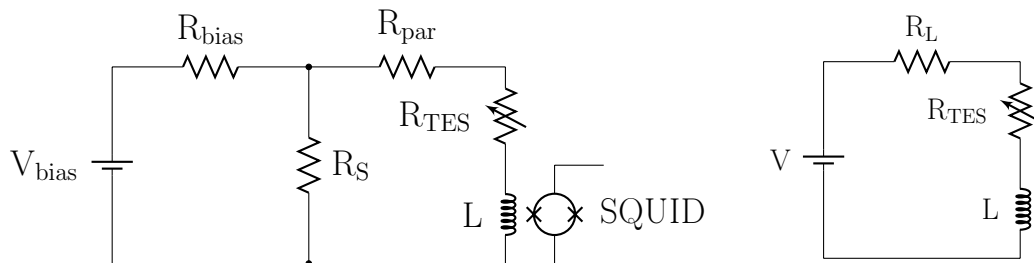
Fig. 4.3: *Left:* The electric circuit used to bias the TES (after Kinnunen, 2011). R_{bias} is the bias resistor, R_{S} is the shunt resistor and R_{par} is an additional parasitic resistance that can exist in the circuit. An input coil in series with the TES that is inductively coupled to a SQUID is typically used to read out the signals from the detector. *Right:* The Thevenin-equivalent of the circuit, where $R_{\text{L}} = R_{\text{S}} + R_{\text{par}}$ and $V = V_{\text{bias}} R_{\text{S}}/R_{\text{bias}}$.

With Eqs. (4.4) and (4.5), Eq. (4.3) becomes

$$R_{\text{TES}}(T, I) \approx R_0 + \alpha \frac{R_0}{T_0}(T - T_0) + \beta \frac{R_0}{I_0}(I - I_0). \tag{4.6}$$

The voltage applied across the TES produces a Joule heating P_{J} given by

$$P_{\text{J}}(t) = R_{\text{TES}}(T(t), I(t))I(t)^2. \tag{4.7}$$

The voltage biasing setup has an additional advantage concerning the detector operation. When the temperature of the TES increases, its resistance increases. For a constant bias voltage V this causes a drop in TES current and thus a decrease of Joule heating. The temperature of the TES cools down until it is in equilibrium again with the heat loss through the weak thermal link. This restoring action is called negative *electrothermal feedback* (ETF) and keeps the TES stably self-regulated within the narrow transition region. Besides stability, the negative ETF also speeds up the recovery back to steady state which increases the possible count rates of the detector.

The heat flow P_{bath} depends on the difference in temperature between the absorber and the cold bath. We assume a power-law dependence which can be modeled as (Irwin & Hilton, 2005)

$$P_{\text{b}}(T, T_{\text{b}}) = \frac{G_{\text{bath}}}{nT^{n-1}}(T^n - T_{\text{b}}^n), \tag{4.8}$$

where G_{bath} is the conductance of the weak thermal link to the cold bath and n is the thermal conductance exponent, a dimensionless constant which depends on the dominant mechanism of heat transport, the geometry of the link, and material.

Adding the additional Joule heating resulting from the voltage biasing to the thermal equation (4.1) yields

$$C\frac{dT(t)}{dt} = -P_{\text{b}}(T, T_{\text{b}}) + R_{\text{TES}}(T, I)I^2 + P_{\text{in}}, \quad T(0) = T_0 \tag{4.9}$$

Equations (4.9) and (4.2) form a system of two coupled differential equations that describe the response of a TES based microcalorimeter. However, like all physical systems with dissipation, the performance of real detectors is affected and limited by various noise processes. To investigate and simulate the effect of noise on the performance of the detector we need to include these noise processes in our detector model. In the next section I explain the main sources of noise that exist in a TES based microcalorimeter.

4.3   Noise Contributions

In an ideal simple detector model as described above there are three main sources of noise (Goldie et al., 2009): Johnson noise generated in the TES and bias resistor, thermal fluctuation noise (TFN) from the connection to the cold bath and noise in the readout circuit.

The TFN is caused by random exchange of energy across the weak thermal link between the TES and the cold bath (Dreyer, 2012). These fluctuations in energy lead to fluctuations of the TES temperature.

Johnson noise results from random thermal motions of the electrons in a resistor (Horowitz & Hill, 2015). Since the motion of electrons constitutes a current, these random motions create fluctuations in voltage across the resistor.

In order to get a realistic simulation of the detector we want to include these noise terms in our analysis. This allows us to provide meaningful data and feedback for studies regarding the capabilities and optimization of the detector. Adding the noise terms to the equations that describe the response of a TES results in a system of so-called *stochastic differential equations*

$$C\frac{dT(t)}{dt} = -P_{\mathrm{b}}(T, T_{\mathrm{b}}) + R(T, I)I^2 + P_{\mathrm{in}} + \text{"noise"}, \tag{4.10}$$

$$L\frac{dI(t)}{dt} = V - IR_{\mathrm{L}} - IR_{\mathrm{TES}}(T, I) + \text{"noise"}, \tag{4.11}$$

with initial conditions $T(0) = T_0$ and $I(0) = I_0$. Stochastic differential equations (SDE) are a generalization of ordinary differential equations for stochastic processes. With SDEs it is possible to accurately model systems that are not only deterministic but that are also subject to stochastic forces like our detector model. The following chapter provides an introduction to the theory of SDEs. In Chapter 6 I present methods to solve such equations numerically.

Chapter 5

Stochastic Differential Equations

Stochastic differential equations occur when a system described by differential equations is influenced by random noise. In the most general sense stochastic differential equations are differential equations where one or more of the terms is a stochastic process. This results in a solution which is itself a stochastic process.

As an example consider the population growth model (Mao, 2007)

$$\frac{dN(t)}{dt} = a(t)N(t), \qquad N(0) = N_0, \tag{5.1}$$

where $N(t)$ is the size of a population at time t, $a(t)$ is the relative rate of growth and $N_0 \geq 0$ is the initial size of the population. The rate of growth $a(t)$ might be influenced by some random environmental effects, e.g.,

$$a(t) = r(t) + \sigma(t)"\text{noise}", \tag{5.2}$$

so Eq. (5.1) becomes

$$\frac{dN(t)}{dt} = r(t)N(t) + \sigma(t)N(t)"\text{noise}", \qquad N(0) = N_0. \tag{5.3}$$

We can also write Eq. (5.3) as an integral equation, i.e.,

$$N(t) = N_0 + \int_0^t r(s)N(s)ds + \int_0^t \sigma(s)N(s)"\text{noise}"ds. \tag{5.4}$$

This equation is an example of a stochastic differential equation. The first integral is an ordinary Riemann integral whereas the second integral is called a *stochastic integral* or *Itô integral*. The integral is named after the Japanese mathematician Itô Kiyoshi who laid the foundations for the theory of stochastic integration and stochastic differential equations (Itô, 1951). How can we describe the "noise" term mathematically and how can we make sense of the second integral in Eq. (5.4)?

In this chapter I present Itô's construction of this stochastic integral. First I review some basic concepts and results of measure theory and probability theory that are used in the following sections. Then I present Itô's construction of the stochastic integral and the *Itô formula*. This formula is a stochastic calculus counterpart of the chain rule. Finally I present the definition of a stochastic differential equation and an existence and uniqueness theorem for such differential equations.

5.1   Measure Theory and Integrals

This section provides a short introduction to measure theory and integrals. The aim of this section is to explain some basic definitions and concepts of measure theory and integration that will be used throughout this thesis.

In the most general sense measure theory is the study of measures. These are functions that assign a number to certain subsets of a given set. It generalizes the intuitive notions of length, area and volume and builds the foundation for many other areas of mathematics such as probability theory or ergodic theory.

The following definitions and theorems are adapted from Cyganowski et al. (2002) unless otherwise stated. Before we can give the definition of a measure, we first need to introduce the concept of σ-algebras. These are families of subsets of a given set on which a measure can be defined.

Definition 5.1. *If Ω is a given set, then a σ-algebra $\mathcal{F}$ on Ω is a family $\mathcal{F}$ of subsets of Ω with the following properties:*

(i)   *$\Omega \in \mathcal{F}$.*
(ii)   *If $A_1, A_2, A_3 \ldots \in \mathcal{F}$, then $\bigcup_{i=1}^{\infty} A_i \in \mathcal{F}$.*
(iii)   *If $A \in \mathcal{F}$, then $A^C \in \mathcal{F}$, where $A^C = \Omega \setminus A$ is the complement of A in Ω.*

The pair $(\Omega, \mathcal{F})$ is called a *measurable space* and the elements of $\mathcal{F}$ are named *$\mathcal{F}$-measurable sets*. Examples of σ-algebras are the family $\mathcal{P}(\Omega)$ of all subsets of Ω or the trivial σ-algebra $\{\emptyset, \Omega\}$.

Given any family $\mathcal{U}$ of subsets of Ω there exists a smallest σ-algebra on Ω containing $\mathcal{U}$. This σ-algebra, denoted by $\sigma(\mathcal{U})$, is called the *σ-algebra generated by $\mathcal{U}$*. For example, if $\Omega = \mathbb{R}^n$ and $\mathcal{U}$ is the family of all open subsets of $\mathbb{R}^n$, then $\mathcal{B}^n = \sigma(\mathcal{U})$ is called the *Borel σ-algebra* and the elements of $\mathcal{B}^n$ are named *Borel sets* (Mao, 2007). The Borel σ-algebra $\mathcal{B}^n$ contains for example all open sets, all closed sets, all countable unions of open sets, all countable intersections of closed sets and so forth.

Definition 5.2. *Let $(\Omega, \mathcal{F})$ be a measurable space. A function $f : \Omega \to \bar{\mathbb{R}}$, where $\bar{\mathbb{R}} = \mathbb{R} \cup \{-\infty, \infty\}$, is called $\mathcal{F}$-measurable (or just measurable) if for any Borel set $B \in \mathcal{B}$ its preimage is $\mathcal{F}$-measurable, that is,*

$$f^{-1}(B) = \{\omega \in \Omega : f(\omega) \in B\} \in \mathcal{F}. \tag{5.5}$$

An example of a measurable function is the *indicator function* $I_A : \Omega \to \mathbb{R}$ of $\mathcal{F}$-measurable sets $A \in \mathcal{F}$ defined as

$$I_A(x) := \begin{cases} 1, & \text{for } x \in A \\ 0, & \text{for } x \notin A. \end{cases} \tag{5.6}$$

The only possible preimages here are $\emptyset$, A, $\Omega \setminus A$ and Ω, which are all $\mathcal{F}$-measurable.

An important property of measurable functions is given in the next theorem (Schilling, 2005).

Theorem 5.3. *Let $(\Omega, \mathcal{F})$ be a measurable space and let $f, g : \Omega \to \bar{\mathbb{R}}$ be $\mathcal{F}$-measurable functions. Then the functions*

$$f + g, \quad f - g, \quad f \cdot g \tag{5.7}$$

are also $\mathcal{F}$-measurable (whenever they are defined).

We can now state the definition of a measure.

Definition 5.4. *Let $(\Omega, \mathcal{F})$ be a measurable space. A function $\mu : \mathcal{F} \to \mathbb{R} \cup \{\infty\}$ is called a* measure *if it satisfies the following properties:*
(i)   *For all sets $A \in \mathcal{F}$, $\mu(A) \geq 0$.*
(ii)   *$\mu(\emptyset) = 0$.*
(iii)   *If sets $A_1, A_2, A_3, \ldots \in \mathcal{F}$ are pairwise disjoint (i.e., $A_i \cap A_j = \emptyset$ if $i \neq j$), then*

$$\mu\left(\bigcup_{i=1}^{\infty} A_i\right) = \sum_{i=1}^{\infty} \mu(A_i). \tag{5.8}$$

A measurable set $N \in \mathcal{F}$ is called a $(\mu-)$ *null set* if $\mu(N) = 0$. We say a property $P = P(\omega)$ holds $(\mu-)$ *almost everywhere* if P is true for all $\omega \in \Omega$ apart from some ω contained in a null set. For example, two functions $f, g : \Omega \to \bar{\mathbb{R}}$ are said to be *equal almost everywhere* if $\mu(\{\omega \in \Omega : f(\omega) \neq g(\omega)\}) = 0$.

This concludes the introduction to measure theory. Next I want to give a brief review of three main concepts of integration: the Riemann integral, the Stieltjes integral and the Lebesgue integral.

Knowledge of the Lebesgue integral will be necessary for the next sections. Understanding the idea and limitations of the other two integrals will be helpful when introducing the Itô integral. For more details see, e.g., Schilling (2005).

The standard integral of elementary calculus is the Riemann integral

$$\int_a^b f(x)dx, \tag{5.9}$$

where f is a scalar function defined on the interval $[a, b]$. The Riemann integral gives the area of the plane under the graph of the function f and above the interval $[a, b]$ if f takes nonnegative values. If the function f is both positive and negative, then the integral corresponds to the signed area under the graph of f, i.e., the area above the x-axis minus the area below the x-axis. The integral is defined as the limit of the sums of areas of approximating rectangles. That is,

$$\int_a^b f(x)dx := \lim \sum_{i=1}^{n} f(\xi_i)(x_i - x_{i-1}), \tag{5.10}$$

where x_i are points of a partition $a = x_0 < x_1 < \ldots < x_n = b$ of the interval $[a, b]$ and the evaluation points ξ_i are arbitrarily chosen points in the subintervals $[x_{i-1}, x_i]$. This limit is understood in such a way that n goes to infinity while the lengths $\delta_i = x_i - x_{i-1}$ of the subintervals tend uniformly to zero. If this limit is the same for all such partitions and any choices of points ξ_i, it is called the Riemann integral of the function f on $[a, b]$. The integral exists and is finite if f is continuous or if f is bounded with at most countably many points of discontinuity.

A possible generalization of the Riemann integral is the Stieltjes integral

$$\int_a^b f(x)dg(x), \tag{5.11}$$

where f and g are two functions defined on the interval $[a, b]$. It is similarly defined to be the limit

$$\int_a^b f(x)dg(x) := \lim \sum_{i=1}^n f(\xi_i)(g(x_i) - g(x_{i-1})) \tag{5.12}$$

of an approximating sum where the x_i are points of a partition $a = x_0 < x_1 < \ldots < x_n = b$ of the interval $[a, b]$ and the $\xi_i \in [x_{i-1}, x_i]$ are arbitrarily chosen points. The limit is again understood in such a way that n goes to infinity while the lengths of the subintervals tend uniformly to zero. As with the Riemann integral one requires the limit to be the same for all such partitions and any choices of evaluation points ξ_i.

The Stieltjes and Riemann integral coincide for the identity function $g(x) = x$. To give a criterion for existence we need the concept of *bounded variation* (Schilling & Partzsch, 2012).

Definition 5.5. *Let $g : [a, b] \to \mathbb{R}$ be a function and let $\Pi = \{a = x_0 < x_1 < \ldots < x_n = b\}$ be a finite partition of the interval $[a, b] \subset \mathbb{R}$. We call*

$$S_a^b(g; \Pi) := \sum_{i=1}^n |g(x_i) - g(x_{i-1})| \tag{5.13}$$

the variation sum. *The supremum of the variation sums over all finite partitions*

$$V_a^b(g) := \sup \left\{ S_a^b(g; \Pi) : \Pi \text{ is a finite partition of } [a, b] \right\} \tag{5.14}$$

is called the total variation *of g on $[a, b]$. If $V_a^b(g) < \infty$, we say that g is of* bounded variation *on $[a, b]$.*

The Stieltjes integral exists if f is continuous and g is of bounded variation on $[a, b]$ (Schilling & Partzsch, 2012). If, additionally, g is differentiable, then

$$\int_a^b f(x)dg(x) = \int_a^b f(x)g'(x)dx. \tag{5.15}$$

More general than the Riemann and Stieltjes integral is the Lebesgue integral or integral with respect to a measure. It extends the concept of integration to a larger class of functions and domains on which these functions can be defined. Let $(\Omega, \mathcal{F})$ be a measurable space, let $\mu : \mathcal{F} \to \mathbb{R} \cup \{\infty\}$ be a measure, and let $f : \Omega \to \bar{\mathbb{R}}$ be a measurable function. The Lebesgue integral of f over Ω with respect to the measure μ is denoted by

$$\int_\Omega f \, d\mu \tag{5.16}$$

and is defined in three stages:

1. First the integral is defined for nonnegative simple functions.

   A simple function $\phi : \Omega \to \mathbb{R}$ on a measurable space $(\Omega, \mathcal{F})$ is a function of the form

   $$\phi(x) = \sum_{i=1}^{k} c_i I_{A_i}(x), \tag{5.17}$$

   where $c_1, c_2, \ldots, c_k \in \mathbb{R}$ and the sets $A_1, A_2, \ldots, A_k \in \mathcal{F}$ are pairwise disjoint.

   Let ϕ be a nonnegative simple function, i.e., with nonnegative coefficients c_i in Eq. (5.17). The Lebesgue integral of ϕ is then defined as

   $$\int_{\Omega} \phi \, d\mu := \sum_{i=1}^{k} c_i \mu(A_i). \tag{5.18}$$

2. Next, assume f to be a nonnegative measurable function. One can show that there exists a sequence of nonnegative simple functions ϕ_n, $n = 1, 2, 3, \ldots$, such that $\phi_n(x) \leq \phi_{n+1}(x)$ for all n and x, and $\lim_{n \to \infty} \phi_n(x) = f(x)$. The Lebesgue integral of f is then defined as

   $$\int_{\Omega} f \, d\mu := \lim_{n \to \infty} \int_{\Omega} \phi_n \, d\mu. \tag{5.19}$$

3. Finally, let f be any measurable function. Then we can write

   $$f = f^+ - f^-, \tag{5.20}$$

   where $f^+(x) = \max\{f(x), 0\}$ and $f^-(x) = -\min\{f(x), 0\}$ which are both nonnegative measurable functions. The Lebesgue integral of f exists if at least one of $\int_{\Omega} f^+ \, d\mu$ and $\int_{\Omega} f^- \, d\mu$ is finite. In this case define

   $$\int_{\Omega} f \, d\mu := \int_{\Omega} f^+ \, d\mu - \int_{\Omega} f^- \, d\mu. \tag{5.21}$$

If $\int_{\Omega} |f| \, d\mu < \infty$, we say that f is *(Lebesgue) integrable*. For a measurable set $A \in \mathcal{F}$ one can define the Lebesgue integral of f over the set A as

$$\int_{A} f \, d\mu := \int_{\Omega} f I_A \, d\mu. \tag{5.22}$$

Finally, an important result from measure theory is Lebesgue's dominated convergence theorem which justifies passage to the limit under the sign of the integral (Koralov & Sinai, 2007).

Theorem 5.6 (Lebesgue Dominated Convergence Theorem). *If a sequence of measurable functions $\{f_n\}$ converges to a measurable function f almost everywhere and*

$$|f_n| \leq \varphi \tag{5.23}$$

where φ is integrable on Ω, then the function f is integrable on Ω and

$$\lim_{n \to \infty} \int_{\Omega} f_n d\mu = \int_{\Omega} f d\mu. \tag{5.24}$$

5.2   Probability Theory

This section provides a short introduction to probability theory, a branch of mathematics that is concerned with the analysis of random phenomena. On the basis of measure theory I will review and explain the definitions and concepts that are necessary for the construction of the Itô integral and definition of a stochastic differential equation.

Let $(\Omega, \mathcal{F})$ be a measurable space. In a probability context, Ω is called the *sample space* and $\mathcal{F}$ is named the *event space*. In probability theory one studies the possible outcomes of given events as well as their likelihoods and distributions. A map that assigns each event a probability, taking values between 0 and 1, is the *probability measure* (Kloeden & Platen, 1995).

Definition 5.7. *A* probability measure P *is a measure on a measurable space* $(\Omega, \mathcal{F})$ *for which* $P(\Omega) = 1$. *The triple* $(\Omega, \mathcal{F}, P)$ *is called a* probability space.

For an event $A \in \mathcal{F}$ we interpret $P(A)$ as the likelihood that the event A occurs and say that *A occurs with probability one* or *almost surely (a.s.)* if $P(A) = 1$. In the remainder of this section let $(\Omega, \mathcal{F}, P)$ be a probability space.

The next definition by Cyganowski et al. (2002) introduces the concept of random variables.

Definition 5.8. *A function* $X : \Omega \to \mathbb{R}$ *is called a* random variable *if it is* $\mathcal{F}$-*measurable, i.e.,*

$$X^{-1}(B) = \{\omega \in \Omega : X(\omega) \in B\} \in \mathcal{F} \tag{5.25}$$

for any set $B \in \mathcal{B}$.

A random variable is a measurable function that assigns a real number to every element in the sample space. For example, if an experiment consists of tossing a fair coin ten times, the random variable X could be defined as the number of times the coin turns up heads.

Why do we require the random variable X to be measurable? One might be interested in the probability that a random variable takes on a value in an interval I. In order to have a probability assigned to that set one needs the function X to be measurable.

Given a random variable X the smallest σ-algebra on Ω with respect to which X is measurable is called the σ-*algebra generated by* X and is denoted by $\sigma(X)$ (Proschan & Shaw, 2016).

A straightforward generalization of random variables are *random vectors*.

Definition 5.9. *A function* $X : \Omega \to \mathbb{R}^n$ *is called a* random vector *if it is* $\mathcal{F}$-*measurable, i.e.,*

$$X^{-1}(B) = \{\omega \in \Omega : X(\omega) \in B\} \in \mathcal{F} \tag{5.26}$$

for any set $B \in \mathcal{B}^n$.

Since a random variable is just a one dimensional random vector, there is no formal reason to distinguish between these terms and they are often used synonymously.

Two sets $A, B \in \mathcal{F}$ are said to be *independent* if $P(A \cap B) = P(A)P(B)$. The following definition by Mao (2007) extends this concept to multiple sets and introduces independence of σ-algebras and random variables.

Definition 5.10. *Let I be an index set.*

(i) *A collection of sets $\{A_i : i \in I\} \subset \mathcal{F}$ is said to be independent if*

$$P(A_{i_1} \cap \cdots \cap A_{i_k}) = P(A_{i_1}) \cdots P(A_{i_k}) \tag{5.27}$$

for all possible choices of indices $i_1, \ldots, i_k \in I$.

(ii) *A collection of sub-σ-algebras $\{\mathcal{F}_i : i \in I\}$ of $\mathcal{F}$ is said to be independent if for every possible choice of indices $i_1, \ldots, i_k \in I$,*

$$P(A_{i_1} \cap \cdots \cap A_{i_k}) = P(A_{i_1}) \cdots P(A_{i_k}) \tag{5.28}$$

holds for all $A_{i_1} \in \mathcal{F}_{i_1}, \ldots, A_{i_k} \in \mathcal{F}_{i_k}$.

(iii) *A family of random variables $\{X_i : I \in I\}$ is said to be independent if the σ-algebras $\sigma(X_i)$, $i \in I$, generated by them are independent.*

(iv) *A random variable X and a σ-algebra $\mathcal{H} \subset \mathcal{F}$ are said to be independent if $\sigma(X)$ and $\mathcal{H}$ are independent.*

The most basic information about a random variable is given by its expectation and variance (Mao, 2007).

Definition 5.11. *Let $X : \Omega \to \mathbb{R}$ be a real-valued random variable. If X is integrable with respect to the probability measure P then the number*

$$E[X] := \int_{\Omega} X dP \tag{5.29}$$

is called the expectation *of X with respect to P. The number*

$$Var(X) = E\left[(X - E[X])^2\right] \tag{5.30}$$

is called the variance *of X. If Y is another real-valued random variable,*

$$Cov(X, Y) = E[(X - E[X])(Y - E[Y])] \tag{5.31}$$

is called the covariance *of X and Y.*

Two random variables X and Y are said to be uncorrelated if $Cov(X, Y) = 0$. If $X = (X_1, \cdots, X_n)^T$ is an $\mathbb{R}^n$-valued random variable, we define $E[X] := (E[X_1], \cdots, E[X_n])^T$. The terms *expected value* or *mean* are sometimes used instead of expectation.

Two important properties of the expectation are summarized in the following theorem (Cyganowski et al., 2002).

Theorem 5.12. *Let X and Y be two real-valued integrable random variables and $\alpha, \beta \in \mathbb{R}$. Then*

(i) $E[\alpha X + \beta Y] = \alpha E[X] + \beta E[Y]$ *(linearity of the expectation).*

(ii) $E[XY] = E[X]E[Y]$ *if X and Y are independent.*

Using the linearity of the expectation one can derive an equivalent formula for the variance which is particularly useful for calculations, namely $Var(X) = E[X^2] - E[X]^2$.

The following definitions introduce the *distribution function* and *density function* of a random variable X (Evans, 2014).

Definition 5.13. *Let $X : \Omega \to \mathbb{R}$ be a random variable. The* distribution function *of X is the function $F_X : \mathbb{R} \to [0, 1]$ defined by*

$$F_X(x) = P(\{\omega \in \Omega : X(\omega) \leq x\}), \quad x \in \mathbb{R}. \tag{5.32}$$

That is, the distribution function of a random variable X, evaluated at x, is the probability that X will take a value less than or equal to x.

Definition 5.14. *Let $X : \Omega \to \mathbb{R}$ be a random variable and F_X its distribution function. If there exists a nonnegative, integrable function $f : \mathbb{R} \to \mathbb{R}$ such that*

$$F_X(x) = \int_{-\infty}^{x} f(t)dt, \tag{5.33}$$

then f is called the density function *for X.*

Example 5.15. If a random variable $X : \Omega \to \mathbb{R}$ has density

$$f(x) = \frac{1}{\sqrt{2\pi\sigma^2}} e^{-\frac{(x-m)^2}{2\sigma^2}} \quad (x \in \mathbb{R}), \tag{5.34}$$

we say X has a *Gaussian* (or *normal*) distribution with mean m and variance σ^2. In this case we write $X \sim N(m, \sigma^2)$ and say

$$X \text{ is an } N(m, \sigma^2) \text{ random variable.}$$

For $p \in [1, \infty)$ we define the L^p-norm $\|X\|_p$ of a random variable $X : \Omega \to \mathbb{R}^n$ by

$$\|X\|_p := (E[|X|^p])^{\frac{1}{p}} \tag{5.35}$$

and the corresponding L^p-spaces by

$$L^p(\Omega, \mathbb{R}^n) := \{X : \Omega \to \mathbb{R}^n | \ \|X\|_p < \infty\}. \tag{5.36}$$

With this norm the L^p-spaces are Banach spaces, i.e., complete normed vector spaces (Øksendal, 2003). *Complete* in this case means that every Cauchy sequence in $L^p(\Omega, \mathbb{R}^n)$ is convergent.

There are two concepts of convergence in the context of probability theory that I will use in the following sections (Mao, 2007).

Definition 5.16. *Let X and X_k, $k \geq 1$, be $\mathbb{R}^n$-valued random variables.*
(a) *If for every $\epsilon > 0$, $P(\{\omega \in \Omega : |X_k(\omega) - X(\omega)| > \epsilon\}) \to 0$ as $k \to \infty$, then $\{X_k\}$ is said to converge to X in* probability.
(b) *If X_k and X belong to $L^p(\Omega, \mathbb{R}^n)$ and $\|X_k - X\|_p \to 0$ as $k \to \infty$, then $\{X_k\}$ is said to converge to X in L^p.*

For two events $A, B \in \mathcal{F}$ with $P(B) > 0$ the *conditional probability of A given B*, denoted by $P(A|B)$, is

$$P(A|B) := \frac{P(A \cap B)}{P(B)}. \tag{5.37}$$

Similarly, one can define the *conditional expectation of a random variable X given B*, denoted by $E[X|B]$, as

$$E[X|B] := \frac{\int_B X dP}{P(B)}, \tag{5.38}$$

provided that the integral is finite. However, one frequently encounters a family of conditions so we need a more general concept of conditional expectation. The next definition by Koralov & Sinai (2007) introduces a generalization of this notion by defining the conditional expectation of a random variable X given a sub-σ-algebra $\mathcal{H} \subset \mathcal{F}$.

Definition 5.17 (Conditional expectation). *Let $X \in L^1(\Omega, \mathbb{R})$. If $\mathcal{H} \subset \mathcal{F}$ is a σ-algebra, then the* conditional expectation of X given $\mathcal{H}$*, denoted by $E[X|\mathcal{H}]$, is a random variable satisfying:*
(i)   *$E[X|\mathcal{H}]$ is $\mathcal{H}$-measurable,*
(ii)   *$\int_H E[X|\mathcal{H}]dP = \int_H X dP$, for all $H \in \mathcal{H}$.*

The conditional expectation $E[X|\mathcal{G}]$ can be interpreted as the best guess of the value of X based on the information provided by $\mathcal{G}$. The existence and uniqueness of $E[X|\mathcal{G}]$ are guaranteed by the Radon-Nikodym Theorem (Øksendal, 2003).

The following theorem summarizes some important properties of the conditional expectation (Øksendal, 2003).

Theorem 5.18. *Suppose $X, Y \in L^1(\Omega, \mathbb{R})$ and $\mathcal{H} \subset \mathcal{F}$ is a σ-algebra. Then*
(a)   *$E[E[X|\mathcal{H}]] = E[X]$.*
(b)   *$E[X|\mathcal{H}] = X$ if X is $\mathcal{H}$-measurable.*
(c)   *$E[X|\mathcal{H}] = E[X]$ if X and $\mathcal{H}$ are independent.*
(d)   *$E[YX|\mathcal{H}] = YE[X|\mathcal{H}]$ if Y is $\mathcal{H}$-measurable.*

Until now we only looked at random variables as functions on a sample space without regard to how these might depend on parameters. The next definition by Mao (2007) introduces the concept of *stochastic processes*. These are families of random variables indexed by a parameter.

Definition 5.19. *A family $\{X_t\}_{t \in I}$ of $\mathbb{R}^n$-valued random variables is called a* stochastic process *with* parameter set *(or* index set*) I and state space $\mathbb{R}^n$.*

Usually the parameter set I is the half-line $\mathbb{R}_+ = [0, \infty)$, which is often thought of as time. For each fixed $t \in I$ we have a random variable

$$\Omega \ni \omega \rightarrow X_t(\omega) \in \mathbb{R}^n. \tag{5.39}$$

On the other hand, for each fixed $\omega \in \Omega$ we have a function

$$I \ni t \rightarrow X_t(\omega) \in \mathbb{R}^n \tag{5.40}$$

which is called a *realization* or *sample path* of the stochastic process. That is why we can use a stochastic process to represent randomly changing numerical values of some system as time evolves. For example, the growth of a bacterial population or the random fluctuations in an electrical signal. If we run an experiment and study the values of X as time evolves, we are in fact looking at a sample path of X for some fixed $\omega \in \Omega$. In general we will observe a different sample path if we rerun the experiment.

In this thesis I will use the notation X_t to denote sample paths of a stochastic process, suppressing the sample space argument ω for compactness of notation when the context is clear.

Next, I present two definitions related to stochastic processes (Mao, 2007).

Definition 5.20. (a) *A* filtration *is a family* $\{\mathcal{F}_t\}_{t\geq 0}$ *of increasing sub-σ-algebras of* $\mathcal{F}$ *(i.e., $\mathcal{F}_t \subset \mathcal{F}_s \subset \mathcal{F}$ for all $0 \leq t < s < \infty$).*
(b) *A* filtered probability space $(\Omega, \mathcal{F}, \{\mathcal{F}_t\}_{t\geq 0}, P)$ *is a probability space equipped with a filtration.*

Intuitively, the σ-algebra $\mathcal{F}$ contains all events which might ever be observed or to which we can assign probabilities. The filtration keeps track of what information is available at each of the times $t \geq 0$, where information only increases with time. So for each $t \geq 0$ the σ-algebra $\{\mathcal{F}_t\}$ tells us which events might be observed at time t.

Definition 5.21. *Let $(\Omega, \mathcal{F}, \{\mathcal{F}_t\}_{t\geq 0}, P)$ be a filtered probability space and let $\{X_t\}_{t\in I}$ be an $\mathbb{R}^n$-valued stochastic process. It is said to be*
(i)   continuous *if for almost all $\omega \in \Omega$ the function $X_t(\omega)$ is continuous on $t \geq 0$.*
(ii) $\{\mathcal{F}_t\}$-adapted *if for every t, X_t is $\{\mathcal{F}_t\}$-measurable.*

A stochastic process $\{X_t\}_{t\geq 0}$ is always adapted to its *natural filtration* $\{\mathcal{F}_t^X\}_{t\geq 0}$ where $\mathcal{F}_t^X = \sigma\left(\cup_{0\leq s\leq t} \sigma(X_s)\right)$ (Grigoriu, 2002). This is the smallest filtration with respect to which $\{X_t\}_{t\geq 0}$ is adapted.

5.3   The Wiener Process and White Noise

We can now state the definition of a Wiener process (Mao, 2007). This process was proposed by Norbert Wiener as a mathematical description of Brownian motion, i.e., the irregular motion of pollen particles on a water surface due to random collisions with the water molecules. That is why the Wiener process is often called *Brownian motion* synonymously due to its connection with the physical process originally observed by Robert Brown in 1828 (Mao, 2007).

Definition 5.22. *Let $(\Omega, \mathcal{F}, \{\mathcal{F}_t\}_{t\geq 0}, P)$ be a filtered probability space. A* one-dimensional Wiener process *is a real-valued continuous $\{\mathcal{F}_t\}$-adapted stochastic process $\{W_t\}_{t\geq 0}$ with the following properties:*
(i) $W_0 = 0$ *a.s.,*
(ii)   *for $0 \leq s < t < \infty$, the increment $W_t - W_s$ is normally distributed with mean zero and variance $t - s$,*
(iii)   *for $0 \leq s, < t < \infty$, the increment $W_t - W_s$ is independent of $\mathcal{F}_s$.*

If $\{W_t\}_{t \geq 0}$ is a Wiener process, then for all times $0 = t_0 < t_1 < \ldots < t_n < \infty$ the increments $(W_{t_i} - W_{t_{i-1}})$, $1 \leq i \leq n$, are independent (Karatzas & Shreve, 1991). We say that the Wiener process has *independent increments*.

Almost all sample paths of the Wiener process are continuous, but they are non differentiable for all $t \geq 0$. Moreover, the sample paths are of unbounded variation almost surely over any finite interval (Socha, 2008).

An appropriate mathematical interpretation for the "noise" term in Eq. (5.4) is the so-called *white noise process* (Kuo, 2006). The white noise process can be formally considered as the generalized derivative of a Wiener process $\{W_t\}_{t \geq 0}$ (Kloeden & Platen, 1995). Before we can state the definition of the white noise process we need to introduce some additional concepts from stochastic calculus (Lefebvre, 2007).

Definition 5.23. *We say that the random vector $(X_1, \ldots, X_n)$ has a* multinormal distribution *if each random variable X_k can be expressed as a linear combination of independent random variables $Z_1, \ldots, Z_m$, where $Z_j \sim N(0, 1)$, for $j = 1, \ldots, m$. That is, if*

$$X_k = \mu_k + \sum_{j=1}^{m} c_{kj} Z_j \qquad \text{for } k = 1 \ldots, n \tag{5.41}$$

where μ_k is a real constant, for all k.

Definition 5.24. *A stochastic process $\{X_t\}_{t \in I}$ is said to be a* Gaussian process *if the random vector $(X_{t_1}, \ldots, X_{t_n})$ has a multinormal distribution, for any n and for all $t_1, \ldots, t_n$.*

Definition 5.25. *Let $\{X_t\}_{t \in I}$ be a stochastic process. The* autocorrelation function *and the* autocovariance function *of the process at the point (t_1, t_2) are defined, respectively, by*

$$R_X(t_1, t_2) = E[X_{t_1} X_{t_2}], \tag{5.42}$$

and

$$C_X(t_1, t_2) = R_X(t_1, t_2) - E[X_{t_1}]E[X_{t_2}]. \tag{5.43}$$

We say that the stochastic process is wide-sense stationary *if there is a constant μ and a function $c : \mathbb{R} \to \mathbb{R}$ such that*

$$E[X_t] = \mu \quad \text{and} \quad R_X(t_1, t_2) = c(t_2 - t_1) \tag{5.44}$$

for all $t_1, t_2 \in I$.

So a wide-sense stationary process has a constant mean and its autocorrelation function only depends of the difference $s = t_2 - t_1$, i.e., it does not change by shifts in time.

Definition 5.26. *The* spectral density *of a wide-sense stationary stochastic process $\{X_t\}_{t \in I}$ is the Fourier transform $S_X(\omega)$ of its autocorrelation function*

$$S_X(\omega) = \int_{-\infty}^{\infty} e^{i\omega s} c(s) ds \tag{5.45}$$

Now we can state the definition of a white noise process (Kuo, 2006).

Definition 5.27. *A* white noise (process) *is defined to be a generalized wide-sense stationary Gaussian process $\{Z_t\}_{t\geq 0}$ with mean zero and autocovariance function $C_Z(t_1, t_2) = \delta(t_2 - t_1)$. Here $\delta(\cdot)$ is the Dirac delta function.*

The Dirac delta function is a generalized function with $\delta(s) = 0$ for all $s \neq 0$ such that

$$\int_{-\infty}^{\infty} f(s)\delta(s)ds = f(0) \tag{5.46}$$

for all functions f continuous at $s = 0$ (Kloeden & Platen, 1995).

Note that, since $E[Z_t] = 0$, we also have $R_Z(t_1, t_2) = \delta(t_2 - t_1)$. The spectral density function of the white noise Z_t is given by

$$S_Z(\omega) = \int_{-\infty}^{\infty} e^{i\omega s}\delta(s)ds = 1. \tag{5.47}$$

So the white noise Z_t has a constant nonzero spectral density. That is where the name white noise comes from as its average power is uniformly distributed in frequency which is a characteristic of white light.

Although the Wiener process is non differentiable in the classical sense, using the concept of generalized functions one can show (Horsthemke & Lefever, 1984) that the white noise is the generalized derivative of a Wiener process. In fact this property is often used as an alternative definition of white noise (Socha, 2008).

This means, in order to give a well-defined meaning to Eq. (5.3)

$$\frac{dN(t)}{dt} = r(t)N(t) + \sigma(t)N(t)"\text{noise}", \qquad N(0) = N_0.$$

we need to rewrite the equation in integral form, that is,

$$N(t) = N_0 + \int_0^t r(s)N(s)ds + \int_0^t \sigma(s)N(s)Z_t\, ds,$$

assuming that the noise can be described by a white noise process Z_t. Since the white noise is the generalized derivative of a Wiener process, we can write the second integral as

$$\int_0^t \sigma(s)N(s)Z_t\, ds = \int_0^t \sigma(s)N(s)dW_s, \tag{5.48}$$

that is, as an integral with respect to a Wiener process (Horsthemke & Lefever, 1984).

Because the sample paths of a Wiener process have unbounded variation almost surely over any finite interval we cannot simply define this integral as a Stieltjes integral (see section 5.1). In the next section I present Itô's idea to give a meaning to this stochastic integral.

5.4 The Itô Integral

In this section I will explain how the stochastic integral

$$\int_a^b X_t dW_t \tag{5.49}$$

of a random variable $X : \Omega \to \mathbb{R}$ with respect to a Wiener process $\{W_t\}_{t>0}$ can be defined. The definitions and theorems in this section are adapted from Mao (2007) unless otherwise stated.

Let $(\Omega, \mathcal{F}, \{\mathcal{F}_t\}_{t\geq0}, P)$ be a filtered probability space and let $\{W_t\}_{t\geq0}$ be a one-dimensional Wiener process defined on the probability space satisfying the following conditions:

(i)   For each t, W_t is $\mathcal{F}_t$-measurable;
(ii)   For any $s \leq t$, the increment $W_t - W_s$ is independent of $\mathcal{F}_s$.

Note that we can always choose the natural filtration $\{\mathcal{F}_t^W\}_{t\geq0}$ as the filtration we are working with if the Wiener process $\{W_t\}_{t\geq0}$ has independent increments. Then $\{W_t\}_{t\geq0}$ is a Wiener process with respect to $\{\mathcal{F}_t^W\}_{t\geq0}$ that satisfies the two assumptions above (Karatzas & Shreve, 1991).

Definition 5.28. *Let* $0 \leq a < b < \infty$. *Denote by* $\mathcal{M}^2([a,b]; \mathbb{R})$ *the space of all real-valued measurable* $\{\mathcal{F}_t\}$-*adapted processes* $X = \{X_t\}_{a\leq t\leq b}$ *such that*

$$\|X\|_{a,b} := \left(E \int_a^b X_t^2 dt \right)^{1/2} < \infty. \tag{5.50}$$

Two processes X *and* $\bar{X}$ *in* $\mathcal{M}^2([a,b]; \mathbb{R})$ *are called equivalent and we write* $X = \bar{X}$ *if* $\|X - \bar{X}\|_{a,b} = 0$.

For a stochastic process $X \in \mathcal{M}^2([a,b]; \mathbb{R})$ it is possible to define the Itô integral $\int_a^b X_t dW_t$. The idea is similar to the definition of the Lebesgue integral: First, we define the Itô Integral for a class of simple processes. Each $X \in \mathcal{M}^2([a,b]; \mathbb{R})$ can be approximated by a sequence X^n of such simple processes and the limit of $\int_a^b X_t^n dW_t$ is then defined as the Itô integral $\int_a^b X_t dW_t$.

Definition 5.29. *A real-valued stochastic process* $X = \{X_t\}_{a\leq t\leq b}$ *is called a simple process if there exists a partition* $a = t_0 < t_1 < \cdots < t_k = b$ *of* $[a,b]$, *and bounded random variables* ξ_i, $0 \leq i \leq k-1$, *such that* ξ_i *is* $\mathcal{F}_{t_i}$-*measurable and*

$$X_t = \sum_{i=0}^{k-1} \xi_i I_{[t_i, t_{i+1})}(t), \tag{5.51}$$

where $I_{[t_i, t_{i+1})}(t)$ *is the indicator function of the interval* $[t_i, t_{i+1})$. *Denote by* $\mathcal{M}_0([a,b]; \mathbb{R})$ *the family of all such processes.*

Definition 5.30. *For a simple process $X \in \mathcal{M}_0([a,b]; \mathbb{R})$ define*

$$\int_a^b X_t dW_t := \sum_{i=0}^{k-1} \xi_i (W_{t_{i+1}} - W_{t_i}). \tag{5.52}$$

This integral is called the stochastic integral *or the* Itô integral *of X with respect to the Wiener process* $\{W_t\}$.

The next lemma is crucial for the definition of the Itô integral. The lemma shows that the mapping associating a step process X with its stochastic integral preserves the norm, i.e., $\|\int_a^b X_t dW_t\|_2 = \|X\|_{a,b}$. Such mappings are called isometries (Vigirdas, 2011). We will use the lemma to proof the existence of the Itô integral.

Lemma 5.31 (The Itô isometry). *If $X \in \mathcal{M}_0([a,b]; \mathbb{R})$, then*

$$E\left[\int_a^b X_t dW_t\right] = 0, \tag{5.53}$$

$$E\left[\left(\int_a^b X_t dW_t\right)^2\right] = E\left[\int_a^b X_t^2 dt\right]. \tag{5.54}$$

Proof. The following proof is adapted from Mao (2007) and Lindström et al. (2015). By the linearity of the expectation,

$$E\left[\int_a^b X_t dW_t\right] = E\left[\sum_{i=0}^{k-1} \xi_i (W_{t_{i+1}} - W_{t_i})\right] = \sum_{i=0}^{k-1} E\left[\xi_i (W_{t_{i+1}} - W_{t_i})\right]. \tag{5.55}$$

Since ξ_i is $\mathcal{F}_{t_i}$-measurable and $W_{t_{i+1}} - W_{t_i}$ is independent of $\mathcal{F}_{t_i}$ by definition,

$$E\left[\xi_i (W_{t_{i+1}} - W_{t_i})\right] \overset{5.18.\,(a)}{=} E\left[E\left[\xi_i (W_{t_{i+1}} - W_{t_i}) | \mathcal{F}_{t_i}\right]\right] \tag{5.56}$$

$$\overset{5.18.\,(d)}{=} E\left[\xi_i E\left[W_{t_{i+1}} - W_{t_i} | \mathcal{F}_{t_i}\right]\right] \tag{5.57}$$

$$\overset{5.18.\,(c)}{=} E\left[\xi_i E\left[W_{t_{i+1}} - W_{t_i}\right]\right] \tag{5.58}$$

$$= 0, \tag{5.59}$$

where the last step follows since $E\left[W_{t_{i+1}} - W_{t_i}\right] = 0$ by definition. This proofs the first part (5.53) of the lemma. Next, I proof the second part (5.54) of the lemma. Again, by the linearity of the expectation,

$$E\left[\left(\int_a^b X_t dW_t\right)^2\right] = E\left[\left(\sum_{i=0}^{k-1} \xi_i (W_{t_{i+1}} - W_{t_i})\right)^2\right] \tag{5.60}$$

$$= E\left[\sum_{i,j=0}^{k-1} \xi_i \xi_j (W_{t_{i+1}} - W_{t_i})(W_{t_{j+1}} - W_{t_j})\right] \tag{5.61}$$

$$= \sum_{i,j=0}^{k-1} E[\xi_i \xi_j (W_{t_{i+1}} - W_{t_i})(W_{t_{j+1}} - W_{t_j})]. \tag{5.62}$$

For $i \neq j$, say $i < j$,

$$E[\xi_i \xi_j (W_{t_{i+1}} - W_{t_i})(W_{t_{j+1}} - W_{t_j})] \tag{5.63}$$

$$\overset{5.18.\,(a)}{=} E[E[\xi_i \xi_j (W_{t_{i+1}} - W_{t_i})(W_{t_{j+1}} - W_{t_j})|\mathcal{F}_{t_j}]]. \tag{5.64}$$

The random variable ξ_j is $\mathcal{F}_{t_j}$-measurable as well as ξ_i, $W_{t_{i+1}}$ and W_{t_i} since $\mathcal{F}_{t_i} \subset \mathcal{F}_{t_j}$ and $t_{i+1} \leq t_j$ for $i < j$. From this fact it follows that $\xi_i \xi_j (W_{t_{i+1}} - W_{t_i})$ is $\mathcal{F}_{t_j}$-measurable by theorem (5.3) and

$$E[E[\xi_i \xi_j (W_{t_{i+1}} - W_{t_i})(W_{t_{j+1}} - W_{t_j})|\mathcal{F}_{t_j}]] \tag{5.65}$$

$$\overset{5.18.\,(d)}{=} E[\xi_i \xi_j (W_{t_{i+1}} - W_{t_i}) E[W_{t_{j+1}} - W_{t_j}|\mathcal{F}_{t_j}]]. \tag{5.66}$$

Because $W_{t_{j+1}} - W_{t_j}$ is independent of $\mathcal{F}_{t_j}$, we have

$$E[\xi_i \xi_j (W_{t_{i+1}} - W_{t_i}) E[W_{t_{j+1}} - W_{t_j}|\mathcal{F}_{t_j}]] \tag{5.67}$$

$$\overset{5.18.\,(c)}{=} E[\xi_i \xi_j (W_{t_{i+1}} - W_{t_i}) E[W_{t_{j+1}} - W_{t_j}]] = 0, \tag{5.68}$$

since $E[W_{t_{j+1}} - W_{t_j}] = 0$ by definition.

On the other hand, for $i = j$ we have

$$E[\xi_i^2 (W_{t_{i+1}} - W_{t_i})^2] \overset{5.18.\,(a)}{=} E[E[\xi_i^2 (W_{t_{i+1}} - W_{t_i})^2|\mathcal{F}_{t_i}]] \tag{5.69}$$

$$\overset{5.18.\,(d)}{=} E[\xi_i^2 E[(W_{t_{i+1}} - W_{t_i})^2|\mathcal{F}_{t_i}]] \tag{5.70}$$

$$\overset{5.18.\,(c)}{=} E[\xi_i^2 E[(W_{t_{i+1}} - W_{t_i})^2]] \tag{5.71}$$

$$= E[\xi_i^2 (t_{i+1} - t_i)], \tag{5.72}$$

since $E[(W_{t_{i+1}} - W_{t_i})^2] = Var(W_{t_{i+1}} - W_{t_i}) + E[W_{t_{i+1}} - W_{t_i}]^2 = t_{i+1} - t_i$ by definition of the Wiener process.

Combining, we obtain

$$\sum_{i,j=0}^{k-1} E[\xi_i \xi_j (W_{t_{i+1}} - W_{t_i})(W_{t_{j+1}} - W_{t_j})] \tag{5.73}$$

$$= \sum_{i=0}^{k-1} E[\xi_i^2 (t_{i+1} - t_i)] \tag{5.74}$$

$$= E\left[\sum_{i=0}^{k-1} \xi_i^2 (t_{i+1} - t_i)\right] \tag{5.75}$$

$$= E\left[\int_a^b X_t^2 dt\right]. \tag{5.76}$$

$\square$

The next lemma shows that every $X \in \mathcal{M}^2([a,b];\mathbb{R})$ can be approximated in $\mathcal{M}^2([a,b];\mathbb{R})$ by a sequence of simple processes.

Lemma 5.32. *For any $X \in \mathcal{M}^2([a,b];\mathbb{R})$ there exists a sequence $\{X^n\}$ of simple processes such that*

$$\lim_{n\to\infty} E\left[\int_a^b (X_t^n - X_t)^2 \, dt\right] = 0. \tag{5.77}$$

Before I continue with the proof of this lemma I will briefly repeat two additional lemmas that are necessary for the proof. The first lemma is the Schwarz inequality (Abramowitz & Stegun, 1972) and the second is about the mean-square continuity of square-integrable functions (Vigirdas, 2011).

Lemma 5.33 (Schwarz's inequality). *Let $f, g : [a,b] \to \mathbb{R}$ be two square integrable functions. Then*

$$\left[\int_a^b f(x)g(x)dx\right]^2 \le \int_a^b [f(x)]^2 \, dx \int_a^b [f(x)]^2 \, dx \tag{5.78}$$

Lemma 5.34. *Let $f : [a,b] \to \mathbb{R}$ be a square integrable function. Then*

$$\int_a^b [f(t+h) - f(t)]^2 \, dt \to 0 \quad \text{as } h \to 0. \tag{5.79}$$

The following proof is adapted from Vigirdas (2011) and Mao (2007).

Proof of Lemma 1.27. The proof of this lemma will be divided into three steps: First, I show that every $X \in \mathcal{M}^2([a,b];\mathbb{R})$ can be approximated by a sequence of bounded processes which in turn can be approximated by a sequence of bounded, continuous processes. Finally, these bounded, continuous processes can then be approximated by a sequence of simple processes.

Step 1. For any $X \in \mathcal{M}^2([a,b];\mathbb{R})$, there exists a sequence $\{Y^n\}$ of bounded processes in $\mathcal{M}^2([a,b];\mathbb{R})$ such that

$$\lim_{n\to\infty} E\left[\int_a^b (Y_t^n - X_t)^2 \, dt\right] = 0. \tag{5.80}$$

Proof. For each n define

$$Y_t^n := \begin{cases} -n & \text{if } X_t < -n \\ X_t & \text{if } -n \le X_t \le n \\ n & \text{if } X_t > n. \end{cases} \tag{5.81}$$

Then $Y^n \in \mathcal{M}^2([a,b];\mathbb{R})$ and $|Y_t^n| \le n$ for each n. Since $Y_t^n = X_t$ when $|X_t| \le n$, one has $\lim_{n\to\infty} Y_t^n = X_t$, and thus $\lim_{n\to\infty} (Y_t^n - X_t)^2 = 0$. On the other hand, using the inequality $(a-b)^2 \le 2(a^2 + b^2)$ and $|Y_t^n| \le |X_t|$, one has

$$\int_a^b (Y_t^n - X_t)^2 dt \le 2 \int_a^b (Y_t^n)^2 + X_t^2 dt \le 4 \int_a^b X_t^2 dt. \tag{5.82}$$

Since $X \in \mathcal{M}^2([a, b]; \mathbb{R})$,

$$E\left[\int_a^b X_t^2 dt\right] < \infty. \tag{5.83}$$

So (5.80) follows by the dominated convergence theorem (5.6). □

Step 2. Let $Y \in \mathcal{M}^2([a, b]; \mathbb{R})$ be bounded. Then there exists a sequence $\{Z^n\}$ of bounded continuous processes in $\mathcal{M}^2([a, b]; \mathbb{R})$ such that

$$\lim_{n \to \infty} E\left[\int_a^b (Z_t^n - Y_t)^2 dt\right] = 0. \tag{5.84}$$

Proof. Assume $|Y_t| \le C$ for all $t \in [a, b]$. For each n define

$$Z_t^n := n \int_{t-1/n}^t Y_s ds \tag{5.85}$$

with the convention that $Y_s = 0$ for $s < 0$. Then the processes Z^n are adapted since Z_t^n depends only on the values of the adapted process Y until the time t. Since $|Y_t| \le C$, one has $|Z_t^n| \le n(1/n)C = C$, implying that Z_t^n is bounded. Moreover,

$$|Z_{t'}^n - Z_t^n| = \left| n \int_{t'-1/n}^{t'} Y_s ds - n \int_{t-1/n}^t Y_s ds \right| \tag{5.86}$$

$$\le n \left(\left| \int_{t'-1/n}^{t'} Y_s ds \right| + \left| \int_{t-1/n}^t Y_s ds \right| \right) \tag{5.87}$$

$$= n \left(\left| \int_{t'}^{t'-1/n} Y_s ds \right| + \left| \int_{t-1/n}^t Y_s ds \right| \right) \tag{5.88}$$

$$\le n \left(\int_{t'}^{t'-1/n} |Y_s| \, ds + \int_{t-1/n}^t |Y_s| \, ds \right) \tag{5.89}$$

$$\le nC(t' - \frac{1}{n} - t') + nC(t - t + \frac{1}{n}) \tag{5.90}$$

$$= nC(t - t') + nC(t' - t) \tag{5.91}$$

$$\le 2nC|t' - t|. \tag{5.92}$$

This estimate implies that Z_t^n is also continuous. It follows that

$$E\left[\int_a^b (Z_t^n - Y_t)^2\, dt\right] = \int_a^b E\left[(Z_t^n - Y_t)^2\right] dt \tag{5.93}$$

$$= \int_a^b E\left[\left(n\int_{t-1/n}^t Y_s ds - Y_t\right)^2\right] dt \tag{5.94}$$

$$= \int_a^b E\left[\left(n\int_{t-1/n}^t Y_s - Y_t ds\right)^2\right] dt \tag{5.95}$$

$$\text{(Schwarz's inequality)} \quad \leq \int_a^b E\left[n\int_{t-1/n}^t (Y_s - Y_t)^2 ds\right] dt \tag{5.96}$$

$$\text{(change of variables } s = t - \bar{s}) \quad = \int_a^b E\left[n\int_{1/n}^0 -(Y_{t-\bar{s}} - Y_t)^2 d\bar{s}\right] dt \tag{5.97}$$

$$= \int_a^b E\left[n\int_0^{1/n} (Y_{t-\bar{s}} - Y_t)^2 d\bar{s}\right] dt \tag{5.98}$$

$$= n\int_0^{1/n} E\left[\int_0^T (Y_{t-\bar{s}} - Y_t)^2 dt\right] d\bar{s}. \tag{5.99}$$

By the mean-square continuity (5.34),

$$\int_a^b (Y_{t-\bar{s}} - Y_t)^2 dt \to 0 \quad \text{as } \bar{s} \to 0. \tag{5.100}$$

Since $(Y_{t-\bar{s}} - Y_t)^2 \leq 4C^2$,

$$E\left[\int_a^b (Y_{t-\bar{s}} - Y_t)^2 dt\right] \to 0 \quad \text{as } \bar{s} \to 0 \tag{5.101}$$

by the dominated convergence theorem (5.6). Therefore, for every $\varepsilon > 0$, there is $n_0 \in \mathbb{N}$ such that

$$E\left[\int_a^b (Y_{t-\bar{s}} - Y_t)^2 dt\right] < \varepsilon \quad \text{for} \quad 0 < \bar{s} < 1/n_0, \tag{5.102}$$

and thus

$$E\left[\int_a^b (Z_t^n - Y_t)^2 dt\right] < n\int_0^{1/n} \varepsilon\, d\bar{s} = \varepsilon \quad \text{for } n > n_0 \tag{5.103}$$

which implies (5.84). $\qquad\square$

Step 3. If $Z \in \mathcal{M}^2([a,b];\mathbb{R})$ is bounded and continuous, then there exists a sequence $\{X^n\}$ of simple processes such that

$$\lim_{n\to\infty} E\left[\int_a^b (X_t^n - Z_t)^2 \, dt\right] = 0. \tag{5.104}$$

Proof. Assume $|Z_t| \le M$ for all $t \in [a,b]$. Let $\Pi^n = \{a = t_0^n < t_1^n < \ldots < t_{k_n}^n = b\}$, $n \in \mathbb{N}$, be a sequence of partitions of the interval $[a,b]$ such that $\max|t_{i+1}^n - t_i^n| \to 0$ as $n \to \infty$.

For each n define

$$X_t^n := Z_{t_i^n}, \quad t \in [t_i^n, t_{i+1}^n). \tag{5.105}$$

This process is simple and adapted to $\mathcal{F}_t$. Since Z is continuous, $|X_t^n - Z_t|^2 \to 0$ as $n \to \infty$. On the other hand, since $|Z_t| \le M$, one has $|X_t^n| \le M$. Therefore,

$$|X_t^n - Z_t|^2 \le 2[(X_t^n)^2 + Z_t^2] \le 4M^2, \quad t \in [a,b]. \tag{5.106}$$

Since

$$E\left[\int_a^b 4M^2\right] < \infty, \tag{5.107}$$

statement (5.104) follows by the dominated convergence theorem (5.6). $\qquad\square$

The conclusion of lemma (5.32) then follows from steps 1-3. $\qquad\square$

We can now use lemma (5.32) to define the Itô integral

$$\int_a^b X_t \, dW_t \tag{5.108}$$

for a process $X \in \mathcal{M}^2([a,b];\mathbb{R})$. By lemma (5.32) there exists a sequence $\{X^n\}$ of simple processes such that

$$\lim_{n\to\infty} E\left[\int_a^b (X_t^n - X_t)^2 dt\right] = 0. \tag{5.109}$$

The Itô integral is then defined as the limit

$$\int_a^b X_t \, dW_t := \lim_{n\to\infty} \int_a^b X_t^n \, dW_t \qquad \text{in } L^2(\Omega, \mathbb{R}). \tag{5.110}$$

To show the existence of this limit we use lemma (5.31) together with the inequality $(a+b)^2 \le 2(a^2 + b^2)$. Then one has that

$$E\left[\left(\int_a^b X_t^n \, dW_t - \int_a^b X_t^m \, dW_t\right)^2\right] = E\left[\left(\int_a^b X_t^n - X_t^m \, dW_t\right)^2\right] \tag{5.111}$$

$$\stackrel{(5.31)}{=} E\left[\int_a^b (X_t^n - X_t^m)^2 \, dt\right] = E\left[\int_a^b ((X_t^n - X_t) + (X_t - X_t^m))^2 \, dt\right] \tag{5.112}$$

$$\le 2E\left[\int_a^b (X_t^n - X_t)^2 dt\right] + 2E\left[\int_a^b (X_t^m - X_t)^2 dt\right] \to 0, \quad \text{as } n, m \to \infty. \tag{5.113}$$

This means that $\{\int_a^b X_t^n\, dW_t\}$ is a Cauchy sequence in $L^2(\Omega, \mathbb{R})$. Since $L^2(\Omega, \mathbb{R})$ is complete, the Cauchy sequence converges. Therefore the limit exists. This leads to the following definition.

Definition 5.35 (Itô integral). *Let $X \in \mathcal{M}^2([a, b]; \mathbb{R})$. The* Itô integral *of X with respect to $\{W_t\}$ is defined by*

$$\int_a^b X_t\, dW_t = \lim_{n \to \infty} \int_a^b X_t^n\, dW_t \quad \text{in } L^2(\Omega, \mathbb{R}), \tag{5.114}$$

where $\{X^n\}$ is a sequence of simple processes such that

$$\lim_{n \to \infty} E\left[\int_a^b (X_t^n - X_t)^2 dt\right] = 0. \tag{5.115}$$

The above definition does not depend on the choice of the particular sequence $\{X^n\}$. Let $\{\tilde{X}^n\}$ be another sequence of simple processes converging to X in the sense that

$$\lim_{n \to \infty} E\left[\int_a^b (\tilde{X}_t^n - X_t)^2 dt\right] = 0. \tag{5.116}$$

Define the new sequence $\{Y^n\}$, where $Y^{2n-1} = X^n$ and $Y^{2n} = \tilde{X}^n$. Then $\{Y^n\}$ is also convergent to X in the same sense and the sequence of integrals $\{\int_a^b Y_t^n\, dW_t\}$ is convergent in $L^2(\Omega, \mathbb{R})$ as shown before. This means that its subsequences $\{\int_a^b X_t^n\, dW_t\}$ and $\{\int_a^b \tilde{X}_t^n\, dW_t\}$ have the same limit.

The space $\mathcal{M}^2([a, b]; \mathbb{R})$ is still quite restrictive and for various applications we need to extend the Itô integral to a larger class of integrands. In the following section I will explain how the integral can be extended to random processes X for which

$$\int_0^T X_t^2 dt < \infty \qquad \text{a.s. for every } T > 0. \tag{5.117}$$

Furthermore we will extend the Itô integral to the multi-dimensional case. This will be necessary to study multidimensional stochastic differential equations. The following definitions and theorems as well as their proofs can be found in Mao (2007) unless otherwise stated.

Definition 5.36. *Let $X \in \mathcal{M}^2([0, T]; \mathbb{R})$. Define*

$$I(t) := \int_0^t X_s\, dW_s \qquad \text{for } 0 \le t \le T, \tag{5.118}$$

where, by definition, $I(0) = \int_0^0 X_s\, dW_s = 0$. We call $I(t)$ the indefinite Itô integral *of X.*

The next theorem states that for stochastic processes $X \in \mathcal{M}^2([0,T];\mathbb{R})$ the indefinite Itô integral can be chosen to depend continuously on t.

Theorem 5.37. *If $X \in \mathcal{M}^2([0,T];\mathbb{R})$, then the indefinite integral $\{I(t)\}_{0 \leq t \leq T}$ has a continuous version, i.e., there exists a continuous stochastic process J_t on $(\Omega, \mathcal{F}, P)$ such that*

$$P(J(t) = I(t)) = 1 \qquad \text{for all } \ 0 \leq t \leq T. \tag{5.119}$$

From now on we assume that $\int_0^t X_s \, dW_s$ means a continuous version of the integral.

Definition 5.38. *Let $(\Omega, \mathcal{F}, \{\mathcal{F}_t\}_{t \geq 0}, P)$ be a filtered probability space. Define $\mathcal{F}_\infty := \sigma\left(\bigcup_{t \geq 0} \mathcal{F}_t\right)$. A random variable $\tau : \Omega \to [0, \infty]$ (it may take the value ∞) is called an $\{\bar{F}_t\}$-stopping time (or simply stopping time) if $\{\omega \in \Omega : \tau(\omega) \leq t\} \in \mathcal{F}_t$ for any $t \geq 0$.*

A stopping time is a specific type of random variable. One can interpret the stopping time as the waiting time that goes by until some random event happens. The filtration $\{\mathcal{F}_t\}_{t \geq 0}$ keeps track of what information is available at each of the times $t \geq 0$, i.e., which events might be observed at time t. So the condition $\{\omega \in \Omega : \tau(\omega) \leq t\} \in \mathcal{F}_t$ for any $t \geq 0$ in the above definition means that, for τ to be a stopping time, it should be possible to decide whether this event has already occurred or not by time t.

Definition 5.39. *If τ and ρ are two stopping times with $\tau \leq \rho$ a.s., we define*

$$[[\tau, \rho[[:= \{(t, \omega) \in \mathbb{R}_+ \times \Omega : \tau(\omega) \leq t < \rho(\omega)\} \tag{5.120}$$

and call it a stochastic interval*. Similarly, we can define stochastic intervals $[[\tau, \rho]]$, $]]\tau, \rho]]$ and $]]\tau, \rho[[$.*

Definition 5.40. *Let $X \in \mathcal{M}^2([0,T];\mathbb{R})$ and let τ be a stopping time such that $0 \leq \tau \leq T$. Then $\{I_{[[0,\tau]]}(t)X_t\}_{0 \leq t \leq T} \in \mathcal{M}^2([0,T];\mathbb{R})$ and we define*

$$\int_0^\tau X_s \, dW_s := \int_0^T I_{[[0,\tau]]}(s) X_s \, dW_s. \tag{5.121}$$

Furthemore, if ρ is another stopping time with $0 \leq \rho \leq \tau$, we define

$$\int_\rho^\tau X_s \, dW_s := \int_0^\tau X_s \, dW_s - \int_0^\rho X_s \, dW_s. \tag{5.122}$$

The following two definitions extend the Itô integral to the multi-dimensional case. Here and in the remainder of this section I use superscripts to index the components of vectors.

Definition 5.41. *Let $\{W_t\}_{t \geq 0}$ be an m-dimensional Wiener Process adapted to the filtration $\{\mathcal{F}_t\}_{t \geq 0}$. That is, $W_t = (W_t^1, \ldots, W_t^m)^T$ where the W^j for $j = 1, \ldots, m$ are one-dimensional pairwise independent Wiener processes adapted to the filtration $\{\mathcal{F}_t\}_{t \geq 0}$.*

Denote by $\mathcal{M}^2([0,T];\mathbb{R}^{d \times m})$ the family of all $d \times m$-matrix valued measurable $\{\mathcal{F}_t\}$-adapted processes $X = \{(X_t^{ij})_{d \times m}\}_{0 \leq t \leq T}$ such that

$$E\left[\int_0^T \|X_s\|^2 \, dt\right] < \infty. \tag{5.123}$$

Here, $\|A\|$ denotes the trace norm of a matrix A, i.e., $\|A\| = \sqrt{\operatorname{trace}(A^T A)}$.

Definition 5.42. *Let $X \in \mathcal{M}^2([0,T]; \mathbb{R}^{d \times m})$. We define the multi-dimensional indefinite Itô integral*

$$\int_0^t X_s \, dW_s = \int_0^t \begin{pmatrix} X_s^{11} & \cdots & X_s^{1m} \\ \vdots & & \vdots \\ X_s^{d1} & \cdots & X_s^{dm} \end{pmatrix} \begin{pmatrix} dW_s^1 \\ \vdots \\ dW_s^m \end{pmatrix} \tag{5.124}$$

to be the d-column-vector-valued process whose i'th component is the following sum of one-dimensional Itô integrals

$$\sum_{j=1}^m \int_0^t X_s^{ij} dW_s^j. \tag{5.125}$$

Next, we extend the Itô integral to a larger class of integrands.

Definition 5.43. *Let $0 \le a < b < \infty$.*
(i) *Denote by $\mathcal{L}^2([a,b]; \mathbb{R}^{d \times m})$ the family of all $d \times m$-matrix valued measurable $\{\mathcal{F}_t\}$-adapted processes $X = \{(X_t^{ij})_{d \times m}\}_{a \le t \le b}$ such that*

$$\int_a^b \|X_t\|^2 \, dt < \infty \qquad a.s. \tag{5.126}$$

(ii) *Let $\mathcal{L}^2(\mathbb{R}_+; \mathbb{R}^{d \times m})$ denote the family of all $d \times m$-matrix-valued measurable $\{\mathcal{F}_t\}$-adapted processes $X = \{(X_t^{ij})_{d \times m}\}_{t \ge 0}$ such that $X \in \mathcal{L}^2([0,T]; \mathbb{R}^{d \times m})$ for every $T > 0$.*
(iii) *Let $\mathcal{M}^2(\mathbb{R}_+; \mathbb{R}^{d \times m})$ denote the family of all processes $X \in \mathcal{L}^2(\mathbb{R}_+; \mathbb{R}^{d \times m})$ such that*

$$E\left[\int_0^T \|X_t\|^2 \, dt\right] < \infty \qquad \text{for every } T > 0. \tag{5.127}$$

We want to define the Itô integral for all processes in $\mathcal{L}^2(\mathbb{R}_+; \mathbb{R}^{d \times m})$. Clearly, if $X \in \mathcal{M}^2(\mathbb{R}_+; \mathbb{R}^{d \times m})$, then $\{X_t\}_{0 \le t \le T} \in \mathcal{M}^2([0,T]; \mathbb{R}^{d \times m})$ for every $T > 0$. This means that the indefinite integral $\int_0^t X_s \, dW_s, t > 0$, is well defined for $X \in \mathcal{M}^2(\mathbb{R}_+; \mathbb{R}^{d \times m})$.

Let $X \in \mathcal{L}^2(\mathbb{R}_+; \mathbb{R}^{d \times m})$. For every integer $n \ge 1$ define the stopping time

$$\tau_n := n \wedge \inf\{t \ge 0 : \int_0^t \|X_s\|^2 \, ds \ge n\} \tag{5.128}$$

where $a \wedge b$ denotes the minimum of a and b. Then $\{X_t I_{[[0,\tau_n]]}(t)\}_{t \ge 0} \in \mathcal{M}^2(\mathbb{R}_+; \mathbb{R}^{d \times m})$. So the indefinite integral

$$I_n(t) = \int_0^t X_s I_{[[0,\tau_n]]}(s) \, dW_s, \qquad t \ge 0 \tag{5.129}$$

is well defined. Moreover, for $1 \le n \le m$ and $t \ge 0$ we have

$$I_m(t \wedge \tau_n) = \int_0^{t \wedge \tau_n} X_s I_{[[0,\tau_m]]}(s) \, dW_s \tag{5.130}$$

$$= \int_0^t X_s I_{[[0,\tau_m]]}(s) I_{[[0,\tau_n]]}(s) \, dW_s \tag{5.131}$$

$$= \int_0^t X_s I_{[[0,\tau_n]]}(s) \, dW_s = I_n(t). \tag{5.132}$$

This implies

$$I_m(t) = I_n(t), \qquad 0 \le t \le \tau_n. \tag{5.133}$$

So we can define the indefinite Itô integral of $X \in \mathcal{L}^2(\mathbb{R}_+; \mathbb{R}^{d \times m})$ as

$$I(t) := I_n(t) \qquad \text{on } 0 \le t \le \tau_n. \tag{5.134}$$

Definition 5.44. *Let $X = \{X_t\}_{t \ge 0} \in \mathcal{L}^2(\mathbb{R}_+; \mathbb{R}^{d \times m})$. The indefinite Itô integral of X with respect to $\{W_t\}$ is the $\mathbb{R}^d$-valued process $\{I(t)\}_{t \ge 0}$ defined by (5.134).*

5.5   Itô's Formula

In the previous section I explained the basic definition and extension of the Itô integral. However, for explicit calculations this definition of the integral can be very arduous. The situation is similar for ordinary Riemann or Lebesgue integrals where one usually uses the fundamental theorem of calculus and the chain rule for actual computations.

The Itô formula, named after Kiyoshi Itô (Itô, 1951), is an identity that serves as the stochastic calculus counterpart of the chain rule. The formula is very useful for evaluating Itô integrals and plays a key role in the derivation of numerical schemes for the approximate solution of stochastic differential equations.

In this section I will show the one-dimensional Itô formula and its generalization to the multi-dimensional case (Mao, 2007). Let $(\Omega, \mathcal{F}, \{\mathcal{F}_t\}_{t \ge 0}, P)$ be a filtered probability space and let $\{W_t\}_{t \ge 0}$ be a one-dimensional Brownian motion adapted to the filtration $\{\mathcal{F}_t\}_{t \ge 0}$.

Definition 5.45. *Let $0 \le a < b < \infty$.*
(i)   *Denote by $\mathcal{L}^1([a,b]; \mathbb{R}^d)$ the family of all $\mathbb{R}^d$-valued measurable $\mathcal{F}_t$-adapted processes $X = \{X_t\}_{a \le t \le b}$ such that*

$$\int_a^b |X_t| dt < \infty \qquad a.s. \tag{5.135}$$

   Here, $|v|$ denotes the Euclidean norm of a vector v.
(ii)   *Let $\mathcal{L}^1(\mathbb{R}_+; \mathbb{R}^d)$ denote   the   family   of   all $\mathbb{R}^d$-valued   measurable $\mathcal{F}_t$-adapted processes $X = \{X_t\}_{t \ge 0}$ such that $X \in \mathcal{L}^1([0,T]; \mathbb{R}^d)$ for every $T > 0$.*

Definition 5.46. *A* one-dimensional Itô process *is a continuous adapted process X_t on $t \ge 0$ of the form*

$$X_t = X_0 + \int_0^t f_s \, ds + \int_0^t g_s \, dW_s, \tag{5.136}$$

where $f \in \mathcal{L}^1(\mathbb{R}_+; \mathbb{R})$ and $g \in \mathcal{L}^2(\mathbb{R}_+; \mathbb{R})$.

The first integral in Eq. (5.136) is an ordinary Riemann integral and the second is an Itô integral. Equation (5.136) is often written in the shorter differential form

$$dX_t = f_t dt + g_t dW_t. \tag{5.137}$$

This is just an abbreviated notation for Eq. (5.136) and we say that X_t has stochastic differential given by (5.137).

Denote by $C^{1,2}(\mathbb{R}_+ \times \mathbb{R}^n; \mathbb{R})$ the family of all real-valued functions $V(t,x)$ defined on $\mathbb{R}_+ \times \mathbb{R}^n$ such that they are continuously twice differentiable in x and once in t. For $V \in C^{1,2}(\mathbb{R}_+ \times \mathbb{R}^n; \mathbb{R})$ we define

$$V_t := \frac{\partial V}{\partial t}, \quad V_x := \left(\frac{\partial V}{\partial x_1}, \cdots, \frac{\partial V}{\partial x_n} \right),$$

$$V_{xx} := \left(\frac{\partial^2 V}{\partial x_i \partial x_j} \right)_{n \times n} = \begin{pmatrix} \frac{\partial^2 V}{\partial x_1 \partial x_1} & \cdots & \frac{\partial^2 V}{\partial x_1 \partial x_d} \\ \vdots & & \vdots \\ \frac{\partial^2 V}{\partial x_d \partial x_1} & \cdots & \frac{\partial^2 V}{\partial x_d \partial x_d} \end{pmatrix}.$$

Theorem 5.47 (The one-dimensional Itô formula). *Let X_t be an Itô process on $t \geq 0$ with the stochastic differential*

$$dX_t = f_t dt + g_t dW_t, \tag{5.138}$$

where $f \in \mathcal{L}^1(\mathbb{R}_+; \mathbb{R})$ and $g \in \mathcal{L}^2(\mathbb{R}_+; \mathbb{R})$. Let $V \in C^{1,2}(\mathbb{R}_+ \times \mathbb{R}; \mathbb{R})$. Then $V(t, X_t)$ is again an Itô process with the stochastic differential given by

$$dV(t, X_t) = \left[V_t(t, X_t) + V_x(t, X_t) f_t + \frac{1}{2} V_{xx}(t, X_t) g_t^2 \right] dt \tag{5.139}$$
$$+ V_x(t, X_t) g_t dW_t \quad \text{a.s.}$$

A proof of the theorem can be found, e.g., in Mao (2007). The following definition and theorem extend the one-dimensional Itô formula to the multi-dimensional case.

Definition 5.48. *Let $\{W_t\}_{t \geq 0}$ be an m-dimensional Wiener process adapted to the filtration $\{\mathcal{F}_t\}_{t \geq 0}$. A d-dimensional Itô process is an $\mathbb{R}^d$-valued continuous adapted process $X_t = (X_t^1, \ldots, X_t^d)^T$ on $t \geq 0$ of the form*

$$X_t = X_0 + \int_0^t f_s \, ds + \int_0^t g_s \, dW_s \tag{5.140}$$

where $f = (f^1, \ldots, f^d)^T \in \mathcal{L}^1(\mathbb{R}_+; \mathbb{R}^d)$ and $g = (g_{ij})_{d \times m} \in \mathcal{L}^2(\mathbb{R}_+; \mathbb{R}^{d \times m})$. We say that X_t has stochastic differential given by

$$dX_t = f_t dt + g_t dW_t. \tag{5.141}$$

This means that

$$dX_t^i = f_t^i dt + \sum_{j=1}^m g_t^{ij} dW_t^j \qquad \text{for } i = 1, \ldots, d. \tag{5.142}$$

Theorem 5.49 (The multi-dimensional Itô formula). *Let X_t be a d-dimensional Itô process on $t \geq 0$ with the stochastic differential*

$$dX_t = f_t dt + g_t dW_t, \tag{5.143}$$

where $f \in \mathcal{L}^1(\mathbb{R}_+; \mathbb{R}^d)$ and $g \in \mathcal{L}^2(\mathbb{R}_+; \mathbb{R}^{d \times m})$. Let $V \in C^{1,2}(\mathbb{R}_+ \times \mathbb{R}^d; \mathbb{R})$. Then $V(t, X_t)$ is again an Itô process with the stochastic differential given by

$$dV(t, X_t) = \left[V_t(t, X_t) + V_x(t, X_t) f_t + \frac{1}{2} \text{trace} \left(g_t^T V_{xx}(t, X_t) g_t \right) \right] dt \tag{5.144}$$
$$+ V_x(t, X_t) g_t dW_t \quad \text{a.s.}$$

The following example illustrates the use of Itô's formula for evaluating Itô integrals.

Example 5.50. Let $\{W_t\}$ be a one-dimensional Wiener process. We want to compute the Itô integral

$$\int_0^t W_t \, dW_t. \tag{5.145}$$

Choose $V(t, x) = x^2$ and $X_t = W_t$, i.e., $f_t = 0$ and $g_t = 1$. Then by Itô's formula (5.47) we get

$$d(W_t^2) = dt + 2W_t dW_t. \tag{5.146}$$

That is,

$$W_t^2 = t + 2 \int_0^t W_t \, dW_t. \tag{5.147}$$

This implies that

$$\int_0^t W_t \, dW_t = \frac{1}{2} W_t^2 - \frac{1}{2} t. \tag{5.148}$$

5.6 Stochastic Differential Equations

Let $(\Omega, \mathcal{F}, \{\mathcal{F}_t\}_{t \geq 0}, P)$ be a filtered probability space. Throughout this section let $\{W_t = (W_t^1, \ldots W_t^m)^T\}_{t \geq 0}$ be an m-dimensional Wiener process defined on the space. Let t_0 and T be two nonnegative real numbers such that $0 \leq t_0 < T < \infty$. Let X_0 be an $\mathcal{F}_{t_0}$-measurable $\mathbb{R}^d$-valued random variable such that $E\left[|X_0|^2\right] < \infty$. Let $f : [t_0, T] \times \mathbb{R}^d \to \mathbb{R}^d$ and $g : [t_0, T] \times \mathbb{R}^d \to \mathbb{R}^{d \times m}$ be two measurable functions.

A *d-dimensional stochastic differential equation of Itô type* is an equation of the form

$$dX_t = f(t, X_t)dt + g(t, X_t)dW_t \qquad \text{on } t_0 \leq t \leq T \tag{5.149}$$

with initial value $X_{t_0} = X_0$.

As in the previous section Eq. (5.149) is equivalent to the integral equation

$$X_t = X_0 + \int_{t_0}^t f(s, X_s)ds + \int_{t_0}^t g(s, X_s)dW_s \qquad \text{on } t_0 \leq t \leq T \tag{5.150}$$

with components

$$X_t^i = X_0^i + \int_{t_0}^t f^i(s, X_s)ds + \sum_{j=1}^m \int_{t_0}^t g^{ij}(s, X_s)dW_s^j, \qquad i = 1, \ldots, d. \tag{5.151}$$

The function f in Eq. (5.149) is referred to as the *drift coefficient* and g is called the *diffusion coefficient*. If the drift and diffusion coefficients do not depend on the variable t, that is, if $f(t, x) \equiv f(x)$ and $g(t, x) \equiv g(x)$, then we say that the stochastic equation is *autonomous*.

A solution $\{X_t\}_{t_0 \leq t \leq T}$ of (5.149) must have properties which ensure that the integrals are well defined. The following definition (Mao, 2007) states what we understand by a solution of Eq. (5.149).

Definition 5.51. *An $\mathbb{R}^d$-valued stochastic process $\{X_t\}_{t_0 \leq t \leq T}$ is called a* solution *of Eq. (5.149) if it has the following properties:*

(i)   *$\{X_t\}_{t_0 \leq t \leq T}$ is continuous and $\mathcal{F}_t$-adapted,*

(ii)   *$\{f(t, X_t)\}_{t_0 \leq t \leq T} \in \mathcal{L}^1([t_0, T]; \mathbb{R}^d)$ and*
        $\{g(t, X_t)\}_{t_0 \leq t \leq T} \in \mathcal{L}^2([t_0, T]; \mathbb{R}^{d \times m})$,

(iii)   *Eq. (5.149) holds for every $t \in [t_0, T]$ with probability 1.*

A solution $\{X_t\}_{t_0 \leq t \leq T}$ is said to be unique *if any other solution $\{\bar{X}_t\}_{t_0 \leq t \leq T}$ is indistinguishable from $\{X_t\}_{t_0 \leq t \leq T}$, that is,*

$$P\left(X_t = \bar{X}_t \text{ for all } t_0 \leq t \leq T\right) = 1. \tag{5.152}$$

Example 5.52. In financial mathematics stochastic processes are used to model the evolution of stock prices. Consider a stock whose price at time t is X_t. Assume a constant appreciation rate $\mu \in \mathbb{R}$ and suppose that the price fluctuations of the stock are proportional to the current price of the stock. Then the evolution of the stock price process is assumed to be described by the linear differential equation (Musiela & Rutkowski, 2005)

$$dX_t = \mu X_t dt + \sigma X_t dW_t, \qquad \text{on } t_0 \leq t \leq T, \ X_{t_0} = X_0, \tag{5.153}$$

where $X_0 \in \mathbb{R}_+$ is the initial stock price, W_t is a one-dimensional Wiener process and $\sigma > 0$ is a constant volatility coefficient.

Using Itô's formula one can show that the solution to this stochastic differential equations is given by

$$X_t = X_0 \exp(\sigma W_t + (\mu - \frac{1}{2}\sigma^2)t), \qquad t_0 \leq t \leq T. \tag{5.154}$$

As with ordinary differential equations, the first question which arises is that of the existence and uniqueness of solutions to Eq. (5.149). We generally cannot find explicit formulas like (5.154) for the solutions of stochastic differential equations and need to use numerical methods to determine the solutions approximately. This is why we need to know if the equation actually does have a solution for a given initial value and if this solution is unique.

For an ordinary differential equation

$$\frac{dx}{dt}(t) = f(t, x), \quad x(t_0) = x_0, \tag{5.155}$$

a sufficient condition (Adkins & Davidson, 2012) for the existence and uniqueness of a solution is that the function $f = f(t, x)$ is continuous and satisfies the Lipschitz condition

$$|f(t, x) - f(t, y)| \leq K|x - y| \tag{5.156}$$

for some constant $K > 0$ and for all $(t, x), (t, y)$ in $\mathcal{S} := \{(t, x) : a \leq t \leq b, -\infty < y < \infty\}$. If (t_0, x_0) is an interior point of $\mathcal{S}$, then there exists a unique solution to Eq. (5.155) on the interval $[a, b]$.

A similar result exists for stochastic differential equations (Kuo, 2006).

Theorem 5.53. *Assume that there exists a constant $K > 0$ such that for all $x, y \in \mathbb{R}^d$ and $t \in [t_0, T]$*
(i)   (Lipschitz condition)

$$|f(t, x) - f(t, y)|^2 \leq K |x - y|^2, \quad \|g(t, x) - g(t, y)\|^2 \leq K |x - y|^2, \quad (5.157)$$

(ii)   (Linear growth condition)

$$|f(t, x)|^2 \leq K(1 + |x|^2), \quad \|g(t, x)\|^2 \leq K(1 + |x|^2). \quad (5.158)$$

Then there exists a unique solution to Eq. (5.149).

5.7   The Stratonovich Integral

The *Stratonovich integral* is an alternative definition of a stochastic integral introduced by the Russian physicist R. L. Stratonovich in 1966 (Stratonovich, 1966). Since the Stratonovich integral is often used in numerical methods for stochastic differential equations I will briefly explain its construction and difference from the Itô integral in the remainder of this chapter.

As shown in Kloeden & Platen (1995), the Itô integral $\int_0^T X_t \, dW_t$ of a stochastic process $X \in \mathcal{M}^2([a, b]; \mathbb{R})$ as defined in (5.35) is equal to the L^2-limit of the sums

$$S_n = \sum_{j=1}^n X_{\xi_j^{(n)}} \left(W_{t_{j+1}^{(n)}} - W_{t_j^{(n)}} \right), \quad (5.159)$$

with evaluation points $\xi_j^{(n)} = t_j^{(n)}$ for partitions $0 = t_1^{(n)} < t_2^{(n)} < \ldots < t_{n+1}^{(n)} = T$ of the interval $[0, T]$ such that

$$\delta^{(n)} = \max_{1 \leq j \leq n} \left(t_{j+1}^{(n)} - t_j^{(n)} \right) \to 0 \quad \text{as} \quad n \to \infty. \quad (5.160)$$

The Stratonovich integral is now defined by choosing the midpoint

$$\tau_j^{(n)} = \frac{1}{2}(t_j^{(n)} + t_{j+1}^{(n)}) \quad (5.161)$$

of each partition subinterval $[t_j^{(n)}, t_{j+1}^{(n)}]$ as the evaluation point in the sum (5.159) instead of the lower endpoint $t_j^{(n)}$ (Cyganowski et al., 2002).

Definition 5.54 (Stratonovich Integral). *Let $X \in \mathcal{M}^2([a, b]; \mathbb{R})$. The* Stratonovich integral *of X with respect to $\{W_t\}$ is defined as the limit*

$$\int_0^T X_t \circ dW_t := \lim_{n \to \infty} \sum_{j=1}^n X_{\tau_j^{(n)}} \left(W_{t_{j+1}^{(n)}} - W_{t_j^{(n)}} \right) \quad \text{in } L^2, \quad (5.162)$$

where $\tau_j^{(n)}$ is chosen as in Eq. (5.161).

The symbol " $\circ$ " before the differential dW_t is used here to distinguish between the Stratonovich integral and the Itô integral. The Stratonovich integral can be extended to a larger class of integrands in the same way as the Itô integral.

If the Stratonovich integral is used in a stochastic differential equation instead of the Itô integral, the resulting equation is called a *Stratonovich stochastic differential equation*. Stratonovich and Itô stochastic differential equations with the same coefficients normally do not have the same solution. But, as shown in Kloeden & Platen (1995), if X_t is the solution of an Itô stochastic differential equation

$$X_t = X_{t_0} + \int_{t_0}^{t} a(s, X_s)ds + \int_{t_0}^{t} b(s, X_s)dW_s, \qquad (5.163)$$

then X_t satisfies the modified Stratonovich stochastic differential equation

$$X_t = X_{t_0} + \int_{t_0}^{t} \underline{a}(s, X_s)ds + \int_{t_0}^{t} b(s, X_s) \circ dW_s, \qquad (5.164)$$

with a modified drift coefficient

$$\underline{a}(t, x) = a(t, x) - \frac{1}{2}b(t, x)\frac{\partial b}{\partial x}(t, x). \qquad (5.165)$$

Depending on the particular context the Stratonovich integral can be more convenient to work with than the Itô integral sometimes. Nevertheless, it is possible to switch between the two integrals via relation (5.165).

This summary of the Stratonovich integral concludes the introduction to stochastic differential equations. In the next chapter I will present methods to solve such equations numerically.

Chapter 6

Numerical Methods for Stochastic Differential Equations

In this chapter I give an introduction to numerical methods for stochastic differential equations (SDE). Because most SDEs do not have explicit solutions, we need to use numerical methods to compute the solutions approximately. Since SDE models find application in many areas, the development of appropriate numerical schemes is still a very active research topic.

First, I present the stochastic Taylor expansion which allows the approximation of a stochastic process in a similar way to the Taylor series for ordinary functions. Then I show how numerical methods for SDEs can be derived from the Taylor expansions and present criteria concerning the accuracy of such methods. Finally, I present a Runge-Kutta type method for SDEs that I used for the numerical simulations of transition-edge sensors in Chapter 7.

6.1 Stochastic Taylor Expansions

In this section I describe the construction of stochastic Taylor expansions. The stochastic Taylor expansion is the stochastic calculus counterpart to the Taylor series for real-valued ordinary functions and is based on the iterated application of the Itô formula (5.47). Many numerical methods for the integration of SDEs are built from stochastic Taylor expansions.

The following derivation is adapted from Cyganowski et al. (2002). Let $(\Omega, \mathcal{F}, \{\mathcal{F}_t\}_{t \geq 0}, P)$ be a filtered probability space. Let X_t be the solution of the one-dimensional SDE in integral form

$$X_t = X_{t_0} + \int_{t_0}^t a(s, X_s)ds + \int_{t_0}^t b(s, X_s)dW_s \tag{6.1}$$

for $t \in [t_0, T]$, where $a : [t_0, T] \times \mathbb{R} \to \mathbb{R}$ and $b : [t_0, T] \times \mathbb{R} \to \mathbb{R}$ are two measurable real-valued functions such that $\{a(t, X_t)\}_{t_0 \leq t \leq T} \in \mathcal{L}^1([t_0, T]; \mathbb{R})$ and $\{b(t, X_t)\}_{t_0 \leq t \leq T} \in \mathcal{L}^2([t_0, T]; \mathbb{R})$. Let $f : \mathbb{R} \times \mathbb{R} \to \mathbb{R}$ be any twice continuously differentiable function. Then the Itô formula (5.47) for $V(t, x) = f(t, x)$ gives

$$f(t, X_t) = f(t_0, X_{t_0}) + \int_{t_0}^t L^0 f(s, X_s)ds + \int_{t_0}^t L^1 f(s, X_s)dW_s, \tag{6.2}$$

where we have introduced the operators

$$L^0 := \frac{\partial}{\partial t} + a\frac{\partial}{\partial x} + \frac{1}{2}b^2\frac{\partial^2}{\partial x^2} \tag{6.3}$$

$$L^1 := b\frac{\partial}{\partial x}. \tag{6.4}$$

We now apply Eq. (6.2) for different choices of f. For $f(t, x) \equiv x$ we have $L^0 f = a$ and $L^1 f = b$ and Eq. (6.2) recovers to the original SDE

$$X_t = X_{t_0} + \int_{t_0}^t a(s, X_s)ds + \int_{t_0}^t b(s, X_s)dW_s. \tag{6.5}$$

Choosing $f = a$ in Eq. (6.2) yields

$$a(t, X_t) = a(t_0, X_{t_0}) + \int_{t_0}^t L^0 a(s, X_s)ds + \int_{t_0}^t L^1 a(s, X_s)dW_s. \tag{6.6}$$

Similarly, if we choose $f = b$, then Eq. (6.2) becomes

$$b(t, X_t) = b(t_0, X_{t_0}) + \int_{t_0}^t L^0 b(s, X_s)ds + \int_{t_0}^t L^1 b(s, X_s)dW_s. \tag{6.7}$$

Substituting Eqs. (6.6) and (6.7) into Eq. (6.5) leads to

$$X_t = X_{t_0} + \int_{t_0}^t \left\{ a(t_0, X_{t_0}) + \int_{t_0}^s L^0 a(z, X_z)dz + \int_{t_0}^s L^1 a(z, X_z)dW_z \right\} ds \tag{6.8}$$

$$+ \int_{t_0}^t \left\{ b(t_0, X_{t_0}) + \int_{t_0}^s L^0 b(z, X_z)dz + \int_{t_0}^s L^1 b(z, X_z)dW_z \right\} dW_s.$$

Summarizing the four double integrals in Eq. (6.8) into one remainder expression R we obtain

$$X_t = X_{t_0} + a(t_0, X_{t_0}) \int_{t_0}^t ds + b(t_0, X_{t_0}) \int_{t_0}^t dW_s + R \tag{6.9}$$

with remainder

$$R = \int_{t_0}^t \int_{t_0}^s L^0 a(z, X_z)dz\, ds + \int_{t_0}^t \int_{t_0}^s L^1 a(z, X_z)dW_z\, ds \tag{6.10}$$

$$+ \int_{t_0}^t \int_{t_0}^s L^0 b(z, X_z)dz\, dW_s + \int_{t_0}^t \int_{t_0}^s L^1 b(z, X_z)dW_z\, dW_s.$$

Equation (6.9) is the simplest nontrivial Itô-Taylor expansion of X_t. One can continue this procedure to replace the integrands in the remainder (6.10) by using Eq. (6.2) with appropriately chosen functions f. For example, by applying Eq. (6.2) to $f = L^1 b$ in the last term of the remainder R we get

$$X_t = X_{t_0} + a(t_0, X_{t_0}) \int_{t_0}^t ds + b(t_0, X_{t_0}) \int_{t_0}^t dW_s \tag{6.11}$$

$$+ L^1 b(t_0, X_{t_0}) \int_{t_0}^t \int_{t_0}^s dW_z\, dW_s + \bar{R},$$

with remainder

$$\bar{R} = \int_{t_0}^{t} \int_{t_0}^{s} L^0 a(z, X_z) dz\, ds + \int_{t_0}^{t} \int_{t_0}^{s} L^1 a(z, X_z) dW_z\, ds \qquad (6.12)$$

$$+ \int_{t_0}^{t} \int_{t_0}^{s} L^0 b(z, X_z) dz\, dW_s + \int_{t_0}^{t} \int_{t_0}^{s} \int_{t_0}^{z} L^0 L^1 b(u, X_u) du\, dW_z\, dW_s$$

$$+ \int_{t_0}^{t} \int_{t_0}^{s} \int_{t_0}^{z} L^1 L^1 b(u, X_u) dW_u\, dW_z\, dW_s. \qquad (6.13)$$

By using this substitution repeatedly we obtain constant integrands in higher and higher order terms. This way we get an expansion for X_t that involves multiple Itô integrals multiplied by certain constants and a remainder R containing the next multiple Itô integrals with non-constant integrands. We can now use the stochastic Taylor expansion to design numerical methods for SDEs. By applying Taylor expansions of the form (6.9) or (6.11) over successive subintervals of the interval of integration $[t_0, T]$ while neglecting the remainder terms, we can gradually construct an approximation of the solution X_t of the SDE (6.1).

6.2 The Euler-Maruyama Method

The Euler-Maruyama method (Maruyama, 1955) is one of the simplest methods for the approximate numerical solution of SDEs. The method is obtained by truncating the stochastic Taylor expansion after the first order terms. As in the previous section let X_t be the solution of the SDE

$$dX_t = a(t, X_t)dt + b(t, X_t)dW_t \qquad (6.14)$$

on $t_0 \leq t \leq T$ with the initial value $X_{t_0} = X_0$.

Let $t_0 = \tau_0 < \tau_1 < \ldots < \tau_n < \ldots < \tau_N = T$ be a discretization of the time interval $[t_0, T]$. Then the Euler-Maruyama approximation is a continuous stochastic process $Y = \{Y_t\}_{t_0 \leq t \leq T}$ that satisfies the iterative scheme (Kloeden & Platen, 1995)

$$Y_0 = X_0, \qquad (6.15)$$
$$Y_{n+1} = Y_n + a(\tau_n, Y_n)\Delta_n + b(\tau_n, Y_n)\Delta W_n,$$

for $n = 0, 1, 2, \ldots, N - 1$, where $Y_n \coloneqq Y_{\tau_n}$ denotes the value of the approximation at the discretization time τ_n,

$$\Delta_n = \int_{\tau_n}^{\tau_{n+1}} dt = \tau_{n+1} - \tau_n \qquad (6.16)$$

is the length of the time discretization subinterval $[\tau_n, \tau_{n+1}]$ and

$$\Delta W_n = \int_{\tau_n}^{\tau_{n+1}} dW_t = W_{\tau_{n+1}} - W_{\tau_n}. \qquad (6.17)$$

When the diffusion coefficient is zero, i.e., $b \equiv 0$, the iterative scheme (6.15) is identical to the Euler scheme for ordinary differential equations.
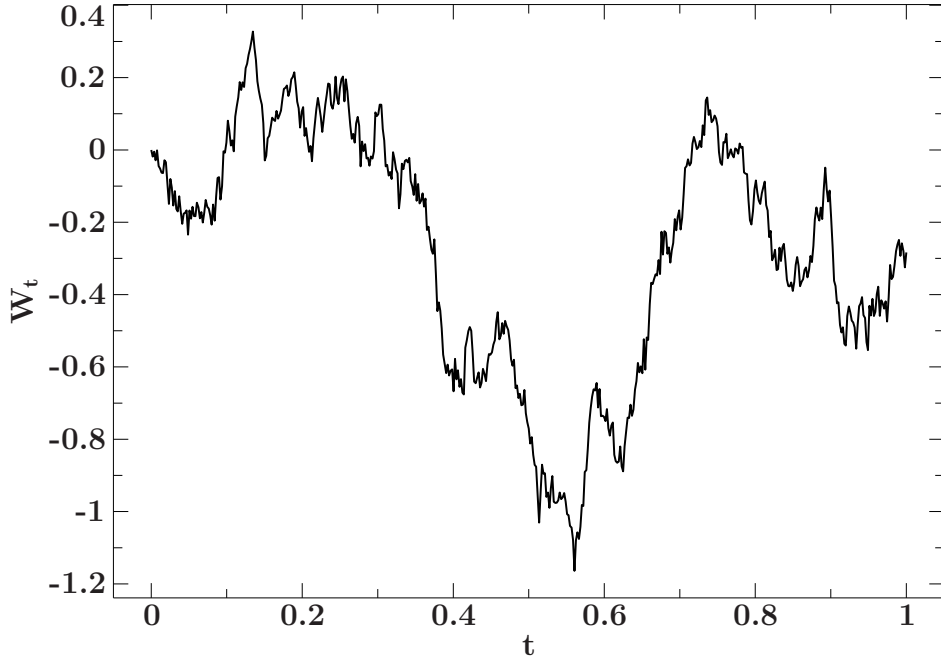
Fig. 6.1: Linearly interpolated sample path of a time discrete Wiener process over the time interval $[0, 1]$.

The Euler-Maruyama scheme (6.15) gives the values of the approximating process Y only at the discretization times τ_n. The values of Y at intermediate times can be computed by appropriate interpolation methods if required. For example, one can use linear interpolation, as suggested by Platen & Bruti-Liberati (2010), given by

$$Y_t = Y_{n_t} + \frac{t - \tau_{n_t}}{\tau_{n_t+1} - \tau_{n_t}}(Y_{n_t+1} - Y_{n_t}), \tag{6.18}$$

where

$$n_t = \max\{n = 0, 1, \ldots, N : \tau_n \leq t\}. \tag{6.19}$$

We can now compute the approximating sequence $\{Y_n, n = 0, 1, \ldots, N\}$ recursively, similar to numerical methods for ordinary differential equations. The only difference is that we need to generate the increments ΔW_n of the Wiener process W_t for each time step. From the definition of the Wiener process (5.22) we know that the process starts at zero and that the increments are independent and normally distributed with mean zero and variance Δ_n. In practice one can use a pseudo-random number generator to compute a sequence of independent random numbers with these properties numerically. For this thesis I use the function *gsl_ran_gaussian* of the GNU Scientific Library by Galassi et al. (2009). More details about the algorithm can be found in L'Ecuyer (1996). This way we can generate a time discrete sample path of a Wiener process recursively by

$$W_0 = 0, \tag{6.20}$$
$$W_{n+1} = W_n + \Delta W_n,$$

for $n = 0, 1, 2, \ldots, N - 1$, where $W_n := W_{\tau_n}$ denotes the value of the Wiener process at the discretization time τ_n and $\Delta W_n \sim N(0, \Delta_n)$. A linearly interpolated sample

path of a Wiener process that I generated with this method over the interval $[0, 1]$ at equidistant discretization times $\tau_n = n2^{-9}$ for $n = 0, 1, \ldots, 2^9$ is shown in Fig. 6.1.

Example 6.1. To illustrate the outcome of the Euler-Maruyama method I applied the scheme to the SDE from Example (5.52)

$$dX_t = \mu X_t dt + \sigma X_t dW_t, \tag{6.21}$$

for $t \in [0, T]$ with initial value $X_{t_0} = X_0 \in \mathbb{R}$. From Example (5.52) we know that the SDE (6.21) has the explicit solution

$$X_t = X_0 \exp(\sigma W_t + (\mu - \frac{1}{2}\sigma^2)t), \tag{6.22}$$

for $t \in [0, T]$ and the given Wiener process $W = \{W_t\}_{t \geq 0}$. This way we can compare the Euler approximation with the exact solution and also calculate the errors.

Applying the Euler-Maruyama scheme (6.15) to the SDE (6.21) yields the iterative scheme

$$Y_0 = X_0, \tag{6.23}$$
$$Y_{n+1} = Y_n + \mu Y_n \Delta_n + \sigma Y_n \Delta W_n,$$

for $n = 0, 1, 2, \ldots$, and $\Delta W_n \sim N(0, \Delta_n)$. The corresponding values of the exact solution for the same sample path of the Wiener process are given by

$$X_{\tau_n} = X_0 \exp(\sigma \sum_{i=1}^{n} \Delta W_{i-1} + (\mu - \frac{1}{2}\sigma^2)\tau_n). \tag{6.24}$$

I implemented the Euler-Maruyama method as a program in the S-Lang programming language, executed within the *Interactive Spectral Interpretation System* (ISIS) (Houck & Denicola, 2000). The black lines in Fig. 6.2 show a linearly interpolated plot of the exact solution of SDE (6.21) for $X_0 = 1$, $\mu = 2$, and $\sigma = 1$, corresponding to the sample path of the Wiener process from Fig. 6.1. The red lines show the result of the Euler-Maruyama approximation for an equidistant step size of $\Delta_n = 2^{-4}$ and $\Delta_n = 2^{-6}$.

Example (6.1) clearly shows that the quality of the approximation Y improves for the smaller step size. If we repeat the simulation with smaller step sizes, we expect the approximation to be even closer to the exact solution X. It looks like some kind of convergence is taking place. A measure for the quality of the approximation used in the context of SDEs is the *absolute error* defined as (Kloeden et al., 1994)

$$\epsilon = E(|X_T - Y_T|). \tag{6.25}$$

That is, the absolute error is the expectation of the absolute value of the difference between the exact solution and the approximation at the end time T. There are now two types of convergence that are used to describe the accuracy of stochastic numerical schemes. The first is *strong convergence* and the second is *weak convergence* (Kloeden et al., 1994).
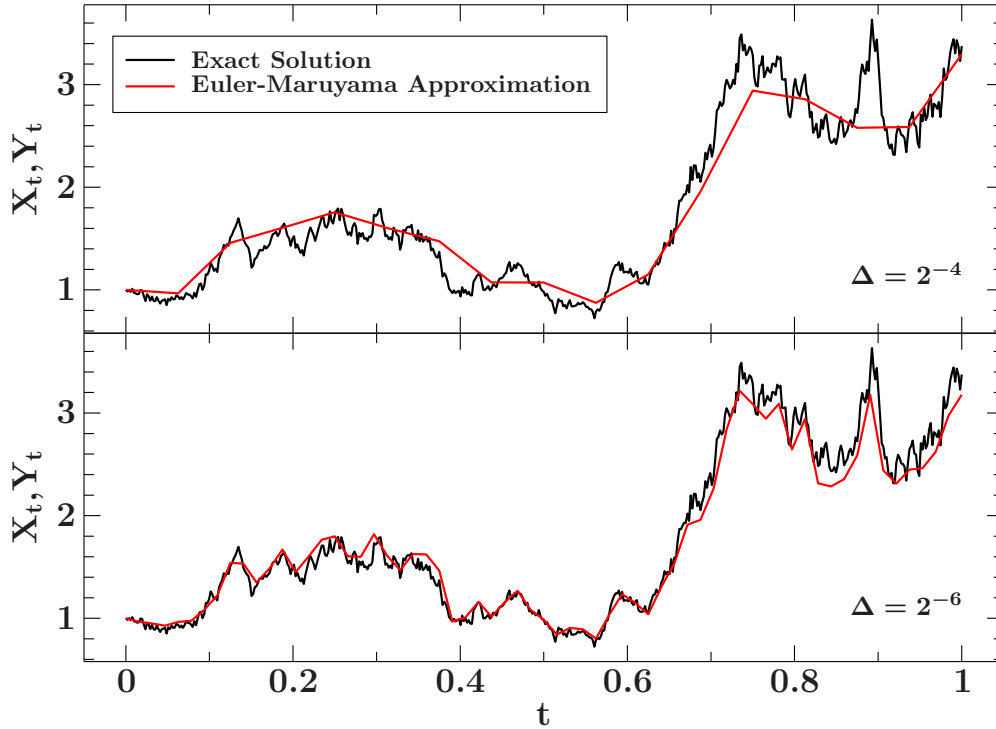
Fig. 6.2: Euler-Maruyama method applied to the SDE (6.21) for $X_0 = 1$, $\mu = 2$, and $\sigma = 1$ over the time interval $[0, 1]$. The red lines show the resulting approximations for different step sizes. For comparison, the exact solution is shown in black.

Definition 6.2. *Let $\mathcal{I}_\delta = \{\tau_0, \tau_1, \ldots, \tau_N\}$ with $t_0 = \tau_0 < \tau_1 < \ldots < \tau_N = T$ be a discretization of the time interval $[t_0, T]$. Denote by δ the maximum step size of the discretization. We say that a time discrete approximation $Y = \{Y_t\}_{t \in \mathcal{I}_\delta}$*

(i)   *converges strongly with order $\gamma > 0$ at time T to the solution X of a given SDE if there exists a positive constant C, which does not depend on δ, and a $\delta_0 > 0$ such that*

$$\epsilon(\delta) = E\left(\|X_T - Y_T\|\right) \leq C\delta^\gamma \tag{6.26}$$

for each $\delta \in (0, \delta_0)$.

(ii) *converges weakly with order $\beta > 0$ at time T to the solution X of a given SDE if for each polynomial $g : \mathbb{R}^d \to \mathbb{R}$ there exists a constant $C > 0$, which does not depend on δ, and a $\delta_0 > 0$ such that*

$$|E(g(X_T)) - E(g(Y_T))| \leq C\delta^\beta \tag{6.27}$$

for each $\delta \in (0, \delta_0)$.

The strong convergence of a numerical scheme is of interest when a good pathwise approximation is required, for example in direct simulations. This is also the type of convergence I am interested in because I want to directly simulate the resulting current and temperature response of the transition-edge sensor to an absorption event.

The weak convergence is of interest when we want to approximate the expectations of functionals of Itô processes. This is the case when one is not interested in the direct simulations but only in the statistical properties of the solution such as its probability distribution or its moments.

For example, the Euler-Maruyama approximation has strong order of convergence $\gamma = 0.5$ and weak order of convergence $\beta = 1$ Kloeden & Platen (1995). Although the method is simple to implement, the order of convergence is still very low. To obtain higher-order methods one can add further terms of the stochastic Taylor expansion to the approximation.

6.3 Higher Order Numerical Methods

In this section I present the construction of higher order numerical methods for general d-dimensional SDEs. Let $(\Omega, \mathcal{F}, \{\mathcal{F}_t\}_{t\geq0}, P)$ be a filtered probability space and let $I = [t_0, T]$ for some $0 \leq t_0 < T < \infty$. Denote by $X = \{X_t\}_{t \in I}$ the solution of the d-dimensional SDE system

$$X_t = X_{t_0} + \int_{t_0}^t a(s, X_s)ds + \int_{t_0}^t b(s, X_s)dW_s \quad \text{on } t_0 \leq t \leq T, \tag{6.28}$$

with initial value $X_{t_0} \in L^2(\Omega, \mathbb{R}^d)$, where $\{W_t = (W_t^1, \ldots, W_t^m)^T\}_{t\geq0}$ is an m-dimensional Wiener process defined on the space for $m \geq 1$. Suppose that $a : I \times \mathbb{R}^d \to \mathbb{R}^d$ and $b : I \times \mathbb{R}^d \to \mathbb{R}^{d \times m}$ are two continuous functions that satisfy the Lipschitz and linear growth condition from theorem (5.53) to ensure the existence and uniqueness of the solution. The k-th component of Eq. (6.28) is

$$X_t^k = X_{t_0}^k + \int_{t_0}^t a^k(s, X_s)ds + \sum_{j=1}^m \int_{t_0}^t b^{k,j}(s, X_s)dW_s^j, \tag{6.29}$$

where a^k denotes the k-th component of the d-dimensional vector valued function a and $b^{k,j}$ denotes the (k, j)-th component of the $d \times m$-matrix valued function $b = (b^{k,j})$. Let $t_0 = \tau_0 < \tau_1 < \ldots < \tau_N = T$ be a discretization of the interval $[t_0, T]$ with step sizes $\Delta_n = \tau_{n+1} - \tau_n$ for $n = 0, 1, \ldots, N - 1$.

To simplify the representation of the multiple Itô and Stratonovic integrals as well as the derivatives that will occur in these schemes I use the compact notation introduced by Kloeden & Platen (1995) for this section.

For the operators that were introduced for the stochastic Taylor expansion at the beginning of this chapter we will use the generalizations

$$L^0 = \frac{\partial}{\partial t} + \sum_{k=1}^d a^k \frac{\partial}{\partial x^k} + \frac{1}{2} \sum_{k,l=1}^d \sum_{j=1}^m b^{k,j} b^{l,j} \frac{\partial^2}{\partial x^k \partial x^l}, \tag{6.30}$$

$$\underline{L}^0 = \frac{\partial}{\partial t} + \sum_{k=1}^d \underline{a}^k \frac{\partial}{\partial x^k}, \tag{6.31}$$

and

$$L^j = \underline{L}^j = \sum_{k=1}^d b^{k,j} \frac{\partial}{\partial x^k}, \tag{6.32}$$

for $j = 1, 2, \ldots, m$, where

$$\underline{a}^k = a^k - \frac{1}{2} \sum_{j=1}^m \underline{L}^j b^{k,j}, \tag{6.33}$$

for $k = 1, 2, \ldots, d$. Additionally, we will abbreviate multiple Itô integrals by

$$I_{(j_1,\ldots,j_l)}[\tau_n, \tau_{n+1}] := \int_{\tau_n}^{\tau_{n+1}} \cdots \int_{\tau_n}^{s_2} dW_{s_1}^{j_1} \cdots dW_{s_l}^{j_l} \tag{6.34}$$

and multiple Stratonovich integrals by

$$J_{(j_1,\ldots,j_l)}[\tau_n, \tau_{n+1}] := \int_{\tau_n}^{\tau_{n+1}} \cdots \int_{\tau_n}^{s_2} \circ dW_{s_1}^{j_1} \cdots \circ dW_{s_l}^{j_l}, \tag{6.35}$$

for a multi-index $\alpha = (j_1, j_2, \ldots, j_l) \in \{0, 1, \ldots, m\}^l$ with the convention that

$$W_t^0 = t, \tag{6.36}$$

for all $t \geq 0$. In the remainder of this section I will use the abbreviation

$$f = f(\tau_n, Y_n), \tag{6.37}$$

for $n = 0, 1, 2, \ldots$, in the numerical schemes for any function f defined on $\mathbb{R}^+ \times \mathbb{R}^d$.

One can construct stochastic Taylor expansions for d-dimensional Itô processes in a similar way as shown at the beginning of this chapter for the one dimensional case. The derivation of a general stochastic Taylor expansion for the multi dimensional case is shown in Kloeden & Platen (1995). The main difference to the one dimensional case is that there will occur multiple stochastic integrals of the form (6.34) and (6.35) as well as multiple derivatives of the form (6.30)–(6.33) in such expansions.

We can then construct numerical methods with higher order of convergence for general d-dimensional SDEs as Eq. (6.28) by including appropriately many terms of this general stochastic Taylor expansion. For example, by adding one more term to the Euler-Maruyama scheme (6.15) one obtains the *Milstein scheme*. For the general multi-dimensional case with $d, m \geq 1$, the k-th component of the Milstein scheme is given by (Kloeden & Platen, 1995)

$$Y_{n+1}^k = Y_n^k + a^k \Delta_n + \sum_{j=1}^m b^{k,j} \Delta W_n^j + \sum_{j_1,j_2=1}^m L^{j_1} b^{k,j_2} I_{(j_1,j_2)}[\tau_n, \tau_{n+1}], \tag{6.38}$$

for $n = 0, 1, \ldots, N - 1$. Alternatively, if multiple Stratonovich integrals are used, the Milstein scheme has the form

$$Y_{n+1}^k = Y_n^k + \underline{a}^k \Delta_n + \sum_{j=1}^m b^{k,j} \Delta W_n^j + \sum_{j_1,j_2=1}^m \underline{L}^{j_1} b^{k,j_2} J_{(j_1,j_2)}[\tau_n, \tau_{n+1}], \tag{6.39}$$

for $n = 0, 1, \ldots, N - 1$. The Milstein scheme has strong order of convergence $\gamma = 1.0$ under certain conditions on the functions a and b (Kloeden & Platen, 1995).

We immediately see another problem that arises for higher order numerical methods like the Milstein scheme. For the implementation of the scheme we need to calculate the multiple stochastic integrals $I_{(j_1,j_1)}[\tau_n, \tau_{n+1}]$ and $J_{(j_1,j_1)}[\tau_n, \tau_{n+1}]$ in the approximations (6.38) and (6.39). When $j_1 = j_2$ we can apply the Itô formula to obtain (Kloeden & Platen, 1995)

$$I_{(j_1,j_1)}[\tau_n, \tau_{n+1}] = \frac{1}{2} \left\{ \left(\Delta W_n^{j_1}\right)^2 - \Delta_n \right\} \quad \text{and} \quad J_{(j_1,j_1)}[\tau_n, \tau_{n+1}] = \frac{1}{2} \left(\Delta W_n^{j_1}\right)^2. \tag{6.40}$$

However, when $j_1 \neq j_2$ we cannot write the multiple integrals $I_{(j_1,j_2)}[\tau_n, \tau_{n+1}]$ and $J_{(j_1,j_2)}[\tau_n, \tau_{n+1}]$ just in terms of the increments $\Delta W_n^{j_1}$ and $\Delta W_n^{j_2}$. Nevertheless, for the implementation of a scheme that requires the computation of such integrals one can approximate them numerically instead. In the next section I describe a method for the approximation of such multiple stochastic integrals based on a random Fourier series expansion.

6.4 Approximation of Multiple Stochastic Integrals

In this section I present a method to approximate multiple stochastic Integrals numerically as proposed by Kloeden & Platen (1995). The method is based on the component wise Fourier expansion of a *Brownian bridge process.*

A Brownian bridge process $\{B_t\}_{0 \leq t \leq T}$ is a modification of an m-dimensional Wiener process $W_t = (W_t^1, \ldots, W_t^m)$ defined by (Kloeden & Platen, 1995)

$$B_t = x + W_t - \frac{t}{T} \{W_T - y + x\}, \tag{6.41}$$

for $0 \leq t \leq T$ and $x, y \in \mathbb{R}^d$. The Brownian bridge process satisfies the constraints $B_0 = x$ and $B_T = y$, i.e., all sample paths of the process pass through the same initial point x and end point y.

In this section we will work with a Brownian bridge process that starts at $x = 0$ and ends at $y = 0$ on the time interval $[0, \Delta]$ with $\Delta > 0$, i.e.,

$$\left\{ W_t - \frac{t}{\Delta} W_\Delta \right\}_{0 \leq t \leq \Delta}. \tag{6.42}$$

As shown in Kloeden & Platen (1995) the j-th component of the Fourier expansion of this process has the form

$$W_t^j - \frac{t}{\Delta} W_\Delta^j = \frac{1}{2} a_{j,0} + \sum_{r=1}^{\infty} \left(a_{j,r} \cos\left(\frac{2r\pi t}{\Delta}\right) + b_{j,r} \sin\left(\frac{2r\pi t}{\Delta}\right) \right) \tag{6.43}$$

with random coefficients

$$a_{j,r} = \frac{2}{\Delta} \int_0^\Delta \left(W_s^j - \frac{s}{\Delta} W_\Delta^j \right) \cos\left(\frac{2r\pi s}{\Delta}\right) ds, \tag{6.44}$$

$$b_{j,r} = \frac{2}{\Delta} \int_0^\Delta \left(W_s^j - \frac{s}{\Delta} W_\Delta^j \right) \sin\left(\frac{2r\pi s}{\Delta}\right) ds, \tag{6.45}$$

for $r = 0, 1, 2, \ldots$, and $j = 1, \ldots, m$. One can show that the coefficients $a_{j,r}$ and $b_{j,r}$ are $N(0, \Delta/2\pi^2 r^2)$ distributed random variables (Kloeden & Platen, 1995). By truncating the series (6.43) we obtain an approximation

$$W_t^{j,p} = \frac{t}{\Delta} W_\Delta^j + \frac{1}{2} a_{j,0} + \sum_{r=1}^{p} \left(a_{j,r} \cos\left(\frac{2r\pi t}{\Delta}\right) + b_{j,r} \sin\left(\frac{2r\pi t}{\Delta}\right) \right), \tag{6.46}$$

for each $p \in \mathbb{N}$. The process (6.46) has differentiable sample paths on the time interval $[0, \Delta]$ and one can show that Riemann-Stieltjes integrals with respect to such a process

converge to Stratonovich stochastic integrals (Kloeden & Platen, 1995). Thus, we can use such integrals to approximate multiple Stratonovich integrals $J_{(j_1,\ldots,j_l)}[0,t]$. Denote by

$$J^p_{(j_1,j_2,\ldots,j_l)}[0,t] = \int_0^t \int_0^{s_l} \cdots \int_0^{s_2} dW^{j_1,p}_{s_1} dW^{j_2,p}_{s_2} \ldots dW^{j_l,p}_{s_l} \qquad (6.47)$$

the corresponding Riemann-Stieltjes integrals. I will omit the lengthy derivations here and just present the resulting approximations. A detailed derivation of the approximations as well as more details on this subject can be found in Kloeden & Platen (1995).

We define for all $j = 1,\ldots,m$ and $r = 1,\ldots,p$ with $p \in \mathbb{N}$ random variables ξ_j, $\zeta_{j,r}$, $\eta_{j,r}$, $\mu j, p$ and $\phi_{j,p}$, which are independent and normally distributed with mean zero and variance one, by

$$\xi_j = \frac{1}{\sqrt{\Delta}}W^j_\Delta, \quad \zeta_{j,r} = \sqrt{\frac{2}{\Delta}}\pi r a_{j,r}, \quad \eta_{j,r} = \sqrt{\frac{2}{\Delta}}\pi r b_{j,r}, \qquad (6.48)$$

$$\mu_{j,p} = \frac{1}{\sqrt{\Delta}\rho_p}\sum_{r=p+1}^\infty a_{j,r}, \quad \Phi_{j,p} = \frac{1}{\sqrt{\Delta}\alpha_\rho}\sum_{r=p+1}^\infty \frac{1}{r}b_{j,r},$$

where

$$\rho_p = \frac{1}{12} - \frac{1}{2\pi^2}\sum_{r=1}^p \frac{1}{r^2} \quad \text{and} \quad \alpha_p = \frac{\pi^2}{180} - \frac{1}{2\pi^2}\sum_{r=1}^p \frac{1}{r^4}. \qquad (6.49)$$

With these random variables we can approximate a multiple Stratonovich integral $J_{(j_1,\ldots,j_l)}[0,\Delta]$ by $J^p_{(j_1,\ldots,j_l)}[0,\Delta]$ for $p \in \mathbb{N}$ as described below. To simplify the notation I will omit the argument $[0,\Delta]$ from the J^p_α from now on. For $j, j_1, j_2, j_3 \in \{1,\ldots,m\}$ we have

$$J^p_{(0)} = \Delta, \quad J^p_{(j)} = \sqrt{\Delta}\xi_j, \qquad (6.50)$$

$$J^p_{(0,0)} = \frac{1}{2}\Delta^2, \quad J^p_{(j,0)} = \frac{1}{2}\Delta\left(\sqrt{\Delta}\xi_j + a_{j,0}\right), \quad J^p_{(0,j)} = \frac{1}{2}\Delta\left(\sqrt{\Delta}\xi_j - a_{(j,0)}\right), \quad (6.51)$$

where

$$a_{j,0} = -2\sqrt{\Delta\rho_p}\mu_{j,p} - \frac{1}{\pi}\sqrt{2\Delta}\sum_{r=1}^p \frac{1}{r}\zeta_{j,r}, \qquad (6.52)$$

and

$$J^p_{(j_1,j_2)} = \frac{1}{2}\Delta\xi_{j_1}\xi_{j_2} - \frac{1}{2}\sqrt{\Delta}\left(a_{j_2,0}\xi_{j_1} - a_{j_1,0}\xi_{j_2}\right) + \Delta A^p_{j_1,j_2}, \qquad (6.53)$$

with

$$A^p_{j_1,j_2} = \frac{1}{2\pi}\sum_{r=1}^p \frac{1}{r}\left(\zeta_{j_1,r}\eta_{j_2,r} - \eta_{j_1,r}\zeta_{j_2,r}\right). \qquad (6.54)$$

Triple Stratonovich integrals can be approximated by

$$J_{(0,0,0)}^p = \frac{1}{3!}\Delta^3, \tag{6.55}$$

$$J_{(0,j,0)}^p = \frac{1}{3!}\Delta^{5/2}\xi_j - \frac{1}{\pi}\Delta^2 b_j, \tag{6.56}$$

$$J_{(j,0,0)}^p = \frac{1}{3!}\Delta^{5/2}\xi_j + \frac{1}{4}\Delta^2 a_{j,0} + \frac{1}{2\pi}\Delta^2 b_j, \tag{6.57}$$

$$J_{(0,0,j)}^p = \frac{1}{3!}\Delta^{5/2}\xi_j - \frac{1}{4}\Delta^2 a_{j,0} + \frac{1}{2\pi}\Delta^2 b_j, \tag{6.58}$$

with

$$b_j = \sqrt{\Delta\alpha_p}\Phi_{j,p} + \sqrt{\frac{\Delta}{2}}\sum_{r=1}^p \frac{1}{r^2}\eta_{j,r}, \tag{6.59}$$

$$J_{(j_1,0,j_2)}^p = \frac{1}{3!}\Delta^2\xi_{j_1}\xi_{j_2} + \frac{1}{2}a_{j_1,0}J_{(0,j_2)}^p + \frac{1}{2\pi}\Delta^{3/2}\xi_{j_2}b_{j_1} \tag{6.60}$$
$$- \Delta^2 B_{j_1,j_2}^p - \frac{1}{4}\Delta^{3/2}a_{j_2,0}\xi_{j_1} + \frac{1}{2\pi}\Delta^{3/2}\xi_{j_1}b_{j_2},$$

$$J_{(0,j_1,j_2)}^p = \frac{1}{3!}\Delta^2\xi_{j_1}\xi_{j_2} - \frac{1}{\pi}\Delta^{3/2}\xi_{j_2}b_{j_1} + \Delta^2 B_{j_1,j_2}^p \tag{6.61}$$
$$- \frac{1}{4}\Delta^{3/2}a_{j_2,0}\xi_{j_1} + \frac{1}{2\pi}\Delta^{3/2}\xi_{j_1}b_{j_2} + \Delta^2 C_{j_1,j_2}^p + \frac{1}{2}\Delta^2 A_{j_1,j_2}^p,$$

with

$$B_{j_1,j_2}^p = \frac{1}{4\pi^2}\sum_{r=1}^p \frac{1}{r^2}\left(\zeta_{j_1,r}\zeta_{j_2,r} + \eta_{j_1,r}\eta_{j_2,r}\right), \tag{6.62}$$

and

$$C_{j_1,j_2}^p = -\frac{1}{2\pi^2}\sum_{\substack{r,l=1 \\ r\neq l}}^p \frac{r}{r^2-l^2}\left(\frac{1}{l}\zeta_{j_1,r}\zeta_{j_2,l} - \frac{l}{r}\eta_{j_1,r}\eta_{j_2,l}\right), \tag{6.63}$$

$$J_{(j_1,j_2,0)}^p = \frac{1}{2}\Delta^2\xi_{j_1}\xi_{j_2} - \frac{1}{2}\Delta^{3,2}\left(a_{j_2,0}\xi_{j_1} - a_{j_1,0}\xi_{j_2}\right) \tag{6.64}$$
$$+ \Delta^2 A_{j_1,j_2}^p - J_{(j_1,0,j_2)}^p - J_{(0,j_1,j_2)}^p,$$

$$J_{(j_1,j_2,j_3)}^p = \frac{1}{\sqrt{\Delta}}\xi_{j_1}J_{(0,j_2,j_3)}^p + \frac{1}{2}a_{j_1,0}J_{(j_2,j_3)}^p + \frac{1}{2\pi}\Delta b_{j_1}\xi_{j_2}\xi_{j_3} \tag{6.65}$$
$$- \Delta^{3/2}\xi_{j_2}B_{j_1,j_3}^p + \Delta^{3/2}\xi_{j_3}\left(\frac{1}{2}A_{j_1,j_2}^p - C_{j_2,j_1}^p\right) + \Delta^{3/2}D_{j_1,j_2,j_3}^p,$$

with

$$D^p_{j_1,j_2,j_3} = -\frac{1}{\pi^2 2^{5/2}} \sum_{r,l=1}^{p} \frac{1}{l(l+r)} \left[\zeta_{j_2,l}(\zeta_{j_3,l+r}\eta_{j_1,r} - \zeta_{j_1,r}\eta_{j_1,l+r}) \right. \tag{6.66}$$

$$\left. + \eta_{j_2,l}(\zeta_{j_1,r}\zeta_{j_3,l+r} + \eta_{j_1,r}\eta_{j_3,l+r}) \right]$$

$$+ \frac{1}{\pi^2 2^{5/2}} \sum_{l=2}^{p} \sum_{r=1}^{l-1} \frac{1}{r(l-r)} \left[\zeta_{j_2,l}(\zeta_{j_1,r}\eta_{j_3,l-r} + \zeta_{j_3,l-r}\eta_{j_1,r}) \right.$$

$$\left. - \eta_{j_2,l}(\zeta_{j_1,r}\zeta_{j_3,l-r} - \eta_{j_1,r}\eta_{j_3,l-r}) \right]$$

$$+ \frac{1}{\pi^2 2^{5/2}} \sum_{l=1}^{p} \sum_{r=l+r}^{2p} \frac{1}{r(r-l)} \left[\zeta_{j_2,l}(\zeta_{j_3,r-l}\eta_{j_1,r} - \zeta_{j_1,r}\eta_{j_3,r-l}) \right. \quad ,$$

$$\left. + \eta_{j_2,l}(\zeta_{j_1,r}\zeta_{j_3,r-l} + \eta_{j_1,r}\eta_{j_3,r-l}) \right]$$

where we set $\zeta_{j,r} = 0$ and $\eta_{j,r} = 0$ for $r > p$. Kloeden & Platen (1995) show that mean-square error of the above approximations for multi-indices $\alpha = (j_1, j_2, j_3) \in \{0, 1, \dots, m\}^3$ is given by

$$E\left(\left| J^p_\alpha - J_\alpha \right|^2 \right) \le \Delta^2 \varrho_p, \tag{6.67}$$

where

$$\varrho_p = \frac{1}{2\pi^2} \sum_{r=p+1}^{\infty} \frac{1}{r^2}. \tag{6.68}$$

This inequality allows us to estimate the quality of our approximations and to calculate an upper bound for the error. For the implementation of the above approximation one can again use random number generators to generate realizations of the random variables (6.48).

We can approximate multiple Itô integrals in a similar way by using the following correlations between Itô and Stratonovich integrals (Kloeden & Platen, 1995). For j_1, j_2, $j_3 \in \{0, 1, \dots, m\}$ we have

$$I_{(j_1)} = J_{j_1} \tag{6.69}$$

$$I_{(j_1,j_2)} = J_{(j_1,j_2)} - \frac{1}{2}\mathcal{I}_{\{j_1=j_2\neq 0\}}\Delta \tag{6.70}$$

$$I_{(j_1,j_2,j_3)} = J_{(j_1,j_2,j_3)} - \frac{1}{2}\mathcal{I}_{\{j_1=j_2\neq 0\}}J_{(0,j_3)} - \frac{1}{2}\mathcal{I}_{\{j_2=j_3\neq 0\}}J_{(j_1,0)}, \tag{6.71}$$

where $\mathcal{I}_A$ denotes of indicator function which equals 1 if A is true and 0 otherwise. Additionally, for the implementation of the above approximations in numerical schemes we can use the following relations between multiple Itô integrals to save computation time. For $j \in \{1, \dots, m\}$ and $\Delta W^j := W^j_\Delta - W^j_0$ we have (Kloeden & Platen, 1995)

$$I_{(j,j)} = \frac{1}{2}\left((\Delta W^j)^2 - \Delta \right), \tag{6.72}$$

$$I_{(j,j,j)} = \frac{1}{3!}\left((\Delta W^j)^2 - 3\Delta \right)\Delta W^j, \tag{6.73}$$

$$\Delta W^j \Delta = I_{(j,0)} + I_{(0,j)}. \tag{6.74}$$

That is, we can compute the double and triple Itô integrals $I_{(j,j)}$ and $I_{(j,j,j)}$ directly from the Wiener increments. The double integral $I_{(j,0)}$ can easily be computed from $I_{(j,0)}$ and vice versa.

In this section I explained how the multiple stochastic integrals in higher order numerical schemes can be approximated numerically. By including more terms of the general stochastic Taylor expansion one can construct even higher order numerical methods for SDEs. However, a disadvantage of such Taylor-expansion methods is that the partial derivatives of various orders of the drift and diffusion coefficients must be calculated first and then evaluated at each time step. Depending on the SDE system one is working with this fact can make the implementation of such a method very impractical. There are however numerical methods for the strong approximation of SDEs that do not use the derivatives of the drift and diffusion coefficients, similar to Runge-Kutta schemes for ordinary differential equations. In the next section I will present such a Runge-Kutta method for SDEs that has strong order of convergence 1.5.

6.5 Runge-Kutta Methods

In this section we consider numerical methods for SDEs which avoid the use of derivatives, similar to Runge-Kutta schemes for ordinary differential equations. We will also call them Runge-Kutta schemes in analogy to the deterministic case. I will continue to use the abbreviations and notations introduced in the last section.

Stochastic Runge-Kutta schemes are obtained from the Taylor-expansion methods by replacing the derivatives with finite differences expressed in terms of appropriate supporting values. Below, I present a Runge-Kutta approximation for autonomous SDEs from Platen & Bruti-Liberati (2010) with strong order of convergence 1.5. For general multi-dimensional autonomous SDEs (6.28) with $d, m \geq 1$, the k-th component of the scheme satisfies

$$Y_{n+1}^k = Y_n^k + a^k(Y_n)\Delta_n + \sum_{j=1}^{m} b^{k,j}(Y_n)\Delta W_n^j \qquad (6.75)$$

$$+ \frac{1}{2\sqrt{\Delta_n}} \sum_{j_2=0}^{m} \sum_{j_1=1}^{m} \left\{ b^{k,j_2}\left(\bar{\Upsilon}_+^{j_1}\right) - b^{k,j_2}\left(\bar{\Upsilon}_-^{j_1}\right) \right\} I_{(j_1,j_2)}[\tau_n, \tau_{n+1}]$$

$$+ \frac{1}{2\Delta_n} \sum_{j_2=0}^{m} \sum_{j_1=1}^{m} \left\{ b^{k,j_2}\left(\bar{\Upsilon}_+^{j_1}\right) - 2b^{k,j_2} + b^{k,j_2}\left(\bar{\Upsilon}_-^{j_1}\right) \right\} I_{(0,j_2)}[\tau_n, \tau_{n+1}]$$

$$+ \frac{1}{2\Delta_n} \sum_{j_1,j_2,j_3=1}^{m} \left[b^{k,j_3}\left(\bar{\bar{\Phi}}_+^{j_1,j_2}\right) - b^{k,j_3}\left(\bar{\bar{\Phi}}_-^{j_1,j_2}\right) \right.$$

$$\left. - b^{k,j_3}\left(\bar{\Upsilon}_+^{j_1}\right) + b^{k,j_3}\left(\bar{\Upsilon}_-^{j_1}\right) \right] I_{(j_1,j_2,j_3)}[\tau_n, \tau_{n+1}],$$

with the supporting values

$$\bar{\Upsilon}_\pm^j = Y_n + \frac{1}{m}a(Y_n)\Delta_n \pm b^j(Y_n)\sqrt{\Delta_n}, \qquad (6.76)$$

$$\bar{\bar{\Phi}}_\pm^{j_1,j_2} = \bar{\Upsilon}_+^{j_1} \pm b^{j_2}\left(\bar{\Upsilon}_+^{j_1}\right)\sqrt{\Delta_n}, \qquad (6.77)$$
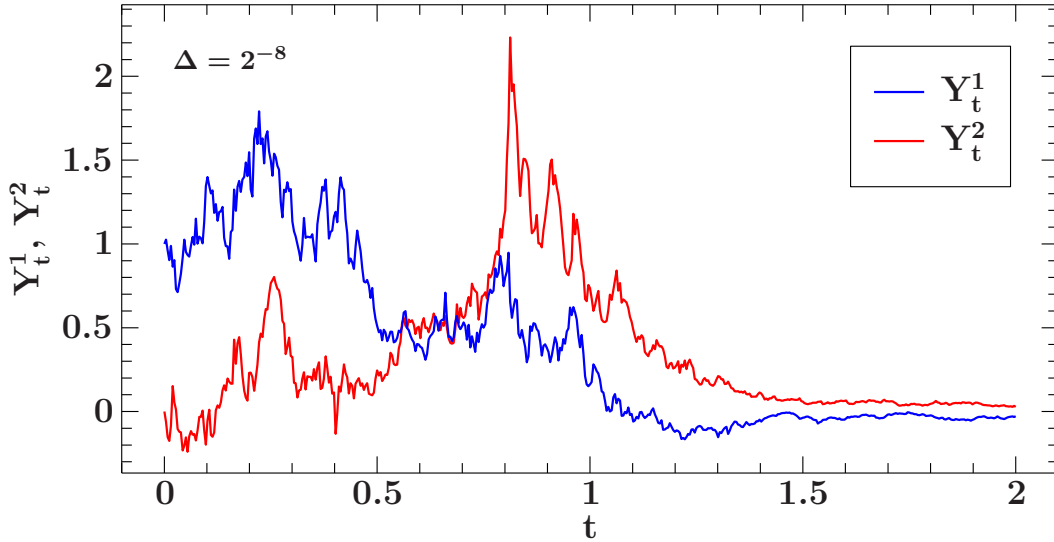
Fig. 6.3: Result of the Runge-Kutta method (6.75) applied to the SDE system (6.78) with constant step size $\Delta = 2^{-8}$ over the time interval $[0, 2]$.

where we set $b^{k,0} := a^k$. The multiple Itô integrals in this scheme can be approximated as described in Sect. 6.4. This Runge-Kutta method is also the method that I used for the numerical simulations of transition-edge sensors in Chapter 7. I implemented the above scheme in the C programming language. To illustrate and verify the output of my program I applied it to a simple two-dimensional SDE system that also has an explicit solution.

Example 6.3. In this example I apply the Runge-Kutta method (6.75) to a simple SDE system and compare the resulting approximation to the exact solution. Consider the system of two coupled autonomous SDEs

$$dX_t^1 = -\frac{3}{2}X_t^1 dt + X_t^1 dW_t^1 - X_t^1 dW_t^2 - X_t^2 dW_t^3, \qquad (6.78)$$
$$dX_t^2 = -\frac{3}{2}X_t^2 dt + X_t^2 dW_t^1 - X_t^2 dW_t^2 + X_t^1 dW_t^3$$

for $t \in [0, 2]$ with initial value $(X_0^1, X_0^2) = (1, 0)$ and three independent Wiener processes W^1, W^2, and W^3. As shown in Wilkie (2004), this SDE system has the explicit solution

$$X_t^1 = \exp\{-2t + W_t^1 - W_t^2\} \cos W_t^3, \qquad (6.79)$$
$$X_t^2 = \exp\{-2t + W_t^1 - W_t^2\} \sin W_t^3, \qquad (6.80)$$

for $t \in [0, 2]$. In order to apply the method to this system I first generated sample paths of three time discrete Wiener processes over the time interval $[0, 2]$ as in (6.20) with constant step sizes $\Delta = 2^{-9}$. Figure 6.3 shows the result of the Runge-Kutta method (6.75) applied to the SDE system (6.78) with constant step size $\Delta = 2^{-8}$ over the time interval $[0, 2]$, corresponding to the previously generated Wiener processes. The approximation Y_t^1 to the first component X_t^1 of the solution is shown in blue and the approximation Y_t^2 to the second component X_t^2 of the solution is shown in red.

Figures 6.4 and 6.5 show the Runge-Kutta approximations for different step sizes and the exact solution (6.79) corresponding to the three generated Wiener processes for comparison. We can see that the quality of the approximation improves for smaller step sizes and that my implementation of the method is working fine.

I have written my program in such a way that it can be applied to any autonomous multi dimensional system of SDEs with any number of noise terms. The next step to obtain numerical simulations of transition-edge sensors is now to model the noise in a TES in the framework of stochastic differential equations. Then I use my program to solve the resulting SDE system numerically.
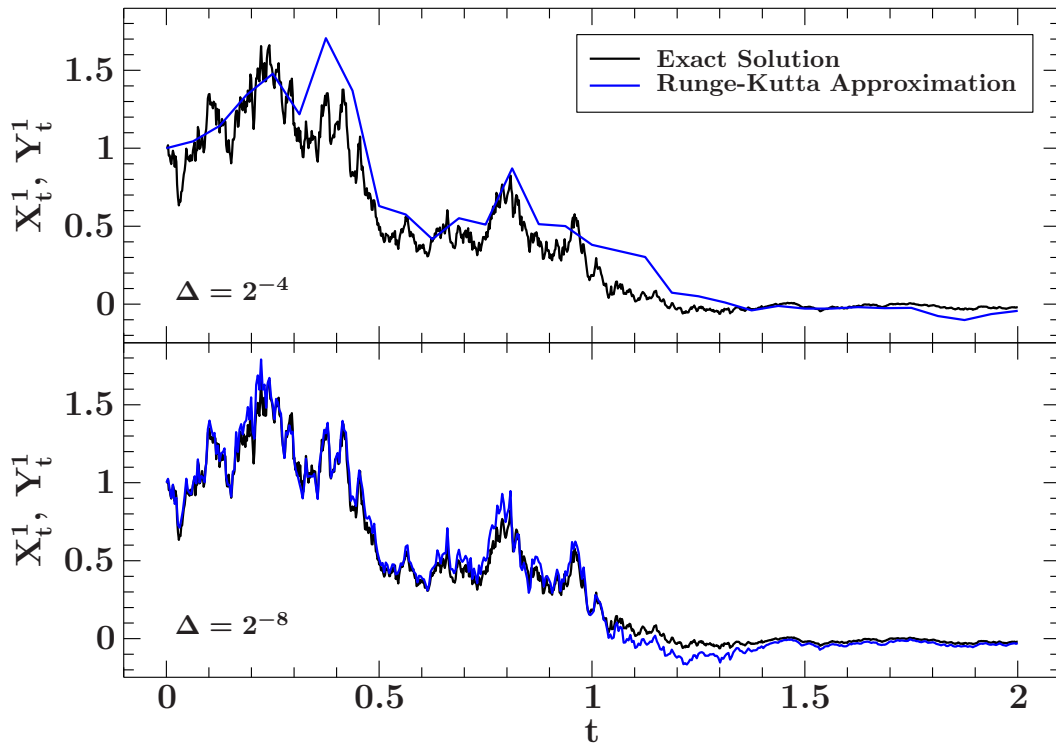
Fig. 6.4: Comparison between the Runge-Kutta approximation Y_t^1 and the exact solution X_t^1 for different step sizes.
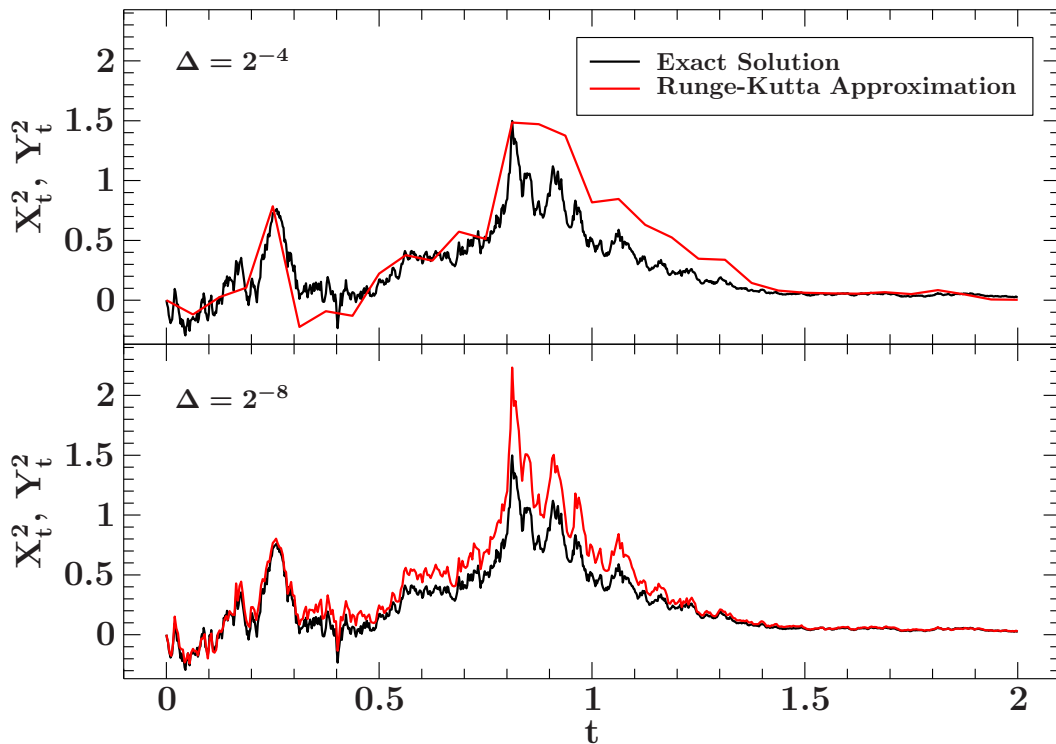
Fig. 6.5: Comparison between the Runge-Kutta approximation Y_t^2 and the exact solution X_t^2 for different step sizes.

Chapter 7

Simulation of Transition-Edge Sensors

In this chapter I present my results of the numerical simulation of TES based microcalorimeters using the stochastic Runge-Kutta scheme from Chapter 6. The simulations include the main noise processes that exist in the detector as described in Chapter 4. First, I describe the noise models used for the simulations and how they are treated in the framework of stochastic differential equations. Then I present the results of my simulations. Finally, I compare my results to the simulations done before with the fourth order Runge-Kutta method for ordinary differential equations.

7.1   Noise Models

To model the Johnson noise from the resistors I follow the approach by Gillespie (1996), Demir (1997) and Allison & Abbot (2005). In these articles, Johnson noise from resistors is modeled as an additional voltage or current source using *Nyquist's theorem*. The following text is a brief summary of this method. For more details see the cited articles.

Shortly after the thermal fluctuations in resistors were observed by John B. Johnson, Harry Nyquist was the first who derived a physical description of this effect in 1928 (Nyquist, 1928). Nyquist's theorem states that the fluctuations in current from a resistor having resistance R at temperature T can be modeled as a wide-sense stationary stochastic process with spectral density given by

$$S_{i_\mathrm{n}}(f) = \frac{2k_\mathrm{b}T}{R}, \tag{7.1}$$

where $k_\mathrm{b} = 1.38 \times 10^{-23}\,\mathrm{JK^{-1}}$ is the Boltzmann constant. The spectral density is constant, i.e., this is the spectral density of a white noise process. As a consequence of the central limit theorem, the thermal noise of a resistor is accurately modeled by a Gaussian process. This means, we can use the formal derivative of the Wiener process as a model for the thermal noise of a resistor.

Based on Nyquist's theorem a noisy resistor can then be modeled as a noise free resistor with the same resistance R in parallel with a noise current source i_n that represents a wide-sense stationary white Gaussian stochastic process whose spectral density is given by Eq. (7.1). This model is called the *Norton equivalent model* for the noisy resistor.
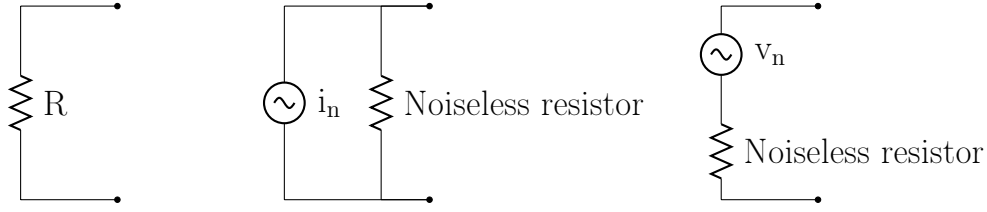
(a) Resistor at temperature T (b) Norton equivalent model (c) Thevenin equivalent model

Fig. 7.1: The noisy resistor at temperature T in figure (a) can be modeled as a noiseless resistor in parallel with a noise-creating current source or in series with a noise-creating voltage source. All three circuits are equivalent.

Alternatively, the noisy resistor can also be modeled as a noise free resistor in series with a noise voltage source v_n whose spectral density is given by

$$S_{v_\mathrm{n}}(f) = 2k_\mathrm{b}TR. \tag{7.2}$$

This model is called the *Thevenin equivalent model* for the noisy resistor. An illustration of the two equivalent circuits describing a noisy resistor is shown in Fig. 7.1.

Using this approach we can model the Johnson noise from the resistors in the bias circuit (Fig. 4.3) of our detector as two additional noise voltage sources in series with the load resistor R_L and the TES. The resulting circuit is shown in Fig. 7.2.

The voltage across the TES is now given by

$$V(t) = I(t)R(T(t), I(t)) + v_\mathrm{dn}(t), \tag{7.3}$$

which leads to additional Joule heating from the noisy voltage source v_{dn}. By including this Joule heating and applying Kirchhoff's voltage law we get the new thermal and electrical circuit equations

$$C\frac{dT(t)}{dt} = -P_\mathrm{b}(T, T_\mathrm{b}) + R(T, I)I^2 + P_\mathrm{in} + Iv_\mathrm{dn}(t), \tag{7.4}$$

$$L\frac{dI(t)}{dt} = V - IR_\mathrm{L} - IR_\mathrm{TES}(T, I) + v_\mathrm{cn}(t) + v_\mathrm{dn}(t), \tag{7.5}$$
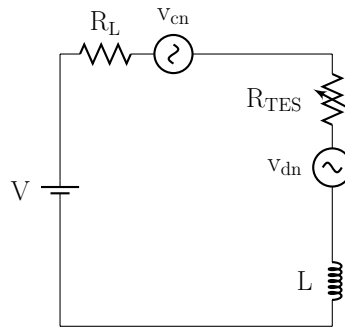

Fig. 7.2: Illustration of the new bias circuit including the Johnson noise from the resistors. The Johnson noise is modeled as two additional noise voltage sources in series with the load resistor and the TES. The first voltage source, named v_dn, models the noise in the detector from the TES and the second voltage source v_cn models the noise in the circuit from the load resistor.

with initial conditions $T(0) = T_0$ and $I(0) = I_0$.

The thermal fluctuation noise across the weak thermal link between the TES and the cold bath is modeled as an additional fluctuating power source in the thermal equation (7.4). Like the Johnson noise, we assume that the thermal fluctuation noise can be modeled as a Gaussian process. As discussed in Irwin & Hilton (2005) the spectral density of the thermal fluctuation noise is given by

$$S_{P_{\mathrm{TFN}}}(f) = 2k_{\mathrm{b}}T_0^2 G_{\mathrm{bath}}. \tag{7.6}$$

That is, the TFN is also a white noise process. Here I use a factor of 2 instead of 4 as in Irwin & Hilton (2005) to be consistent with the previous definition of spectral density.

As discussed above, the noise voltages must be of the form

$$v_{\mathrm{n}}(t) = \sqrt{2k_{\mathrm{b}}TR}\xi(t), \tag{7.7}$$

where $\xi(t)$ is a Gaussian white noise process, i.e., the formal derivative of a Wiener process. Then the spectral density of this process is given by Eq. (7.2). Similarly, the TFN must be of the form

$$P_{\mathrm{TFN}}(t) = \sqrt{2k_{\mathrm{b}}T_0^2 G_{\mathrm{bath}}}\xi(t). \tag{7.8}$$

Including the TFN in the thermal equation and using the notation of stochastic differential equations yields the SDE system

$$dT_t = C^{-1}(-P_{\mathrm{b}}(T_t, T_{\mathrm{b}}) + R_{\mathrm{TES}}(T_t, I_t)I_t^2 + P_{\mathrm{in}})dt \tag{7.9}$$
$$+ C^{-1}I_t\sqrt{2k_{\mathrm{b}}T_t R(T_t, I_t)}dW_t^2 + C^{-1}\sqrt{2k_{\mathrm{b}}T_t^2 G_{\mathrm{bath}}}dW_t^3$$
$$dI_t = L^{-1}(V - I_t R_{\mathrm{L}} - I_t R_{\mathrm{TES}}(T_t, I_t))dt \tag{7.10}$$
$$+ L^{-1}\sqrt{2k_{\mathrm{b}}T_{\mathrm{b}} R_{\mathrm{L}}}dW_t^1 + L^{-1}\sqrt{2k_{\mathrm{b}}T_t R(T_t, I_t)}dW_t^2,$$

on $t_0 \leq t \leq t_{end}$ with initial conditions $T_{t_0} = T_0$, $I_{t_0} = I_0$ and three independent Wiener processes $\{W_t^1\}_{t_0 \leq t \leq t_{end}}$, $\{W_t^2\}_{t_0 \leq t \leq t_{end}}$, $\{W_t^3\}_{t_0 \leq t \leq t_{end}}$. This is the system of stochastic differential equations that I will use for the numerical simulations in the next section.

7.2 Simulation Results

For the simulations I implemented the SDE system (7.9–7.10) and my stochastic Runge-Kutta program from Chapter 6 in the `tessim` software tool within the SIXTE framework. Table 7.1 shows the parameters of the simulated transition-edge sensor. These parameters are stored in a FITS file which is read in during runtime. The photon energies and their arrival times are stored in an additional FITS file. The output generated by `tessim` is a FITS file that contains the current values calculated at the sampling times.

Figure 7.3 shows the resulting current pulses of my simulations for different photon energies with constant step size $\Delta = 6.4 \times 10^{-6}$ seconds. As expected, the current drops when a photon hits the pixel and then recovers back to the steady state value. The higher the photon energy, the larger is the resulting current drop.
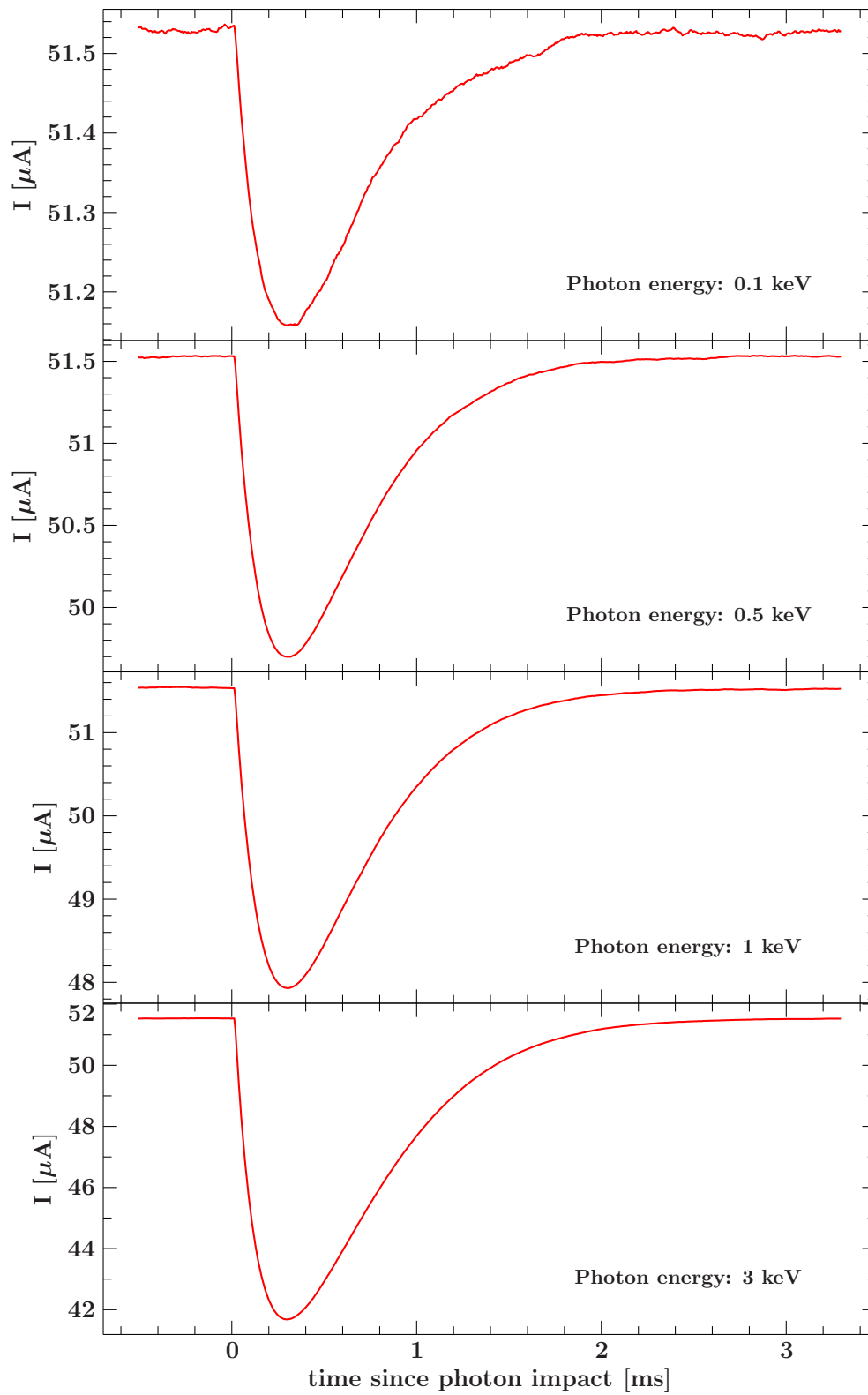
Fig. 7.3: Simulated current pulses for different photon energies.

Table 7.1: The parameters of the simulated TES pixel. The additional parameters `Rpara`, `TTR`, and `Lfilter` are used to calculate the resistance, inductance, and bias voltage of the TES inside `tessim`.

Parameter	Symbol	Value	Explanation
`sample_rate`		156250	Sample rate [Hz]
`delta_t`	Δ	6.4	Step size [μs]
`T_start`	T_0	90.0	Initial temperature [mK]
`I0`	I_0	51.53332	Initial current [μA]
`Ce1`	C	0.8	Heat capacity [pJ/K]
`Gb1`	G_{bath}	114.7	Bath thermal conductance [pW/K]
`Tb`	T_{b}	55	Bath temperature [mK]
`n`	n	3	Thermal exponent
`alpha`	α	75	TES sensitivity
`beta`	β	1.25	TES current dependence
`R0`		1.0	Operating point resistance [mΩ]
`Rpara`		1.0	Parasitic resistor value [mΩ]
`TTR`		4.08	Transformer Turns Ratio
`Lfilter`		2	Filter inductance [μH]

So the stochastic integrator and the implementation are working fine. However, another question that remains to study is how the new results differ from the simulations done before with `tessim`. As mentioned in Chapter 3, `tessim` used a standard fourth order Runge-Kutta method to solve the system of differential equations describing the TES, consisting of Eqs. (4.2) and (4.9). The noise was simulated by adding appropriately scaled random numbers to these differential equations before each integration step. This method is mathematically incorrect, but nevertheless yields very reasonable results. So in the remainder of this chapter I will compare the results of both methods.

Figure 7.4 shows a current pulse obtained with the new integrator and a pulse that is generated with the old code for comparison. We can see that there is not much difference at all between the two pulses. Especially at higher energies the difference is barely visible. To further study the difference between the two methods I also did simulations without noise. The difference between the two solutions obtained this way is shown in Fig. 7.5. The difference is minimal and probably due to the higher order of convergence of the deterministic Runge-Kutta method. This fact could be improved, e.g., by implementing an adaptive step size control for future simulations.

Additionally, I did simulations where I increased the intensity of the noise in both methods by 500 percent. The idea was to investigate if the solutions might deviate from each other for such high noise intensities. However, as the plots in Fig. 7.5 indicate the solutions are still very similar, although the noise seems to be slightly more pronounced for the new method.

The above considerations suggest that the two methods indeed yield very similar results despite the mathematical deficiency of the old approach. In the next section I calculate the noise spectra of a 30 second simulation of just noise using methods from spectral analysis. Perhaps there might be a prominent difference visible between the two methods in their spectra.
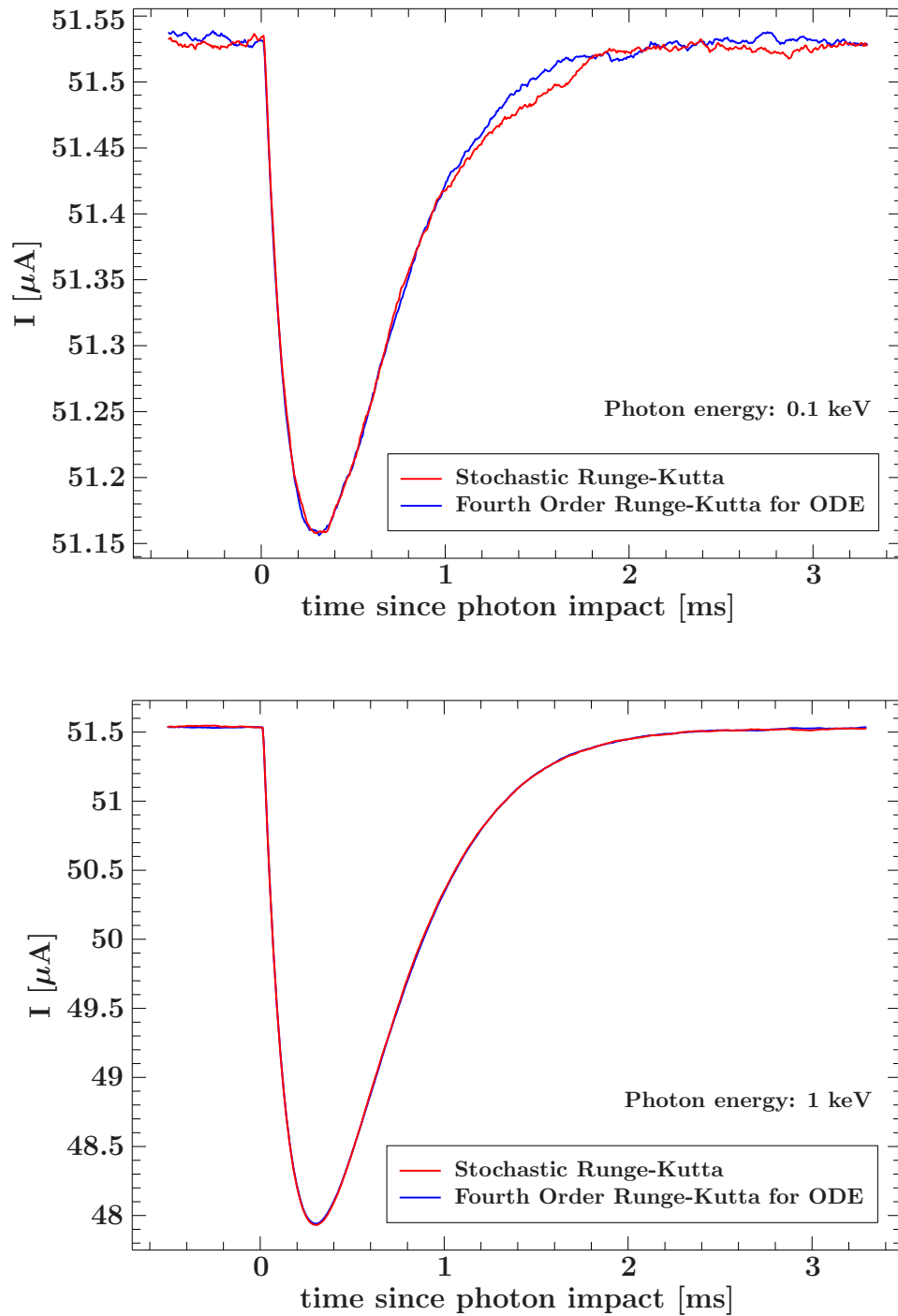
Fig. 7.4: Comparison between the two simulation methods. Shown in red is the solution obtained with the stochastic Runge-Kutta method applied to the SDE system and shown in blue is the result generated with the old method. *Top:* Photon energy: 0.1 keV. *Bottom:* Photon energy: 1 keV.
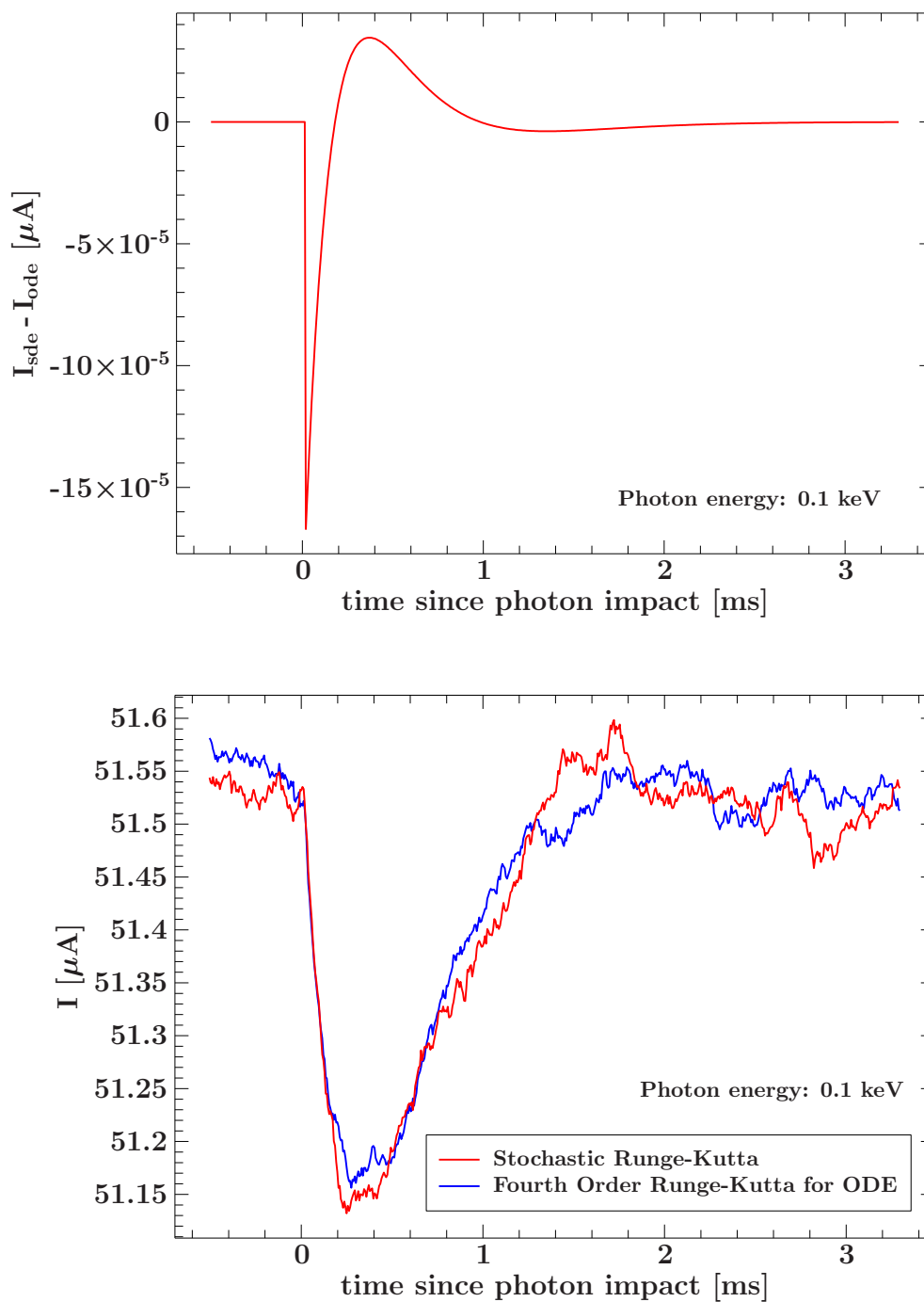
Fig. 7.5: *Top:* The difference between the new simulation result, denoted by I_{sde}, and the old result, denoted by I_{ode}, of a simulation without noise for a photon energy of 0.1 keV. *Bottom:* Current pulses with noise increased by 500 percent.

7.3   Spectral Analysis

In this section I use tools from spectral analysis to compare the noise spectrum of the new simulations with the noise spectrum of the simulations done before and also with theoretical predictions by Irwin & Hilton (2005). First, I give a short introduction to the techniques and concepts of spectral analysis that I will use later in this section such as the discrete Fourier transform and power spectral densities. Then I present and compare the resulting spectra. The following text is based on Stoica & Moses (2015). A thorough introduction to the spectral analysis of signals can be found in this book.

As already shown in Def. 5.26, the spectral density of a signal is defined as the Fourier transform of its autocorrelation function. The spectral density of a signal represents the distribution of signal power over frequencies. For this reason the spectral density is also called *power spectrum* or *power spectral density* (PSD) in the context of signal processing. In this section I will use the term power spectral density. One of the main goals of spectral analysis is to estimate the PSD of a random signal from a sequence of time samples of the signal.

Before dealing with PSDs, we will first define the *energy spectral density* of a deterministic signal. Let $\{y(t) : t = 0, \pm 1, \pm 2, \ldots\}$ be a deterministic discrete-time data sequence that is obtained by sampling a continuous-time signal. To keep the notation simple the time variable t is assumed to be measured in units of the sampling interval, i.e., $y(t) = y_c(t \cdot T_s)$, where $y_c(\cdot)$ is the continuous time signal and T_s is the sampling time interval. If $\{y(t)\}$ has *finite energy*, i.e.,

$$\sum_{t=-\infty}^{\infty} |y(t)|^2 < \infty, \tag{7.11}$$

then, under certain regularity conditions, the sequence $\{y(t)\}$ has a *discrete-time Fourier transform* (DTFT) that is defined as

$$Y(\omega) = \sum_{t=-\infty}^{\infty} y(t)e^{-i\omega t}, \tag{7.12}$$

where $i = \sqrt{-1}$. Here, the *(angular) frequency* ω is measured in radians per sampling interval. The physical frequency variable $\bar{\omega}$ [rad s^{-1}] is given by $\bar{\omega} = \omega/T_s$. We define

$$S(\omega) \coloneqq |Y(\omega)|^2. \tag{7.13}$$

One can show that

$$\sum_{t=-\infty}^{\infty} |y(t)|^2 = \frac{1}{2\pi} \int_{-\pi}^{\pi} S(\omega) d\omega. \tag{7.14}$$

The above equality is called *Parseval's theorem* and shows that $S(\omega)$ represents the distribution of sequence energy. Thus, $S(\omega)$ is called energy spectral density.

We will now turn towards random signals. Usually the signals observed are not deterministic and their variation in the future is unknown. We assume that the discrete-time signal $\{y(t) : t = 0, \pm 1, \pm 2 \ldots\}$ is a wide-sense stationary stochastic process with zero mean, i.e.,

$$E[y(t)] = 0 \quad \text{for all } t. \tag{7.15}$$

The observed signal is just one sample path of the signal and we cannot simply carry over the definitions for deterministic discrete-time signals unchanged because the sample paths do not have finite energy. However, since a random signal usually has a finite *average power*, we can define its PSD. An alternative definition of the PSD $\Phi(\omega)$ is given by

$$\Phi(\omega) = \lim_{N \to \infty} E \left\{ \frac{1}{N} \left| \sum_{t=1}^{N} y(t) e^{-i\omega t} \right|^2 \right\}. \tag{7.16}$$

This definition is similar to the definition of energy spectral density in the deterministic case. From this definition, methods for the numerical approximation of PSDs can be obtained.

The PSD $\Phi(\omega)$ is a periodic function with period 2π. So Φ is fully described by its values in the interval $[-\pi, \pi]$. Alternatively, we can view the PSD as a function of the frequency

$$f = \frac{\omega}{2\pi} \tag{7.17}$$

taking values in the interval $f \in [-1/2, 1/2]$. Furthermore, $\Phi(\omega)$ is symmetric for real-valued signals.

When working with real data we only have a finite number of samples of the signal to work with. How can we estimate the PSD from this record? A common estimator for the PSD is the *periodogram* which is derived from the definition (7.16) of the PSD by neglecting the expectation and limit operation. Let $y = \{y(t)\}_{t=1}^{N}$ be a finite-length record of a wide-sense stationary process. Then the periodogram of y is defined as

$$\hat{\Phi}_p(\omega) = \frac{1}{N} \left| \sum_{t=1}^{N} y(t) e^{-i\omega t} \right|^2. \tag{7.18}$$

In practice we cannot evaluate the periodogram over a continuum of frequencies. For the computation we need to choose an appropriate frequency sampling scheme, e.g.,

$$\omega_k = \frac{2\pi}{N} k, \quad k = 0, \dots, N-1. \tag{7.19}$$

We define

$$W := e^{-i\frac{2\pi}{N}}. \tag{7.20}$$

Then, for the computation of $\bar{\Phi}_p(\omega)$ at the frequency sample ω_k, we only need to calculate the *discrete Fourier transform* (DFT)

$$Y(k) = \sum_{t=1}^{N} y(t) W^k, \quad k = 0, \dots, N-1. \tag{7.21}$$

To calculate the DFT one can use the *fast Fourier transform* (FFT) by Cooley & Tukey (1965). The FFT is a computer algorithm to efficiently compute the DFT of a signal. While the number of complex floating point operations required to perform a DFT is approximately N^2, the number of operations required for the FFT reduces to $(N/2) \log_2(N)$.
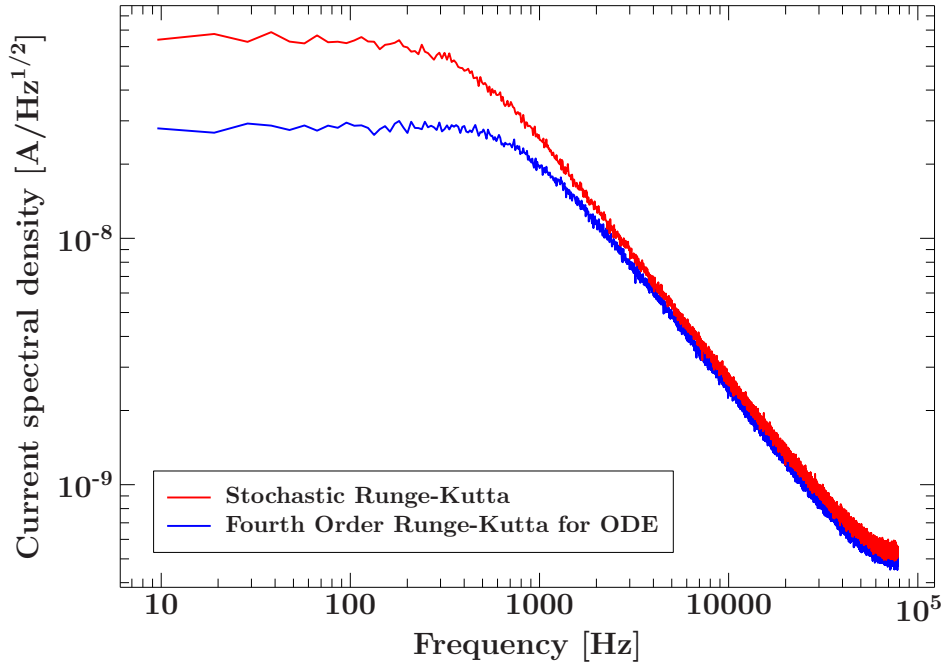
Fig. 7.6: Spectral densities of a 30 second signal of just noise. Shown in red is the PSD for the new method and shown in blue is the PSD of a signal obtained with the old method. The overall shape is very similar, but the intensity is slightly higher for the new method.

7.4 Bartlett's Method and PSD Estimates

A disadvantage of the periodogram as an estimator for the PSD is its high statistical variability. Moreover, the variance at a given frequency does not decrease as the number of samples increases. There are several methods to reduce the variance and fluctuations of the estimated spectrum. One of these methods is *Bartlett's method* (Bartlett, 1950). The basic idea of the Bartlett's method is to subdivide the available sample of N observations into $L = N/M$ subsamples of length M, calculate the periodograms of each segment and then average the periodograms obtained from the individual segments.

Denote by

$$y_j(t) := y((j-1)M + t), \qquad \begin{matrix} t = 1, \dots, M \\ j = 1, \dots, L \end{matrix} \qquad (7.22)$$

the observations of the jth subsample. The corresponding periodograms are given by

$$\hat{\Phi}_j(\omega) = \frac{1}{M} \left| \sum_{t=1}^{M} y_j(t) e^{-i\omega t} \right|^2. \qquad (7.23)$$

Then the Bartlett estimate of the PSD is given by

$$\hat{\Phi}_B(\omega) = \frac{1}{L} \sum_{j=1}^{L} \hat{\Phi}_j(\omega). \qquad (7.24)$$

I implemented the Bartlett's method as an S-Lang program, using the FFT routine from the S-Lang GSL library module[1]. Figure 7.6 shows the resulting PSD estimate

---
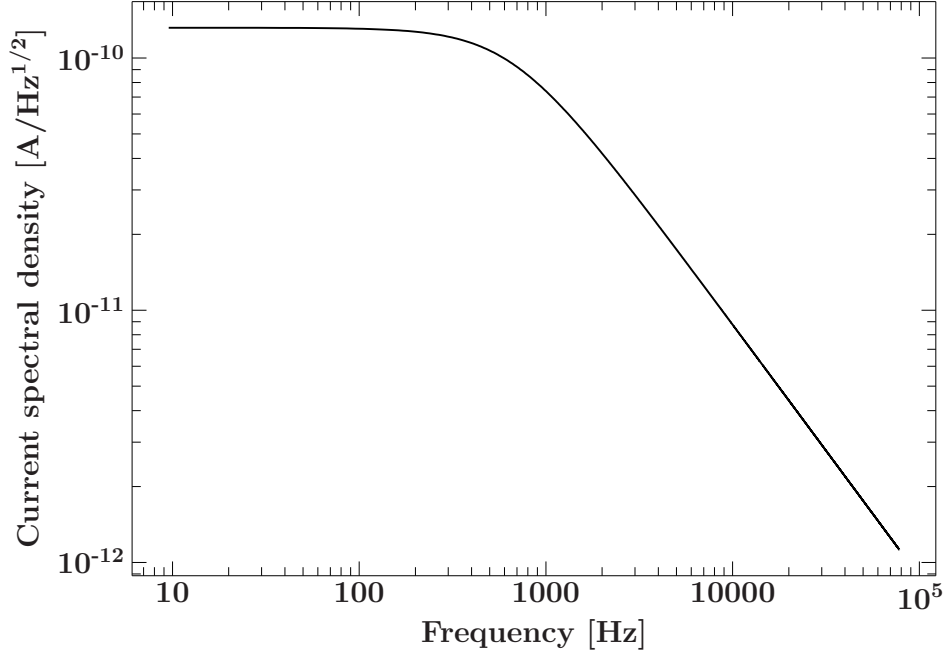[1]http://space.mit.edu/CXC/software/slang/modules/gsl/

Fig. 7.7: Predicted PSD of the steady state current noise as derived by Irwin & Hilton (2005).

of a 30 second simulation output of just noise for a segment length of $M = 2^{14}$. For comparison the PSD of a 30 second noise simulation with the old method is shown in red. We can see that the shape of the two PSDs is very similar. The overall intensity is slightly higher for the new method.

Irwin & Hilton (2005) derived theoretical formulas for the PSDs from different noise sources by using a *nonlinear equilibrium ansatz*. They find that the PSD of the steady state current noise due to Johnson noise in the TES is

$$S_{I_{\text{TES}}}(\omega) = 4k_{\text{B}}T_0 R_0 \frac{\xi_I}{\mathscr{L}_I^2}(1 + \omega^2\tau^2)|s_I(\omega)|^2, \tag{7.25}$$

with

$$s_I(\omega) = -\frac{1}{I_0 R_0}\left[\frac{L}{\tau_{\text{el}}R_0\mathscr{L}_I} + \left(1 - \frac{R_{\text{L}}}{R_0}\right) \right. \tag{7.26}$$

$$\left. + i\omega\frac{L\tau}{R_0\mathscr{L}_I}\left(\frac{1}{\tau_{\text{I}}} + \frac{1}{\tau_{\text{el}}}\right) - \frac{\omega^2\tau}{\mathscr{L}_I}\frac{L}{R_0}\right]^{-1}, \tag{7.27}$$

where $\mathscr{L}_I$ is the low-frequency loop gain, τ is the thermal time constant, τ_{el} is the electrical time constant, τ_{I} is the current-biased thermal time constant, and $\xi(I) = 1 + 2\beta$. Fore more details about these parameters see Irwin & Hilton (2005). Similarly, Irwin & Hilton (2005) find that the PSD of the steady state current noise due to Johnson noise in the load resistor is

$$S_{I_{\text{L}}}(\omega) = 4k_{\text{B}}T_{\text{L}}I_0^2 R_{\text{L}}\frac{(\mathscr{L}_I - 1)^2}{\mathscr{L}_I^2}(1 + \omega^2\tau_{\text{I}}^2)|s_I(\omega)|^2, \tag{7.28}$$

and the PSD due to thermal fluctuation noise is given by

$$S_{I_{\text{TFN}}}(\omega) = 4k_{\text{B}}T_0^2 G \times F_{\text{LINK}}(T_0, T_{\text{bath}})|s_I(\omega)|^2, \tag{7.29}$$

where $F_{\text{LINK}}(T_0, T_{\text{bath}})$ describes the noise power flow over the thermal link. This parameter usually has values between 0.5 and 1 (Kinnunen, 2011). The overall PSD of the steady state current noise due to these three noise sources is then

$$S(\omega) = S_{I_{\text{TES}}}(\omega) + S_{I_{\text{L}}}(\omega) + S_{I_{\text{TFN}}}(\omega). \tag{7.30}$$

Figure 7.7 shows the resulting PSD curve for the parameters of the simulated TES pixel from Table 7.1. We see that the overall shape of the PSD is in fact very similar to the PSD of the simulations shown in Fig. 7.6. The predicted intensity seems to be lower than for the simulations. However, due to several different PSD normalizations that are used in spectral analysis one must be very careful in direct comparisons of the two PSDs. The analysis of this subtle point is still in progress.

To sum up, I can say that my new simulation results do not differ much from the simulations done before. This result is very beneficial because it also confirms all the simulations generated with `tessim` before my work that contributed to the development of the Athena X-IFU detector. However, now we can use a numerical integrator that is especially designed for differential equations affected by noise instead of the heuristic method implemented before.

7.5 Event reconstruction

In this section I briefly describe how the photon energies can be determined from the noisy current pulses. This process is called *event reconstruction* and currently several different reconstruction methods are developed and examined for the Athena X-IFU using simulation results from `tessim` (Peille et al., 2016). The software package aimed at performing the event reconstruction on board Athena is called SIRENA and currently in development (Ceballos et al., 2017). The SIRENA software is also integrated in the SIXTE end-to-end simulator in order to test and evaluate its performance.

The event reconstruction is done in three steps. First, the events have to be detected. Then the events are graded and finally their energy is determined. One of the methods for the event energy determination currently tested for the X-IFU is called *optimal filtering* and uses the noise spectral density (Peille et al., 2016). In this method one assumes that the detector response is linear and that the pulse shapes are identical for all energies. Thus, every pulse is just a scaled version of a single template pulse. A second assumption of this method is that the noise is stationary. Then the scaling factor E of each pulse can be estimated by minimizing the weighted sum

$$\chi^2 = \sum \frac{[D(f) - E \times S(f)]^2}{N^2(f)}, \tag{7.31}$$

where $N(f)$ is the PSD of the noise, $D(f)$ is the DFT of the signal, and $S(f)$ is the DFT of the template pulse. As the X-IFU detector is non-linear, this energy estimate is then transformed by the application of a gain scale in order to obtain the final estimate.

In addition to the optimal filtering method more advanced event reconstruction techniques are currently studied. More details about the different reconstruction algorithms and an in depth study of their performance can be found in Peille et al. (2016).

Chapter 8

Conclusion and Outlook

The aim of this thesis was to model and simulate transition-edge sensor based microcalorimeters by using stochastic differential equations. I successfully implemented a stochastic Runge-Kutta method in the `tessim` software tool within the SIXTE simulation framework in order to solve the resulting system of stochastic differential equations numerically.

The results of my simulations show that the difference between this new approach and the simulations done before with `tessim` is minimal. The simulations show that the effect of noise on the detector signal is greatest at photon energies below 1 keV. Before my work it was not clear how much of a difference this new simulation method would make on the detector signals. Detailed studies of the instrument performance of the Athena X-ray observatory will be performed with the SIXTE software framework in the future. Thus, it was important to make sure that this step in the simulation chain is done correctly.

The fact that my simulations show no drastic differences also confirms all previous studies performed with the `tessim` tool. However, we can now use an integrator that is especially designed for differential equations affected by noise and which can easily be further modified in the future.

The theoretical noise PSD needs to be examined in order to understand where the difference to the simulations originates. Because there was a slight difference between the noise PSDs of the simulations, it would be interesting to see which method is closer to the predicted values.

There are always trade-offs between accuracy and computation time in numerical simulations. Since the stochastic integrator is more complex than the fourth order Runge-Kutta method implemented before, the computation time slightly increases for the new method. This effect will sum up significantly for longer simulation times.

Adaptive step size control could be a possible way to mitigate this effect and reduce the computation time. The current pulses happen in time frames of some milliseconds. It is necessary to simulate these current pulses as accurately as possible in order to calculate their exact energies with the event reconstruction software. The remaining part of the simulation result is just noise where we could increase the step size without great loss of information.

There are some methods proposed for the implementation of variable step sizes in stochastic integrators (see, e.g., Ilie et al., 2015). However, the mathematical theory of

these methods is by far not as well-developed as their deterministic counterparts and still a very active research topic. The biggest challenge with adaptive step size control for stochastic differential equations is the local error estimation. In addition, one has to make sure to stay on the same sample paths of the corresponding Wiener processes when changing the step sizes.

References

Abramowitz M., Stegun I., 1972, Handbook of Mathematical Functions with Formulas, Graphs, and Mathematical Tables, U.S. Department of Commerce, National Bureau of Standards

Adkins W.A., Davidson M.G., 2012, Ordinary Differential Equations, Springer New York

Allison A., Abbot D., 2005, AIP Conf. Proc. 800, 15

Barcons X., Barret D., Decourchelle A., et al., 2017, Astronomische Nachrichten 338, 153

Barcons X., Nandra K., Barret D., et al., 2015, Journal of Physics: Conference Series 610, 012008

Barret D., Lam Trong T., den Herder J.W., et al., 2016, Proc. SPIE 9905, 99055W

Bartlett M., 1950, Biometrika 37, 1

Ceballos M.T., Cobo B., Peille P., et al., 2017, In: Arribas S., Alonso-Herrero A., Figueras F., Hernández-Monteagudo C., Sánchez-Lavega A., Pérez-Hoyos S. (eds.) Highlights on Spanish Astrophysics IX., p.703

Collon M.J., Vacanti G., Günther R., et al., 2015, Proc. SPIE 9603, 96030K

Cooley J., Tukey J., 1965, Math. Comp. 19, 297

Cyganowski S., Kloeden P., Ombach J., 2002, From Elementary Probability to Stochastic Differential Equations with MAPLE®, Springer-Verlag Berlin Heidelberg

Decourchelle A., Costantini E., Badenes C., et al., 2013, arXiv: 1306.2335

Demir A., 1997, Ph.D. thesis, University of California, Berkeley

Dreyer J., 2012, Ph.D. thesis, University of California, Berkeley

Evans L., 2014, An Introduction to Stochastic Differential Equations, American Mathematical Society

Galassi M., Davies J., Theiler J., et al., 2009, GNU Scientific Library Reference Manual (3rd Ed.), Network Theory Ltd.

Gillespie D.T., 1996, Am. J. Phys. 64, 225

Goldie D., Audley M., Glowacka D., et al., 2009, J. Appl. Phys. 105, 074512

Grigoriu M., 2002, Stochastic Calculus: Applications in Science and Engineering, Springer Science+Business Media New York

Horowitz P., Hill W., 2015, The Art of Electronics, Cambridge University Press

Horsthemke W., Lefever R., 1984, Noise-Induced Transitions: Theory and Applications in Physics, Chemistry, and Biology, Springer-Verlag Berlin Heidelberg

Houck J., Denicola L., 2000, In: Manset N., Veillet C., Crabtree D. (eds.) Astronomical Data Analysis Software and Systems IX, Vol. 216. Astronomical Society of the Pacific Conference Series, p. 591

Ilie S., Jackson K.R., Enright W.H., 2015, Numerical Algorithms 68, 791

Irwin K., Hilton G., 2005, Transition-Edge Sensors. In: Enss C. (ed.) Cryogenic Particle Detection, Vol. 99. Topics in Applied Physics Springer-Verlag Berlin Heidelberg

Itô K., 1951, On Stochastic Differential Equations, American Mathematical Society

Jackson B.D., van Weers H., van der Kuur J., et al., 2016, Proc. SPIE 9905, 99052I

Kaastra J., Finoguenov A., Nicastro F., et al., 2013, arXiv: 1306.2324

Karatzas I., Shreve S., 1991, Brownian Motion and Stochastic Calculus, Springer-Verlag New-York

Kinnunen K., 2011, Ph.D. thesis, University of Jyväskylä

Kloeden P., Platen E., 1995, Numerical So-

lution of Stochastic Differential Equations, Springer-Verlag Berlin Heidelberg

Kloeden P., Platen E., Henri S., 1994, Numerical Solution of SDE Through Computer Experiments, Springer-Verlag Berlin Heidelberg

Koralov L., Sinai Y., 2007, Theory of Probability and Random Processes, Springer-Verlag Berlin Heidelberg

Kuo H., 2006, Introduction to Stochastic Integration, Springer-Verlag New York

L'Ecuyer P., 1996, Mathematics of Computation 65, 203

Lefebvre M., 2007, Applied Stochastic Processes, Springer-Verlag New York

Lindström E., Madsen H., Nielsen J., 2015, Statistics for Finance, CRC Press

Mao X., 2007, Stochastic Differential Equations and Applications, Woodhead Publishing

Maruyama G., 1955, Rendiconti del Circolo Matematico di Palermo 4, 48

McCammon D., 2005, Thermal Equilibrium Calorimeters – An Introduction. In: Enss C. (ed.) Cryogenic Particle Detection, Vol. 99. Topics in Applied Physics Springer-Verlag Berlin Heidelberg

Meidinger N., Eder J., Eraerds T., et al., 2017, arXiv: 1702.01079

Musiela M., Rutkowski M., 2005, Martingale Methods in Financial Modelling, Springer-Verlag Berlin Heidelberg

Nyquist H., 1928, Phys. Rev. 32, 110

Øksendal B., 2003, Stochastic Differential Equations: An Introduction with Applications, Springer-Verlag Berlin Heidelberg

Peille P., Ceballos M.T., Cobo B., et al., 2016, In: Space Telescopes and Instrumentation 2016: Ultraviolet to Gamma Ray, Vol. 9905. Proc. SPIE, p. 99055W

Platen E., Bruti-Liberati N., 2010, Numerical Solution of Stochastic Differential Equations with Jumps in Finance, Springer-Verlag Berlin Heidelberg

Proschan M., Shaw P., 2016, Essentials of Probability Theory for Statisticians, CRC Press

Schilling R., 2005, Measures, Integrals and Martingales, Cambridge University Press

Schilling R., Partzsch L., 2012, Brownian Motion: An Introduction to Stochastic Processes, De Gruyter

Schmid C., 2012, Ph.D. thesis, Friedrich-Alexander-Universität Erlangen-Nürnberg

Sciortino S., Rauw G., Audard M., et al., 2013, arXiv: 1306.2333

Socha L., 2008, Linearization Methods for Stochastic Dynamic Systems, Springer-Verlag Berlin Heidelberg

Stoica P., Moses R., 2015, Spectral Analysis of Signals, Prentice Hall

Stratonovich R.L., 1966, SIAM Journal on Control 4, 362

Vigirdas M., 2011, Introduction to Stochastic Analysis: Integrals and Differential Equations, Wiley-ISTE

Wilkie J., 2004, Phys. Rev. E 70, 017701

Willingale R., Pareschi G., Christensen F., den Herder J.W., 2013, arXiv: 1307.1709

Wilms J., Brand T., Barret D., et al., 2014, Proc. SPIE 9144, 91445X

Wilms J., Smith S.J., Peille P., et al., 2016, Proc. SPIE 9905, 990564

Glossary of Notation

a.s. : almost surely.

I_A : the indicator function of a set A, i.e., $I_A(x) = 1$ if $x \in A$ and $I_A(x) = 0$ if $x \notin A$.

$\sigma(\mathcal{U})$: the σ-algebra generated by $\mathcal{U}$.

$a \wedge b$: the minimum of a and b.

$f : A \to B$: the mapping f from a to b.

$\mathbb{R}^n$: the n-dimensional Euclidean space.

$\mathbb{R}^{n \times m}$: the space of all real $n \times m$-matrices.

$\mathbb{R}_+$: the set of all nonnegative real numbers.

$\mathcal{B}^n$: the Borel σ-algebra on $\mathbb{R}^n$.

$\mathcal{B}$: $= \mathcal{B}^1$.

A^T : the transposed of a vector or matrix A.

$\mathrm{trace}(A)$: the trace of a square matrix $A = (a_{ij})_{n \times n} \in \mathbb{R}^{n \times n}$, i.e., $\mathrm{trace}(A) = \sum_{i=1}^n a_{ii}$.

$|v|$: the Euclidean norm of a vector $v \in \mathbb{R}^n$, i.e., $|v| = \sqrt{v_1^2 + \cdots + v_n^2}$.

$\|A\|$: the trace norm of a matrix $A \in \mathbb{R}^{n \times m}$, i.e., $\|A\| = \sqrt{\mathrm{trace}(A^T A)}$.

$\|X\|_p$: $= (E\,[|X|^p])^{1/p}$.

$L^p(\Omega, \mathbb{R}^n)$: the family of all $\mathbb{R}^n$-valued random variables X with $\|X\|_p < \infty$.

$C^m(D, \mathbb{R}^n)$: the family of all continuously m-times differentiable $\mathbb{R}^n$-valued functions defined on D.

$\mathcal{L}^p([a, b]; \mathbb{R}^n)$: the family of all $\mathbb{R}^n$-valued $\mathcal{F}_t$-adapted processes $\{X_t\}_{a \leq t \leq b}$ such that $\int_a^b |X_t|^p dt < \infty$.

$\mathcal{M}^p([a, b]; \mathbb{R}^n)$: the family of all processes $\{X_t\}_{a \leq t \leq b}$ in $\mathcal{L}^p([a, b]; \mathbb{R}^n)$ such that $E \int_a^b |X_t|^p dt < \infty$.

$\mathcal{L}^p(\mathbb{R}_+; \mathbb{R}^n)$: the family of all processes $\{X_t\}_{t \geq 0}$ such that for every $T > 0$, $\{X_t\}_{0 \leq t \leq T} \in \mathcal{L}^p([0, T]; \mathbb{R}^n)$.

$\mathcal{M}^p(\mathbb{R}_+; \mathbb{R}^n)$: the family of all processes $\{X_t\}_{t \geq 0}$ such that for every $T > 0$, $\{X_t\}_{0 \leq t \leq T} \in \mathcal{M}^p([0, T]; \mathbb{R}^n)$.

V_x : $= (\frac{\partial V}{\partial x_1}, \cdots, \frac{\partial V}{\partial x_n})$.

V_{xx} : $= (\frac{\partial^2 V}{\partial x_i \partial x_j})_{n \times n}$.

Acknowledgements

Erklärung

Hiermit versichere ich, dass ich die vorliegende Arbeit selbstständig verfasst und keine anderen als die angegebenen Quellen und Hilfsmittel benutzt habe, dass alle Stellen der Arbeit, die wörtlich oder sinngemäß aus anderen Quellen übernommen wurden, als solche kenntlich gemacht sind und dass die Arbeit in gleicher oder ähnlicher Form noch keiner Prüfungsbehörde vorgelegt wurde.

Erlangen, den 15. September 2017